NUCLEAR MAGNETIC RESONANCE SPECTROSCOPY

Part Five: Advanced NMR Techniques

Since the advent of modern, computer-controlled Fourier transform nuclear magnetic resonance (FT-NMR) instruments, it has been possible to conduct more sophisticated experiments than those described in preceding chapters. Although a great many specialized experiments can be performed, the following discussion examines only a few of the most important ones.

10.1 PULSE SEQUENCES

Chapter 4, Section 4.5, introduced the concept of **pulse sequences.** In an FT-NMR instrument, the computer that operates the instrument can be programmed to control the timing and duration of the excitation pulse—the radiofrequency pulse used to excite the nuclei from the lower spin state to the upper spin state. Chapter 3, Section 3.7B, discussed the nature of this pulse and the reasons why it can excite all the nuclei in the sample simultaneously. Precise timing can also be applied to any decoupling transmitters that operate during the pulse sequence. As a simple illustration, Figure 10.1 shows the pulse sequence for the acquisition of a simple proton NMR spectrum. The pulse sequence is characterized by an excitation pulse from the transmitter; an **acquisition time,** during which the free-induction decay (FID) pattern is collected in digitized form in the computer; and a **relaxation delay,** during which the nuclei are allowed to relax in order to reestablish the equilibrium populations of the two spin states. After the relaxation delay, a second excitation pulse marks the beginning of another cycle in the sequence.

There are many possible variations on this simple pulse sequence. For example, in Chapter 4 we learned that it is possible to transmit *two* signals into the sample. In ^{13}C NMR spectroscopy, a pulse sequence similar to that shown in Figure 10.1 is transmitted at the absorption frequency of the ^{13}C nuclei. At the same time, a second transmitter, tuned to the frequency of the hydrogen (^1H) nuclei in the sample, transmits a broad band of frequencies to **decouple** the hydrogen nuclei from the ^{13}C nuclei. Figure 10.2 illustrates this type of pulse sequence.

The discussion in Chapter 4, Section 4.5, of methods for determining ^{13}C spectra described how to obtain proton-*coupled* spectra and still retain the benefits of nuclear Overhauser enhancement. In this method, which is called an **NOE-enhanced proton-coupled spectrum** or a **gated decoupling spectrum,** the decoupler is turned on during the interval *before* the pulsing of the ^{13}C nuclei. At the moment the excitation pulse is transmitted, the decoupler is switched off. The decoupler is switched on again during the relaxation delay period. The effect of this pulse sequence is to allow the nuclear Overhauser effect to develop while the decoupler is on. Because the decoupler is switched off during the excitation pulse, spin decoupling of the ^{13}C atoms is not observed (a proton-coupled spectrum is seen). The nuclear Overhauser enhancement decays over a relatively long time period; therefore, most of the enhancement is retained as the FID is collected. Once the FID information has been accumulated, the decoupler is switched on again to allow the nuclear Overhauser enhancement to develop before the next excitation pulse. Figure 10.3a shows the pulse sequence for gated decoupling.
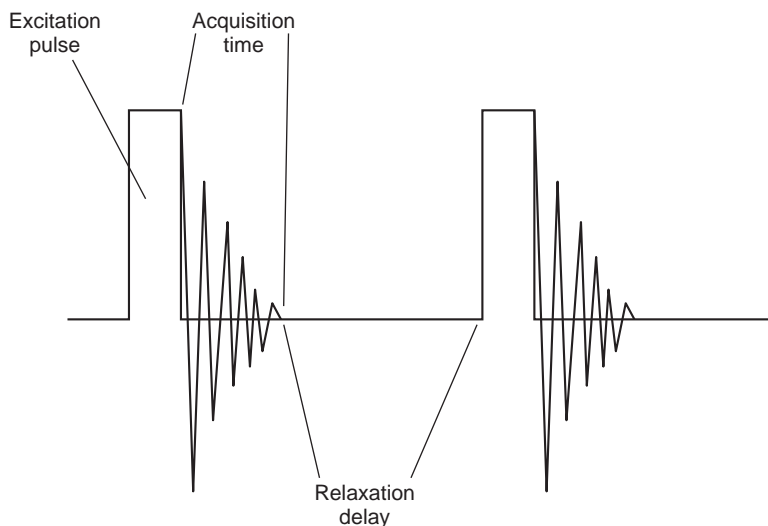
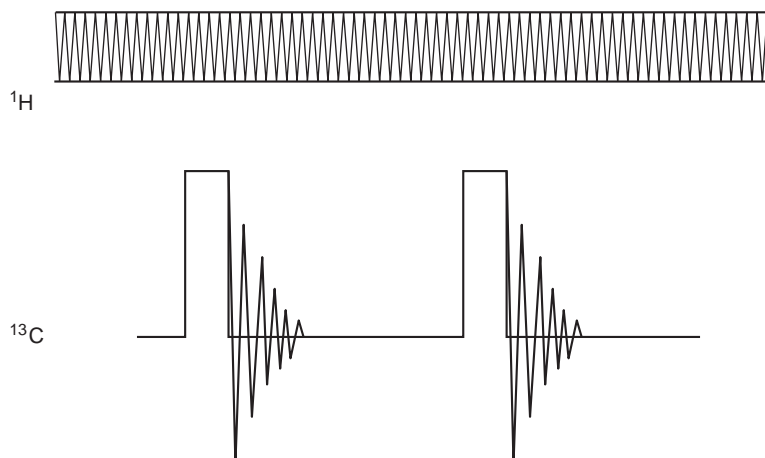**F I G U R E   1 0 . 1**   A simple pulse sequence.

F I G U R E   1 0 . 2   A proton-decoupled ^{13}C NMR pulse sequence.

The opposite result is obtained if the decoupler is not switched on until *the very instant* the excitation pulse is transmitted. Once the FID data have been collected, the decoupler is switched off until the next excitation pulse. This pulse sequence is called **inverse gated decoupling.** The effect of this pulse sequence is to provide a proton-decoupled spectrum with no NOE enhancement. Because the decoupler is switched off before the excitation pulse, the nuclear Overhauser enhancement is not allowed to develop. Proton decoupling is provided since the decoupler is switched on during the excitation pulse and the acquisition time. Figure 10.3b shows the pulse sequence for inverse gated decoupling. This technique is used when it is necessary to determine integrals in a ^{13}C spectrum.

The computer that is built into modern FT-NMR instruments is very versatile and enables us to develop more complex and more interesting pulse sequences than the ones shown here. For example, we can transmit second and even third pulses, and we can transmit them along any of the Cartesian axes. The pulses can be transmitted with varying durations, and a variety of times can also be programmed into the sequence. As a result of these pulse programs, nuclei may exchange energy, they may affect each other's relaxation times, or they may encode information about spin coupling from one nucleus to another.
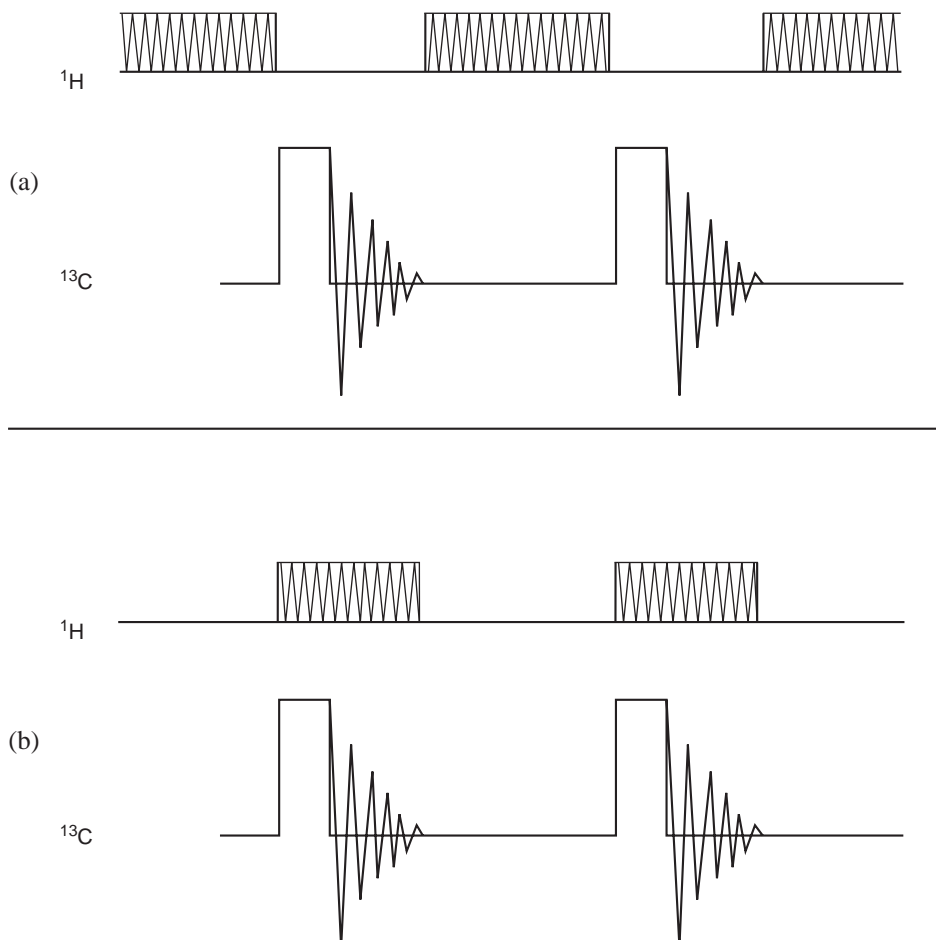
(a)

(b)

F I G U R E   1 0 . 3 A simple pulse sequence. (a) A pulse sequence for gated decoupling; (b) a pulse sequence for inverse gated decoupling.

We will not describe these complex pulse sequences any further; their description and analysis are beyond the scope of this discussion. Our purpose in describing a few simple pulse sequences in this section is to give you an idea of how a pulse sequence is constructed and how its design may affect the results of an NMR experiment. From this point forward, we shall simply describe the *results* of experiments that utilize some complex sequences and show how the results may be applied to the solution of a molecular structure problem. If you want more detailed information about pulse sequences for the experiments described in the following sections, consult one of the works listed in the references at the end of this chapter.

10.2 PULSE WIDTHS, SPINS, AND MAGNETIZATION VECTORS

To gain some appreciation for the advanced techniques that this chapter describes, you must spend some time learning what happens to a magnetic nucleus when it receives a pulse of radiofrequency energy. The nuclei that concern us in this discussion, ^1H and ^{13}C, are magnetic. They have a finite spin, and a spinning charged particle generates a magnetic field. That means that each individual nucleus behaves as a tiny magnet. The nuclear magnetic moment of each nucleus can be illustrated

as a vector (Fig. 10.4a). When the magnetic nuclei are placed in a large, strong magnetic field, they tend to align themselves with the strong field, much as a compass needle aligns itself with the earth's magnetic field. Figure 10.4b shows this alignment. In the following discussion, it would be very inconvenient to continue describing the behavior of each individual nucleus. We can simplify the discussion by considering that the magnetic field vectors for each nucleus give rise to a resultant vector called the **nuclear magnetization vector** or the **bulk-magnetization vector.** Figure 10.4b also shows this vector (**M**). The individual nuclear magnetic vectors precess about the principal magnetic field axis (Z). They have random precessional motions that are not in phase; vector addition produces the resultant, the nuclear (bulk) magnetization vector, which is aligned along the Z axis. We can more easily describe an effect that involves the individual magnetic nuclei by examining the behavior of the nuclear magnetization vector.

The small arrows in Figure 10.4 represent the individual magnetic moments. In this picture, we are viewing the orientations of the magnetic moment vectors from a stationary position, as if we were standing on the laboratory floor watching the nuclei precess inside the magnetic field. This view, or **frame of reference,** is thus known as the **laboratory frame** or the **stationary frame.** We can simplify the study of the magnetic moment vectors by imagining a set of coordinate axes that rotate in the same direction and at the same speed as the average nuclear magnetic moment precesses. This reference frame is called the **rotating frame,** and it rotates about the Z axis. We can visualize these vectors more easily by considering them within the rotating frame, much as we can visualize the complex motions of objects on the earth more easily by first observing their motions from the earth, alone, even though the earth is spinning on its axis, rotating about the sun, and moving through the solar system. We can label the axes of the rotating frames X', Y', and Z' (identical with Z). In this rotating frame, the microscopic magnetic moments are stationary (are not rotating) because the reference frame and the microscopic moments are rotating at the same speed and in the same direction.

Because the small microscopic moments (vectors) from each nucleus add together, what our instrument sees is the *net* or *bulk* magnetization vector for the whole sample. We will refer to this bulk magnetization vector in the discussions that follow.

In a Fourier transform NMR instrument, the radiofrequency is transmitted into the sample in a **pulse** of very short duration—typically on the order of 1 to 10 microseconds (μsec); during this time, the radiofrequency transmitter is suddenly turned on and, after about 10 μsec, suddenly turned off again. The

(a) A collection of magnetic nuclei, showing the individual magnetic moments.

(b) Magnetic nuclei aligned in an external magnetic field; M represents the bulk magnetization vector.
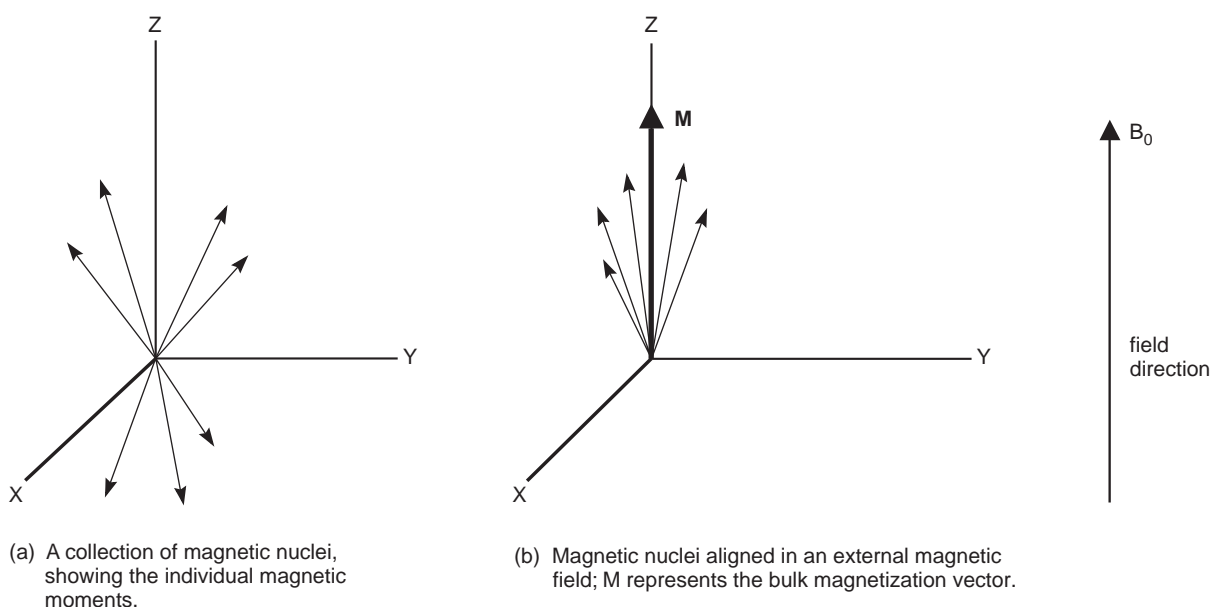
F I G U R E   1 0 . 4   Nuclear magnetization (laboratory frame).
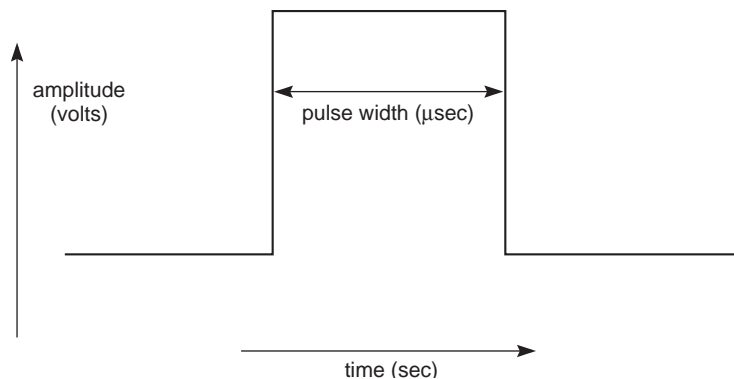
FIGURE 10.5 A square-wave pulse.

pulse can be applied along either the X' or the Y' axis and in either the positive or the negative direction. The shape of the pulse, expressed as a plot of DC voltage versus time, looks like Figure 10.5.

When we apply this pulse to the sample, the magnetization vector of every magnetic nucleus begins to precess about the axis of the new pulse.[1] If the pulse is applied along the X' axis, the magnetization vectors all begin to tip in the same direction at the same time. The vectors tip to greater or smaller extents depending on the duration of the pulse. In a typical experiment, the duration of the pulse is selected to cause a specific **tip angle** of the bulk magnetization vector (the resultant vector of all of the individual vectors), and a pulse duration (known as a **pulse width**) is selected to result in a 90° rotation of the bulk magnetization vector. Such a pulse is known as a **90° pulse.** Figure 10.6 shows its effect along the X' axis. At the same time, if the duration of the pulse were twice as long, the bulk magnetization vector would tip to an angle of 180° (it would point straight down in Fig. 10.6). A pulse of this duration is called a **180° pulse.**

What happens to the magnetization vector following a 90° pulse? At the end of the pulse, the B_0 field is still present, and the nuclei continue to precess about it. If we focus for the moment on the
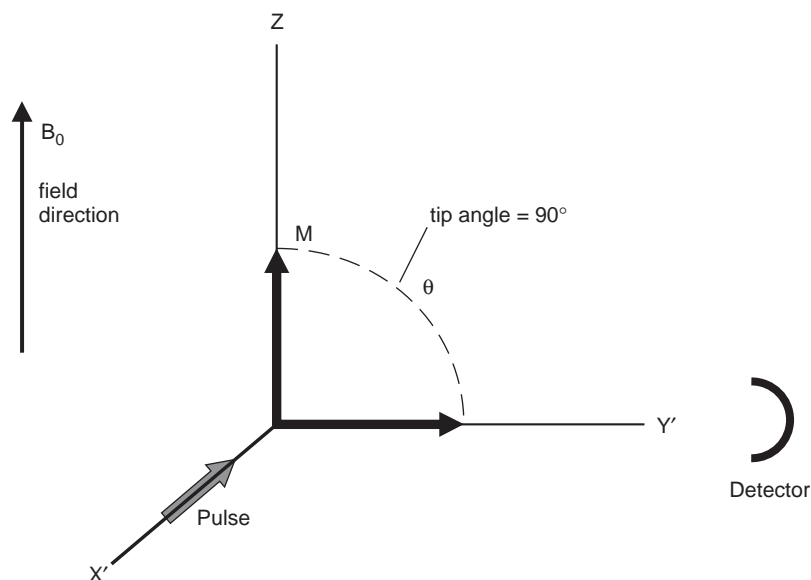

FIGURE 10.6 The effect of a 90° pulse (**M** is the bulk magnetization vector for the sample).

---

[1] Recall from Chapter 3 that if the duration of the pulse is short, the pulse has an uncertain frequency. The range of the uncertainty is sufficiently wide that all of the magnetic nuclei absorb energy from the pulse.

nuclei with precessional frequencies that exactly match the frequency of the rotating frame, we expect the magnetization vector to remain directed along the *Y'* axis (see Fig. 10.6).

In the **laboratory frame,** the *Y'* component corresponds to a magnetization vector rotating in the *XY* plane. The magnetization vector rotates in the *XY* plane because the individual nuclear magnetization vectors are precessing about *Z* (the principal field axis). Before the pulse, individual nuclei have random precessional motions and are not in phase. The pulse causes **phase coherence** to develop so that all of the vectors precess in phase (see Fig. 10.7). Because all of the individual vectors precess about the *Z* axis, **M**, the resultant of all of these vectors, also rotates in the *XY* plane.
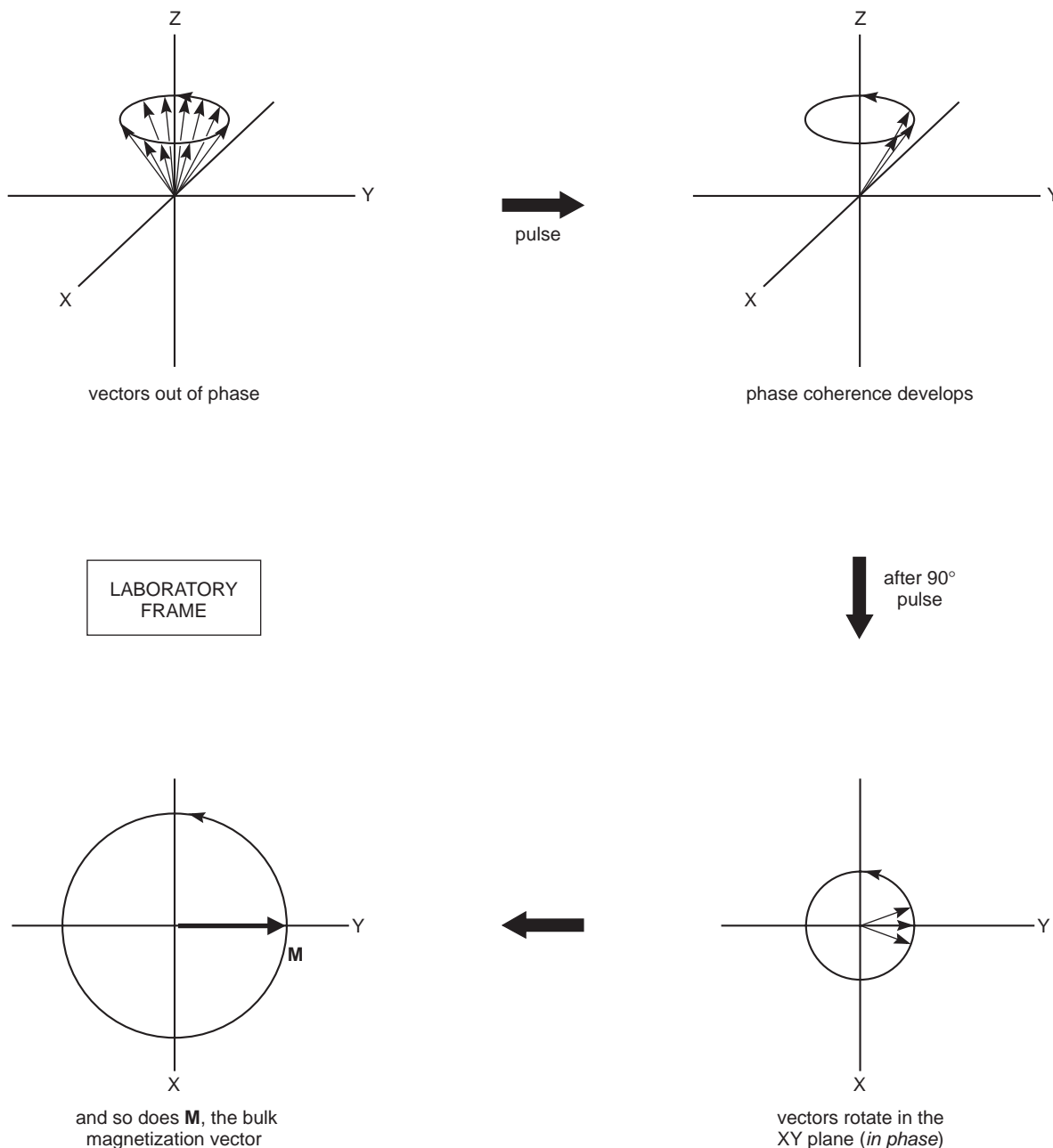
F I G U R E   1 0 . 7 Precession of magnetization vectors in the *XY* plane.
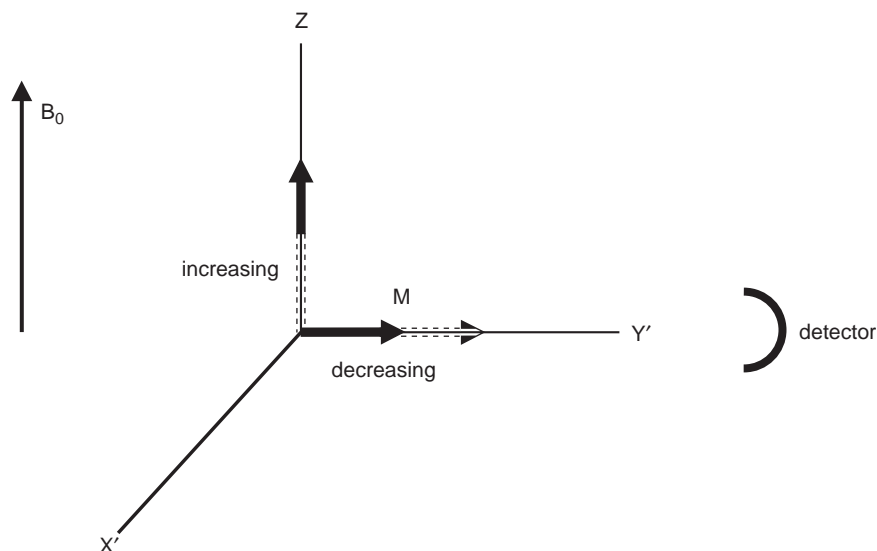
F I G U R E 1 0 . 8 Decay of the magnetization vector components as a function of time.

Once the pulse stops, however, the excited nuclei begin to relax (lose excitation energy and invert their individual nuclear spins). Over time, such **relaxation processes** diminish the magnitude of the bulk magnetization vector along the *Y′* axis and increase it along the *Z* axis, as illustrated in Figure 10.8. These changes in bulk magnetization occur as a result of both spin inversion to restore the Boltzmann distribution (spin–lattice relaxation) *and* loss of phase coherence (spin–spin relaxation). If we wait long enough, eventually the bulk magnetization returns to its equilibrium value, and the bulk magnetization vector points along the *Z* axis.

A receiver coil is situated in the *XY* plane, where it senses the rotating magnetization. As the *Y′* component grows smaller, the oscillating voltage from the receiver coil decays, and it reaches zero when the magnetization has been restored along the *Z* axis. The record of the receiver voltage as a function of time is called the **free-induction decay** (**FID**) because the nuclei are allowed to precess "freely" in the absence of an *X*-axis field. Figure 3.15 in Chapter 3 shows an example of a free-induction decay pattern. When such a pattern is analyzed via a Fourier transform, the typical NMR spectrum is obtained.

To understand how some of the advanced experiments work, it is helpful to develop an appreciation of what an excitation pulse does to the nuclei in the sample and how the magnetization of the sample nuclei behaves during the course of a pulsed experiment. At this point, we shall turn our attention to three of the most important advanced experiments.

10.3 PULSED FIELD GRADIENTS

Before determining an NMR spectrum, it is very important that the magnetic field be **shimmed.** The NMR experiment requires that there be a uniform magnetic field over the entire volume of the sample. If the field is not uniform, the result will be broadened peaks, the appearance of spurious side-band peaks, and a general lack of resolution. This means that every time a sample is introduced into the magnetic field, the field must be adjusted slightly to achieve this uniformity of magnetic field (magnetic field homogeneity).

The shimming process allows one to achieve field homogeneity by carefully adjusting a series of controls to vary the amount of current that passes through a set of coils that generate small magnetic

fields of their own. These adjustable magnetic fields compensate for inhomogeneity in the overall magnetic field. The result of careful shimming is that the spectral lines will have good line shape, and the resolution will be maximized.

The drawback to this manual shimming process is that it is time consuming, and it does not lend itself well to the determination of spectra in an automated environment. With the advent of **pulsed field gradients,** this shimming process becomes much faster, and it can be applied to the determination of spectra automatically.

In a "normal" NMR experiment, one applies a pulse of magnetic field that is uniform along the length of the sample. Figure 10.9a depicts how this pulse might appear. In a pulsed field gradient experiment, the pulse that is applied varies along the length of the sample tube. Figure 10.9b shows what this might look like.

A field gradient pulse causes the nuclei in molecules in different locations along the length of the sample tube to process at different frequencies. The result is that the rotating magnetization vectors of each nucleus will rapidly fall out of phase, resulting in destruction of the signal. By the application of a second gradient pulse, directed in opposite directions along the Z axis, peaks that arise from noise and other artifacts will be eliminated. Magnetization vectors that belong to the sample of interest will be "unwound" with this second pulse, and they will appear as clean signals. Thus, the unwanted peaks are destroyed, and only the peaks of interest remain. To selectively refocus the desired signals correctly, the instrument's computer must already have a **field map** in its memory. This field map is determined for each probe head using a sample that gives a strong signal. Water or the deuterium in the solvent is generally used for this purpose. Once the field map has been created for the probe head that is being used, the computer then uses those values to adjust the field gradient to yield the strongest, sharpest signal.

The advantage of field gradient shimming is that it is usually complete within two or three iterations. Manual shimming, by contrast, can be tedious and time consuming requiring many iterations. The automated nature of field gradient shimming lends itself well to the determination of spectra automatically. This is especially useful when an automatic sample changer is attached to the instrument.

The advantages of field gradient shimming may also be applied to a wide variety of two-dimensional spectroscopic techniques. These will be mentioned in succeeding sections of this chapter.
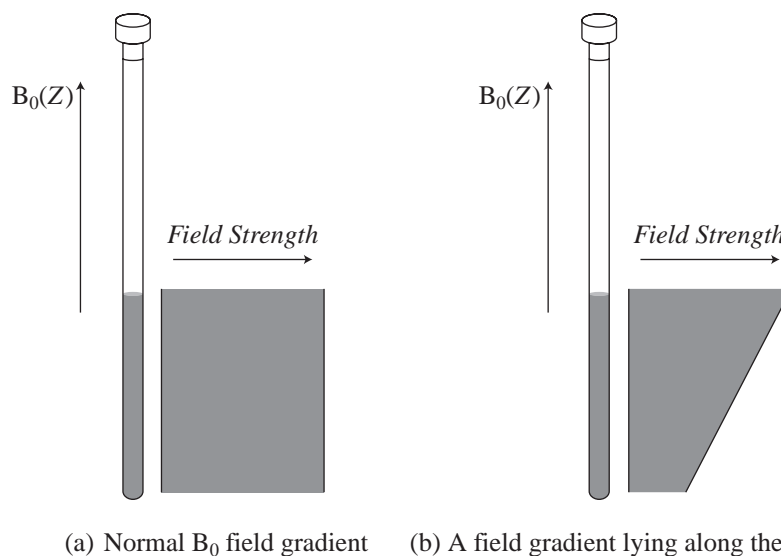

(a) Normal B_0 field gradient   (b) A field gradient lying along the Z direction

F I G U R E   1 0 . 9   Diagram showing the shape of a magnetic field pulse along the Z axis of an NMR sample tube.

10.4 THE DEPT EXPERIMENT

A very useful pulse sequence in ^{13}C spectroscopy is employed in the experiment called **Distortionless Enhancement by Polarization Transfer,** better known as **DEPT.** The DEPT method has become one of the most important techniques available to the NMR spectroscopist for determining the number of hydrogens attached to a given carbon atom. The pulse sequence involves a complex program of pulses and delay times in both the ^1H and ^{13}C channels. The result of this pulse sequence is that carbon atoms with one, two, and three attached hydrogens exhibit different **phases** as they are recorded. The phases of these carbon signals will also depend on the duration of the delays that are programmed into the pulse sequence. In one experiment, called a DEPT-45, only carbon atoms that bear any number of attached hydrogens will produce a peak. With a slightly different delay, a second experiment (called a DEPT-90) shows peaks only for those carbon atoms that are part of a **methine** (CH) group. With an even longer delay, a DEPT-135 spectrum is obtained. In a DEPT-135 spectrum, methine and methyl carbons give rise to positive peaks, whereas methylene carbons appear as inverse peaks. Section 10.5 will develop the reasons why carbon atoms with different numbers of attached hydrogens behave differently in this type of experiment. Quaternary carbons, which have no attached hydrogens, give no signal in a DEPT experiment.

There are several variations on the DEPT experiment. In one form, separate spectra are traced on a single sheet of paper. On one spectrum, only the methyl carbons are shown; on the second spectrum, only the methylene carbons are traced; on the third spectrum, only the methine carbons appear; and on the fourth trace, all carbon atoms that bear hydrogen atoms are shown. In another variation on this experiment, the peaks due to methyl, methylene, and methine carbons are all traced on the same line, with the methyl and methine carbons appearing as positive peaks and the methylene carbons appearing as negative peaks.

In many instances, a DEPT spectrum makes spectral assignments easier than does a proton-decoupled ^{13}C spectrum. Figure 10.10 is the DEPT-135 spectrum of **isopentyl acetate.**
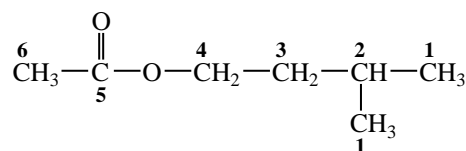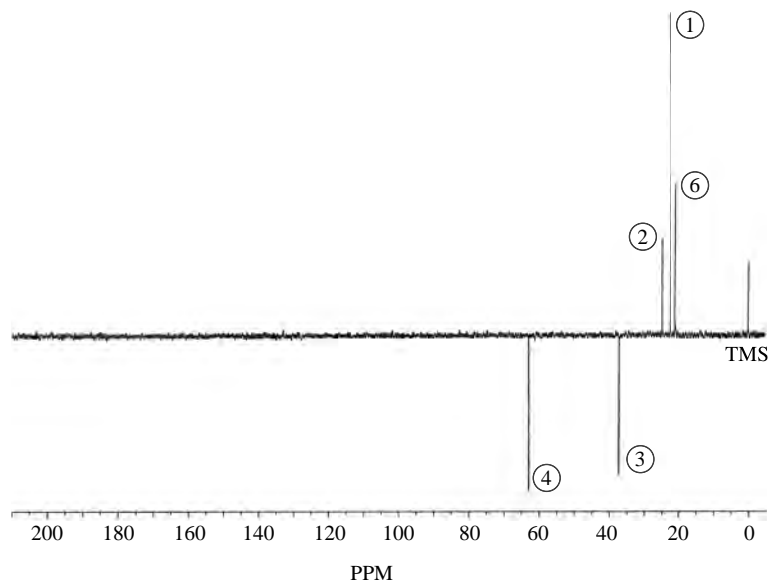

ISOPENTYL ACETATE IN CDCl$_3$—DEPT-135

FIGURE 10.10 DEPT-135 spectrum of isopentyl acetate.

The two equivalent methyl carbons (numbered **1**) can be seen as the tallest peak (at 22.3 ppm), while the methyl group on the acetyl function (numbered **6**) is a shorter peak at 20.8 ppm. The methine carbon (**2**) is a still smaller peak at 24.9 ppm. The methylene carbons produce the inverted peaks: carbon **3** appears at 37.1 ppm, and carbon **4** appears at 63.0 ppm. Carbon **4** is deshielded since it is near the electronegative oxygen atom. The carbonyl carbon (**5**) does not appear in the DEPT spectrum since it has no attached hydrogen atoms.

Clearly, the DEPT technique is a very useful adjunct to ^{13}C NMR spectroscopy. The results of the DEPT experiment can tell us whether a given peak arises from a carbon on a methyl group, a methylene group, or a methine group. By comparing the results of the DEPT spectrum with the original ^{1}H-decoupled ^{13}C NMR spectrum, we can also identify the peaks that must arise from quaternary carbons. Quaternary carbons, which bear no hydrogens, appear in the ^{13}C NMR spectrum but are missing in the DEPT spectrum.

Another example that demonstrates some of the power of the DEPT technique is the terpenoid alcohol **citronellol.**
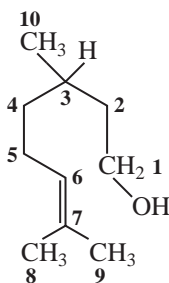
Figure 10.11 is the ^{1}H-decoupled ^{13}C NMR spectrum of citronellol. We can easily assign certain features of the spectrum to particular carbon atoms of the molecule by examining the chemical shifts and intensities. For example, the peak at 131 ppm is assigned to carbon 7, while the taller peak at 125 ppm must arise from carbon 6, which has an attached hydrogen. The pattern appearing between 15 and 65 ppm, however, is much more complex and thus more difficult to interpret.
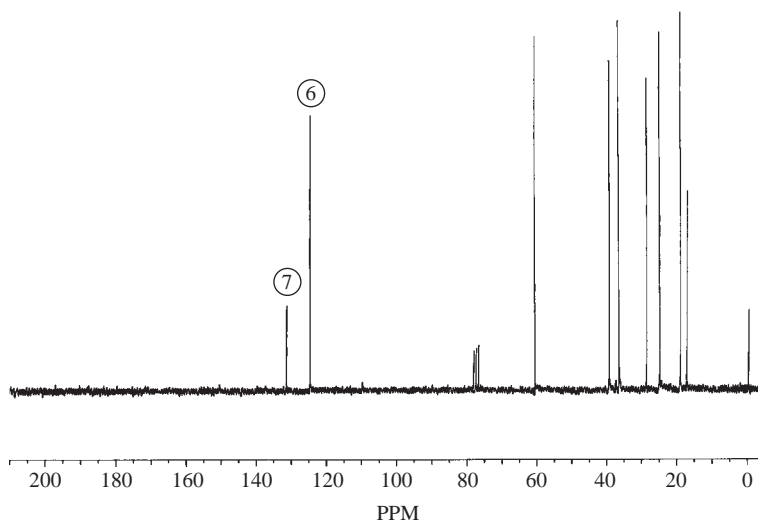
FIGURE 10.11 ^{13}C NMR spectrum of citronellol.
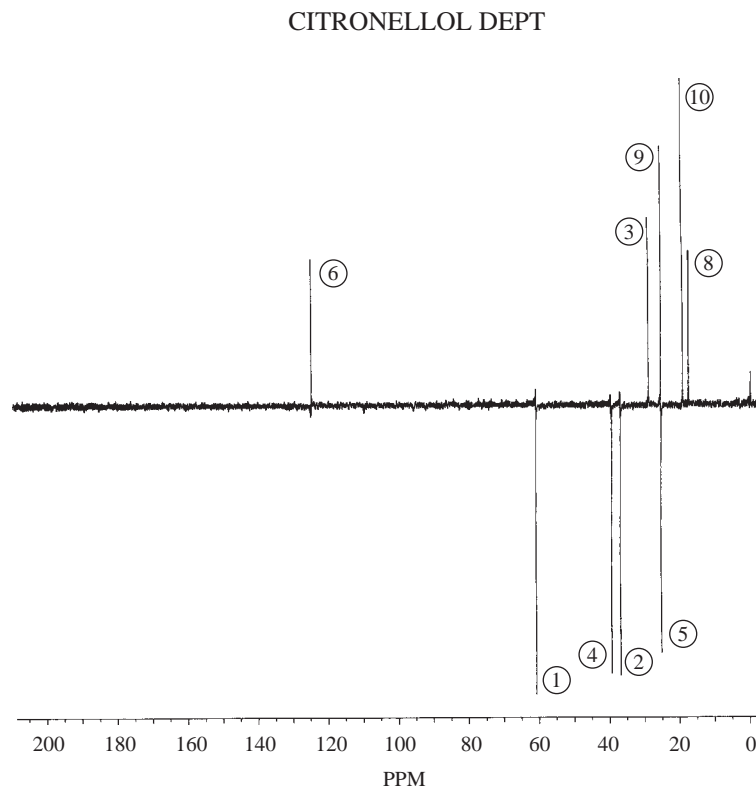
CITRONELLOL DEPT

FIGURE 10.12 DEPT-135 spectrum of citronellol.

The DEPT spectrum of citronellol (Fig. 10.12) makes the specific assignment of individual carbon atoms much easier.[2] Our earlier assignment of the peak at 125 ppm to carbon 6 is confirmed because that peak appears positive in the DEPT-135 spectrum. Notice that the peak at 131 ppm is missing in the DEPT spectrum since carbon 7 has no attached hydrogens. The peak at 61 ppm is negative in the DEPT-135 spectrum, indicating that it is due to a methylene group. Combining that information with our knowledge of the deshielding effects of electronegative elements enables us to assign this peak to carbon 1.

Shifting our attention to the upfield portion of the spectrum, we can identify the three methyl carbons since they appear at the highest values of magnetic field and give positive peaks in the DEPT-135 spectrum. We can assign the peak at 17 ppm to carbon 8 and the peak at 19 ppm to carbon 10 (see Footnote 2).

The most interesting feature of the spectrum of citronellol appears at 25 ppm. When we look carefully at the DEPT-135 spectrum, we see that this peak is actually *two* signals, appearing by coincidence at the same chemical shift value. The DEPT-135 spectrum shows clearly that one of the peaks is positive (corresponding to the methyl carbon at C9) and the other is negative (corresponding to the methylene carbon at C5).

We can assign the remaining peaks in the spectrum by noting that only one positive peak remains in the DEPT-135 spectrum. This peak must correspond to the methine position at C3 (30 ppm). The two remaining negative peaks (at 37 and 40 ppm) are assigned to the methylene carbons at C4 and C2. Without additional information, it is not possible to make a more specific assignment of these two carbons (see Problem 4).

---

[2] Other sources of information besides the DEPT spectrum were consulted in making these assignments (see the references and Problem 4).

These examples should give you an idea of the capabilities of the DEPT technique. It is an excellent means of distinguishing among methyl, methylene, methine, and quaternary carbons in a ^{13}C NMR spectrum.

Certain NMR instruments are also programmed to record the results of a DEPT experiment directly onto a proton-decoupled ^{13}C NMR spectrum. In this variation, called a **^{13}C NMR spectrum with multiplicity analysis**, each of the singlet peaks of a proton-decoupled spectrum is labeled according to whether that peak would appear as a singlet, doublet, triplet, or quartet if proton coupling were considered.

☐ 10.5 DETERMINING THE NUMBER OF ATTACHED HYDROGENS

The DEPT experiment is a modification of a basic NMR experiment called the **attached proton test** (**APT**) experiment. Although a detailed explanation of the theory underlying the DEPT experiment is beyond the scope of this book, an examination of a much simpler experiment (APT) should give you sufficient insight into the DEPT experiment so that you will understand how its results are determined.

This type of experiment uses two transmitters, one operating at the proton resonance frequency and the other at the ^{13}C resonance frequency. The proton transmitter serves as a proton decoupler; it is switched on and off at appropriate intervals during the pulse sequence. The ^{13}C transmitter provides the usual 90° pulse along the X' axis, but it can also be programmed to provide pulses along the Y' axis.

A. Methine Carbons (CH)

Consider a ^{13}C atom with one proton attached to it, where J is the coupling constant:

$$-\overset{|}{\underset{|}{C}}-H \qquad {}^1J_{CH}$$
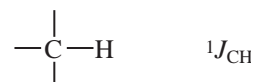
After a 90° pulse, the bulk magnetization vector **M** is directed along the Y' axis. The result of this simple experiment should be a single line since there is only one vector that is rotating at exactly the same frequency as the Larmor precessional frequency.

In this case, however, the attached hydrogen splits this resonance into a doublet. The resonance does not occur exactly at the Larmor frequency; rather, coupling to the proton produces *two* vectors. One of the vectors rotates $J/2$ Hz *faster* than the Larmor frequency, and the other vector rotates $J/2$ Hz *slower* than the Larmor frequency. One vector results from a coupling to the proton with its magnetic moment aligned with the magnetic field, and the other vector results from a coupling to the proton with its magnetic moment aligned against the magnetic field. The two vectors are separated in the rotating frame.
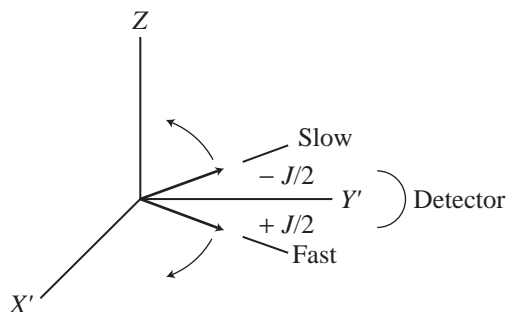
The vectors are moving relative to the rotating frame at a speed of $J/2$ revolutions per second but in opposite directions. The time required for one revolution is therefore the inverse of this speed or $2/J$ seconds per revolution. At time $\frac{1}{4}(2/J), = \frac{1}{2}J$ the vectors have made one-fourth of a revolution and are opposite each other along the X' axis. At this point, no signal is detected by the receiver because there is no component of magnetization along the Y' axis (the resultant of these two vectors is zero).
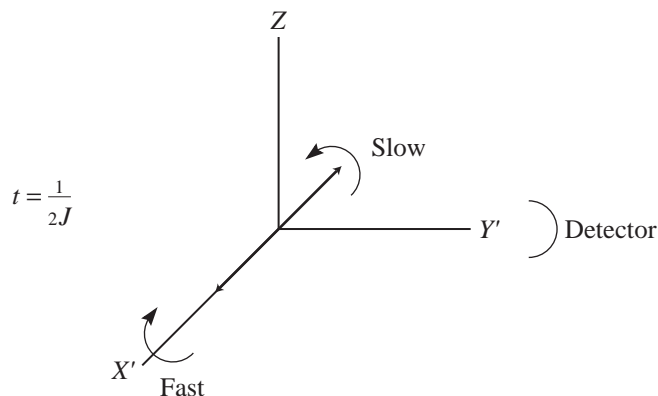
At time $\frac{1}{2}(2/J) = 1/J$, the vectors have realigned along the Y' axis but in the negative direction. An inverted peak would be produced if we collected signal at that time. So, if $t = 1/J$, a methine carbon should show an inverted peak.
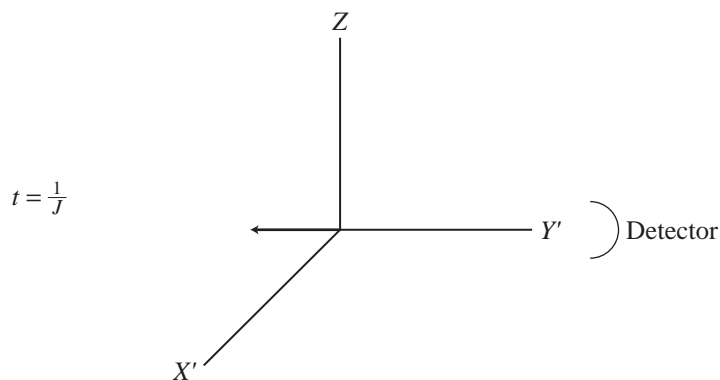
B.   Methylene Carbons (CH₂)

If we examine the fate of a ^{13}C atom with *two* attached protons, we find different behavior:

$$H - \overset{|}{\underset{|}{C}} - H \qquad {}^{1}J_{CH}$$
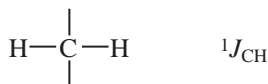
In this case, there are *three* vectors for the ^{13}C nucleus because the two attached protons split the ^{13}C resonance into a triplet. One of these vectors remains stationary in the rotating frame, while the other two move apart with a speed of J revolutions per second.
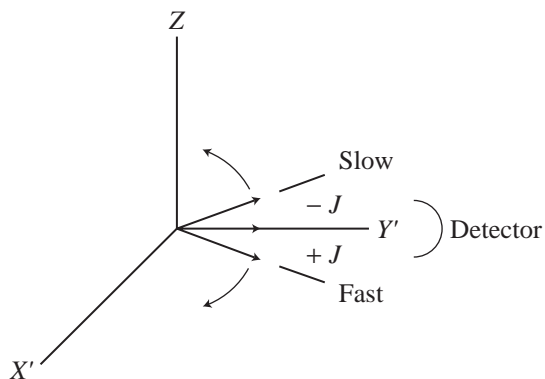
At time $\frac{1}{2}(1/J)$, the two moving vectors have realigned along the negative Y' axis,
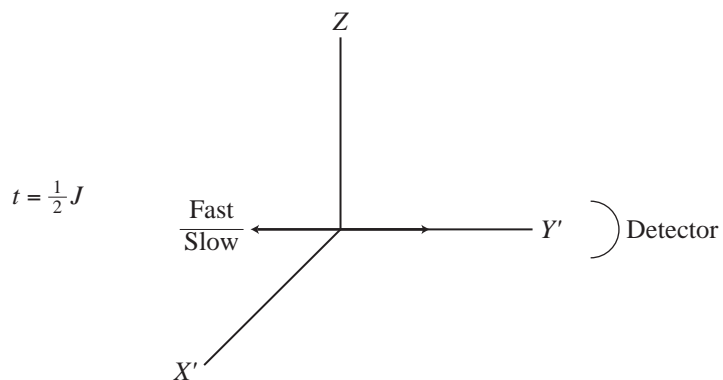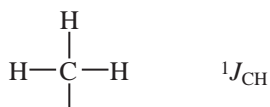

and at time $1/J$, they have realigned along the positive Y axis. The vectors thus produce a normal peak if they are detected at time $t = 1/J$. Therefore, a methylene carbon should show a normal (positive) peak.
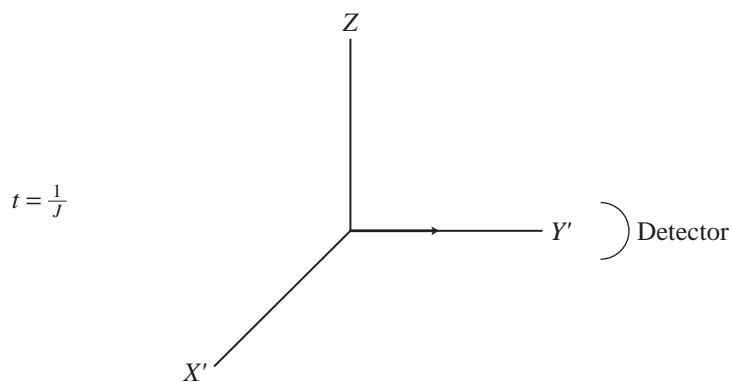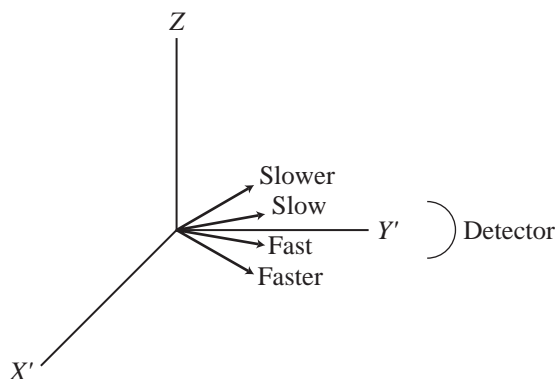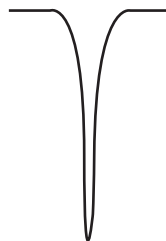
C.   Methyl Carbons (CH$_3$)

In the case of a methyl carbon,

$$H-\underset{|}{\overset{H}{\underset{|}{C}}}-H \qquad {}^1J_{CH}$$

there should be *four* vectors, corresponding to the four possible spin states of a collection of three hydrogen nuclei.

An analysis of the precessional frequencies of these vectors shows that after time $t = 1/J$, the methyl carbon should also show an inverted peak.

D.   Quaternary Carbons (C)

An unprotonated carbon simply shows one magnetization vector, which precesses at the Larmor frequency (i.e., it always points along the Y' axis). A normal peak is recorded at time $t = 1/J$.
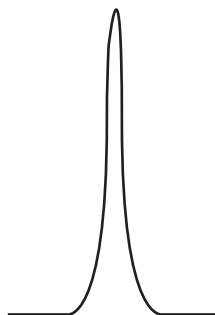
E.   The Final Result

In this type of experiment, we should see a normal peak for every quaternary carbon and methylene carbon and an inverted peak for every methine carbon and methyl carbon. We can thus tell whether the number of hydrogens attached to the carbon is *even* or *odd*.

In the form of this experiment known as the DEPT experiment, the pulse sequence is more complex than those described in the preceding paragraphs. By varying the pulse widths and delay times, it is possible to obtain separate spectra for methyl, methylene, and methine carbons. In the normal manner of presenting DEPT spectra (e.g., a DEPT-135 spectrum), the trace that combines the spectra of all these types of ^{13}C atoms is inverted from the presentation described for the attached proton test (APT). Therefore, in the spectra presented in Figures 10.10 and 10.12, carbon atoms that bear odd numbers of hydrogens appear as positive peaks, carbon atoms that bear even numbers of hydrogens appear as negative peaks, and unprotonated carbon atoms do not appear.

In the DEPT experiment, results similar to those described here for the APT experiment are obtained. A variety of pulse angles and delay times are incorporated into the pulse sequence. The result of the DEPT experiment is that methyl, methylene, methine, and quaternary carbons can be distinguished from one another.

☐ 10.6 INTRODUCTION TO TWO-DIMENSIONAL SPECTROSCOPIC METHODS

The methods we have described to this point are examples of one-dimensional experiments. In a **one-dimensional experiment,** the signal is presented as a function of a single parameter, usually the chemical shift. In a **two-dimensional experiment,** there are two coordinate axes. Generally, these axes also represent ranges of chemical shifts. The signal is presented as a function of each of these chemical shift ranges. The data are plotted as a grid; one axis represents one chemical shift range, the second axis represents the second chemical shift range, and the third dimension constitutes the magnitude (intensity) of the observed signal. The result is a form of contour plot in which contour lines correspond to signal intensity.

In a normal pulsed NMR experiment, the 90° **excitation pulse** is followed immediately by a **data acquisition phase** in which the FID is recorded and the data are stored in the computer. In experiments that use complex pulse sequences, such as DEPT, an **evolution phase** is included before data acquisition. During the evolution phase, the nuclear magnetization vectors are allowed to precess, and information may be exchanged between magnetic nuclei. In other words, a given nucleus may become encoded with information about the spin state of another nucleus that may be nearby.

Of the many types of two-dimensional experiments, two find the most frequent application. One of these is **H−H correlation spectroscopy,** better known by its acronym, **COSY.** In a COSY experiment, the chemical shift range of the proton spectrum is plotted on both axes. The second important technique is **heteronuclear correlation spectroscopy,** better known as the **HETCOR** technique. In a HETCOR experiment, the chemical shift range of the proton spectrum is plotted on one axis, while the chemical shift range of the ^{13}C spectrum for the same sample is plotted on the second axis.

☐ 10.7 THE COSY TECHNIQUE

When we obtain the splitting patterns for a particular proton and interpret it in terms of the numbers of protons located on adjacent carbons, we are using only one of the ways in which NMR spectroscopy can be applied to a structure proof problem. We may also know that a certain proton has two equivalent protons nearby that are coupled with a *J* value of 4 Hz, another nearby proton coupled with a *J* value of 10 Hz, and three others nearby that are coupled by 2 Hz. This gives a very rich

pattern for the proton we are observing, but we can interpret it, with a little effort, by using a tree diagram. Selective spin decoupling may be used to collapse or sharpen portions of the spectrum in order to obtain more direct information about the nature of coupling patterns. However, each of these methods can become tedious and very difficult with complex spectra. What is needed is a simple, unbiased, and convenient method for relating coupled nuclei.

A. An Overview of the COSY Experiment

The pulse sequence for a ^{1}H COSY experiment contains a variable delay time t_1 as well as an acquisition time t_2. The experiment is repeated with different values of t_1, and the data collected during t_2 are stored in the computer. The value of t_1 is increased by regular, small intervals for each experiment, so that the data that are collected consist of a series of FID patterns collected during t_2, each with a different value of t_1.

To identify which protons couple to each other, the coupling interaction is allowed to take place during t_1. During the same period, the individual nuclear magnetization vectors spread as a result of spin-coupling interactions. These interactions modify the signal that is observed during t_2. Unfortunately, the mechanism of the interaction of spins in a COSY experiment is too complex to be described completely in a simple manner. A pictorial description must suffice.

Consider a system in which two protons are coupled to each other:

$$-\overset{\displaystyle |}{\underset{\displaystyle H_a}{C}}-\overset{\displaystyle |}{\underset{\displaystyle H_x}{C}}-$$
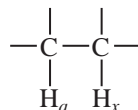
An initial relaxation delay and a pulse **prepare** the spin system by rotating the bulk magnetization vectors of the nuclei by 90°. At this point, the system can be described mathematically as a sum of terms, each containing the spin of only one of the two protons. The spins then **evolve** during the variable delay period (called t_1). In other words, they precess under the influences of both chemical shift and mutual spin–spin coupling. This precession modifies the signal that we finally observe during the acquisition time (t_2). In addition, mutual coupling of the spins has the mathematical effect of converting some of the single-spin terms to **products,** which contain the magnetization components of *both* nuclei. The product terms are the ones we will find most useful in analyzing the COSY spectrum.

Following the evolution period, a second 90° pulse is introduced; this constitutes the next essential part of the sequence, the **mixing period** (which we have not discussed previously). The mixing pulse has the effect of distributing the magnetization among the various spin states of the coupled nuclei. Magnetization that has been encoded by chemical shift during t_1 can be detected at another chemical shift during t_2. The mathematical description of the system is too complex to be treated here. Rather, we can say that two important types of terms arise in the treatment. The first type of term, which does not contain much information that is useful to us, results in the appearance of diagonal peaks in the two-dimensional plot. The more interesting result of the pulse sequences comes from the terms that contain the precessional frequencies of *both* coupled nuclei. The magnetization represented by these terms has been modulated (or "labeled") by the chemical shift of one nucleus during t_1 and, after the mixing pulse, by the precession of the other nucleus during t_2. The resulting off-diagonal peaks (**cross peaks**) show the correlations of pairs of nuclei by means of their spin–spin coupling. When the data are subjected to a Fourier transform, the resulting spectrum plot shows the chemical shift of the first proton plotted along one axis (f_1) and the chemical shift of the second proton plotted along the other axis (f_2). The existence of the off-diagonal peak that corresponds to the chemical shifts of both protons is *proof* of spin coupling between the two protons. If there had been no coupling, their magnetizations would not have given rise to off-diagonal peaks. In

the COSY spectrum of a complete molecule, the pulses are transmitted with short duration and high power so that all possible off-diagonal peaks are generated. The result is a complete description of the coupling partners in a molecule.

Since each axis spans the entire chemical shift range, something on the order of a thousand individual FID patterns, each incremented in t_1, must be recorded. With instruments operating at a high spectrometer frequency (high-field instruments), even more FID patterns must be collected. As a result, a typical COSY experiment may require about a half hour to be completed. Furthermore, since each FID pattern must be stored in a separate memory block in the computer, this type of experiment requires a computer with a large available memory. Nevertheless, most modern instruments are capable of performing COSY experiments routinely.

B. How to Read COSY Spectra

2-Nitropropane. To see what type of information a COSY spectrum may provide, we shall consider several examples of increasing complexity. The first is the COSY spectrum of 2-nitropropane. In this simple molecule, we expect to observe coupling between the protons on the two methyl groups and the proton at the methine position.

$$CH_3-\underset{\underset{NO_2}{|}}{CH}-CH_3$$
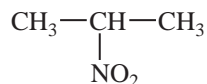
Figure 10.13 is the COSY spectrum of 2-nitropropane. The first thing to note about the spectrum is that the proton NMR spectrum of the compound being studied is plotted along both the horizontal and vertical axes, and each axis is calibrated according to the chemical shift values (in parts per million). The COSY spectrum shows distinct spots on a diagonal, extending from the upper right corner of the spectrum down to the lower left corner. By extending vertical and horizontal lines from each spot on the diagonal, you can easily see that each spot on the diagonal corresponds with the same peak on each coordinate axis. The diagonal peaks serve only as reference points. The important peaks in the spectrum are the **off-diagonal peaks.** In the spectrum of 2-nitropropane, we can extend a horizontal line from the spot at 1.56 ppm (which is labeled **A** and corresponds to the methyl protons). This horizontal line eventually encounters an off-diagonal spot **C** (at the upper left of the COSY spectrum) that corresponds to the methine proton peak at 4.66 ppm (labeled **B**). A vertical line drawn from this off-diagonal spot intersects the spot on the diagonal that corresponds to the methine proton (**B**). The presence of this off-diagonal spot **C**, which correlates the methyl proton spot and the methine proton spot, confirms that the methyl protons are coupled to the methine protons, as we would have expected. A similar result would have been obtained by drawing a vertical line from the 1.56-ppm spot (**A**) and a horizontal line from the 4.66-ppm spot (**B**). The two lines would have intersected at the second off-diagonal spot **D** (at the lower right of the COSY spectrum). The vertical and horizontal lines described in this analysis are drawn on the COSY spectrum in Figure 10.13.

Isopentyl Acetate. In practice, we would not require a COSY spectrum to fully interpret the NMR spectrum of 2-nitropropane. The preceding analysis illustrated how to interpret a COSY spectrum using a simple, easy-to-understand example. A more interesting example is the COSY spectrum of **isopentyl acetate** (Fig. 10.14).
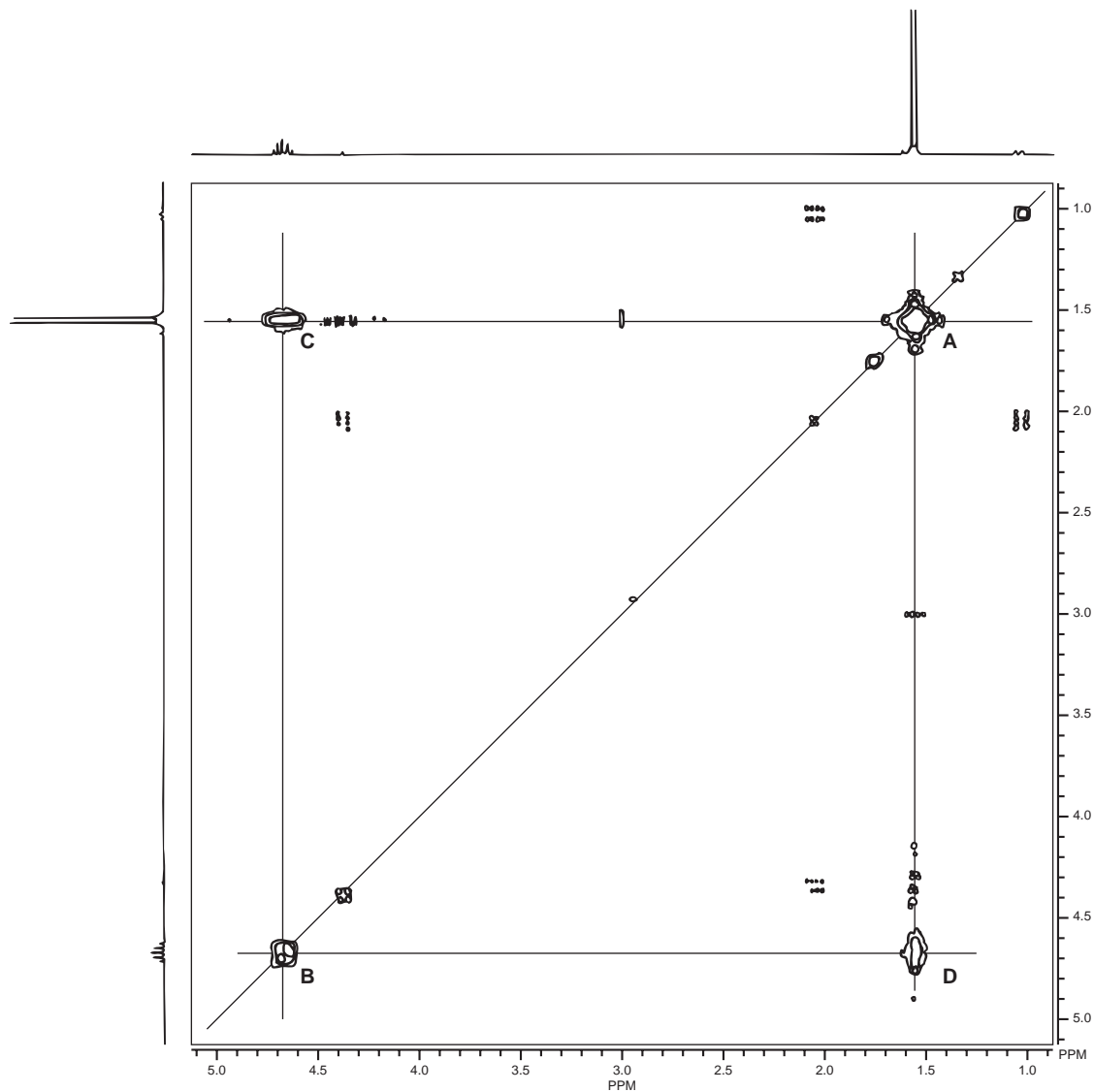
$$\overset{6}{CH_3}-\overset{\overset{O}{\|}}{\underset{5}{C}}-O-\overset{4}{CH_2}-\overset{3}{CH_2}-\underset{\underset{1}{\underset{|}{CH_3}}}{\overset{2}{CH}}-\overset{1}{CH_3}$$
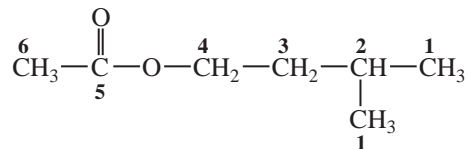
FIGURE 10.13 COSY spectrum of 2-nitropropane.

Again we see coordinate axes; the proton spectrum of isopentyl acetate is plotted along each axis. The COSY spectrum shows a distinct set of spots on a diagonal, with each spot corresponding to the same peak on each coordinate axis. Lines have been drawn to help you identify the correlations. In the COSY spectrum of isopentyl acetate, we see that the protons of the two equivalent methyl groups (**1**) correlate with the methine proton (**2**) at **A**. We can also see correlation between the two methylene groups (**3** and **4**) at **B** and between the methine proton (**2**) and the neighboring methylene (**3**) at **C**. The methyl group of the acetate moiety (**6**) does not show off-diagonal peaks because the acetyl methyl protons are not coupled to other protons in the molecule.

You may have noticed that each of the COSY spectra shown in this section contains additional spots besides the ones examined in our discussion. Often these "extra" spots have much lower intensities than the principal spots on the plot. The COSY method can sometimes detect interactions between nuclei over ranges that extend beyond three bonds. Besides this long-range coupling,
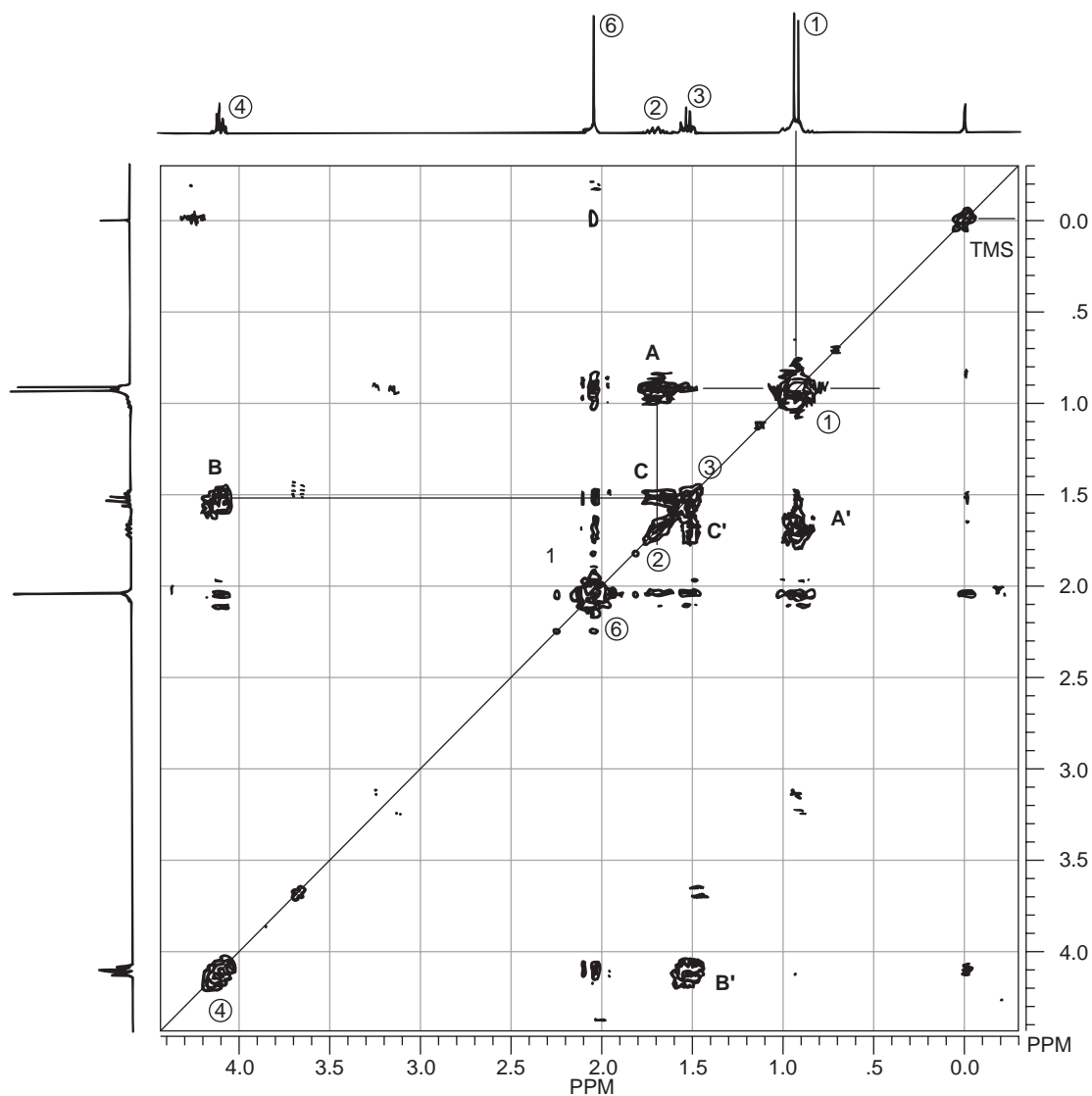
FIGURE 10.14 COSY spectrum of isopentyl acetate. Notice the paired symmetry (**AA′**, **BB′**, **CC′**) around the diagonal line.

nuclei that are several atoms apart but that are close together *spatially* also may produce off-diagonal peaks. We learn to ignore these minor peaks in our interpretation of COSY spectra. In some variations of the method, however, spectroscopists make use of such long-range interactions to produce two-dimensional NMR spectra that specifically record this type of information.

Citronellol. The COSY spectrum of citronellol (see the structural formula on p. 607) is a third example. The spectrum (Fig. 10.15) is rather complex in appearance. Nevertheless, we can identify certain important coupling interactions. Again, lines have been drawn to help you identify the correlations. The proton on C6 is clearly coupled to the protons on C5 at **A**. Closer examination of the spectrum also reveals that the proton on C6 is coupled through allylic (four-bond) coupling to the two methyl groups at C8 and C9 at **B**. The protons on C1 are coupled to two nonequivalent protons on C2 (at 1.4 and 1.6 ppm) at **C** and **D**. They are nonequivalent, owing to the presence of a
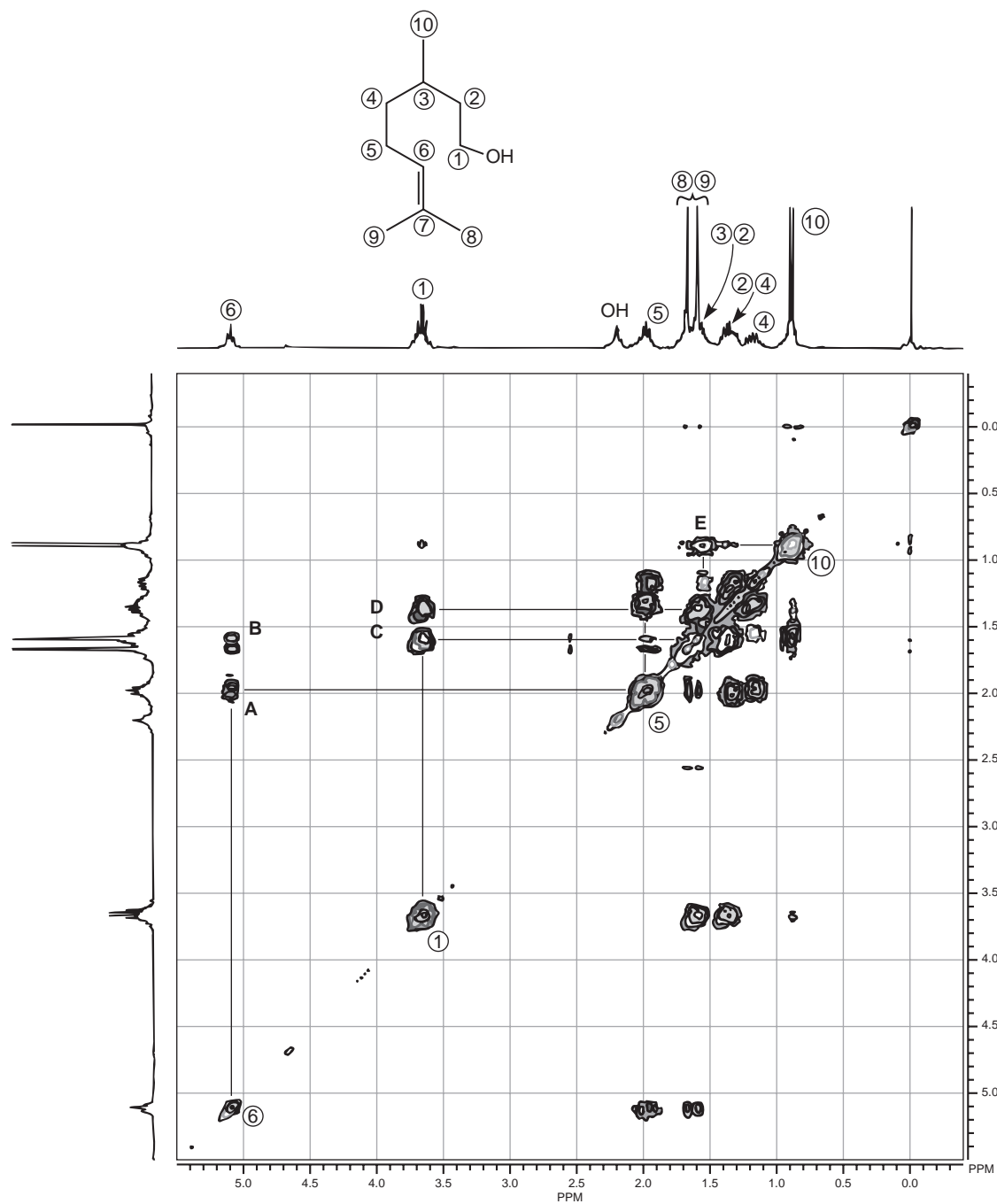
FIGURE 10.15 COSY spectrum of citronellol.

stereocenter in the molecule at C3. The splitting of the methyl protons at C10 by the methine proton at C3 at **E** can also be seen, although the C3 spot on the diagonal line is obscured by other spots that are superimposed on it. However, from the COSY spectrum we can determine that the methine proton at C3 must occur at the same chemical shift as one of the C8 or C9 methyl groups (1.6 ppm). Thus, a great deal of useful information can be obtained even from a complicated COSY pattern.

Pulsed field gradients were introduced in Section 10.3. The COSY method can be combined with the use of pulsed field gradients to produce a result that contains the same information as a COSY spectrum but that has much better resolution and can be obtained in a shorter time. This type of experiment is known as a **gradient-selected COSY** (sometimes known as a **gCOSY**). A gCOSY spectrum can be obtained in as little as 5 min; by contrast, a typical COSY spectrum requires as much as 40 min for data acquisition.

☐ 10.8 THE HETCOR TECHNIQUE

Protons and carbon atoms interact in two very important ways. First, they both have magnetic properties, and they can induce relaxation in one another. Second, the two types of nuclei can be spin-coupled to each other. This latter interaction can be very useful since directly bonded protons and carbons have a *J* value that is at least a power of 10 larger than nuclei related by two-bond or three-bond couplings. This marked distinction between orders of coupling provides us with a sensitive way of identifying carbons and protons that are directly bonded to one another.

To obtain a correlation between carbons and attached protons in a two-dimensional experiment, we must be able to plot the chemical shifts of the ^{13}C atoms along one axis and the chemical shifts of the protons along the other axis. A spot of intensity in this type of two-dimensional spectrum would indicate the existence of a C—H bond. The heteronuclear chemical shift correlation (HETCOR) experiment is designed to provide the desired spectrum.

A.   An Overview of the HETCOR Experiment

As we did in the COSY experiment, we want to allow the magnetization vectors of the protons to precess according to different rates, as dictated by their chemical shifts. Therefore, we apply a 90° pulse to the protons, then include an evolution time (t_1). This pulse tips the bulk magnetization vector into the $X'Y'$ plane. During the evolution period, the proton spins precess at a rate determined by their chemical shifts and the coupling to other nuclei (both protons and carbons). Protons bound to ^{13}C atoms experience not only their own chemical shifts during t_1 but also homonuclear spin coupling and heteronuclear spin coupling to the attached ^{13}C atoms. It is the interaction between ^1H nuclei and ^{13}C nuclei that produces the correlation that interests us. After the evolution time, we apply simultaneous 90° pulses to both the protons and the carbons. These pulses transfer magnetization from protons to carbons. Since the carbon magnetization was "labeled" by the proton precession frequencies during t_1, the ^{13}C signals that are detected during t_2 are modulated by the chemical shifts of the coupled protons. The ^{13}C magnetization can then be detected in t_2 to identify a particular carbon carrying each type of proton modulation.

A HETCOR experiment, like all two-dimensional experiments, describes the environment of the nuclei during t_1. Because of the manner in which the HETCOR pulse sequence has been constructed, the only interactions that are responsible for modulating the proton spin states are the proton chemical shifts and homonuclear couplings. Each ^{13}C atom may have one or more peaks appearing on the f_2 axis that correspond to its chemical shift. The proton chemical shift modulation causes the two-dimensional intensity of the proton signal to appear at an f_1 value that corresponds to the proton chemical shift. Further proton modulations of much smaller frequency arise from homonuclear (H—H) couplings. These provide fine structure on the peaks along the f_1 axis. We can interpret the fine structure exactly as we would in a normal proton spectrum, but in this case we understand that the proton chemical shift value belongs to a proton that is attached to a specific ^{13}C nucleus that appears at its own carbon chemical shift value.

We can thus assign carbon atoms on the basis of known proton chemical shifts, or we can assign protons on the basis of known carbon chemical shifts. For example, we might have a crowded proton spectrum but a carbon spectrum that is well resolved (or vice versa). This approach makes the

HETCOR experiment particularly useful in the interpretation of the spectra of large, complex molecules. An even more powerful technique is to use results from both the HETCOR and COSY experiments together.

B.   How to Read HETCOR Spectra

2-Nitropropane. Figure 10.16 is an example of a simple HETCOR plot. In this case, the sample substance is 2-nitropropane.

$$CH_3-CH-CH_3$$
$$|$$
$$NO_2$$
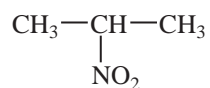
It is common practice to plot the proton spectrum of the compound being studied along one axis and the carbon spectrum along the other axis. Each spot of intensity on the two-dimensional plot indicates a carbon atom that bears the corresponding protons. In Figure 10.16, you should be able to see a peak corresponding to the methyl carbons, which appear at 21 ppm in the carbon spectrum (horizontal axis), and a peak at 79 ppm corresponding to the methine carbon. On the vertical axis, you should also
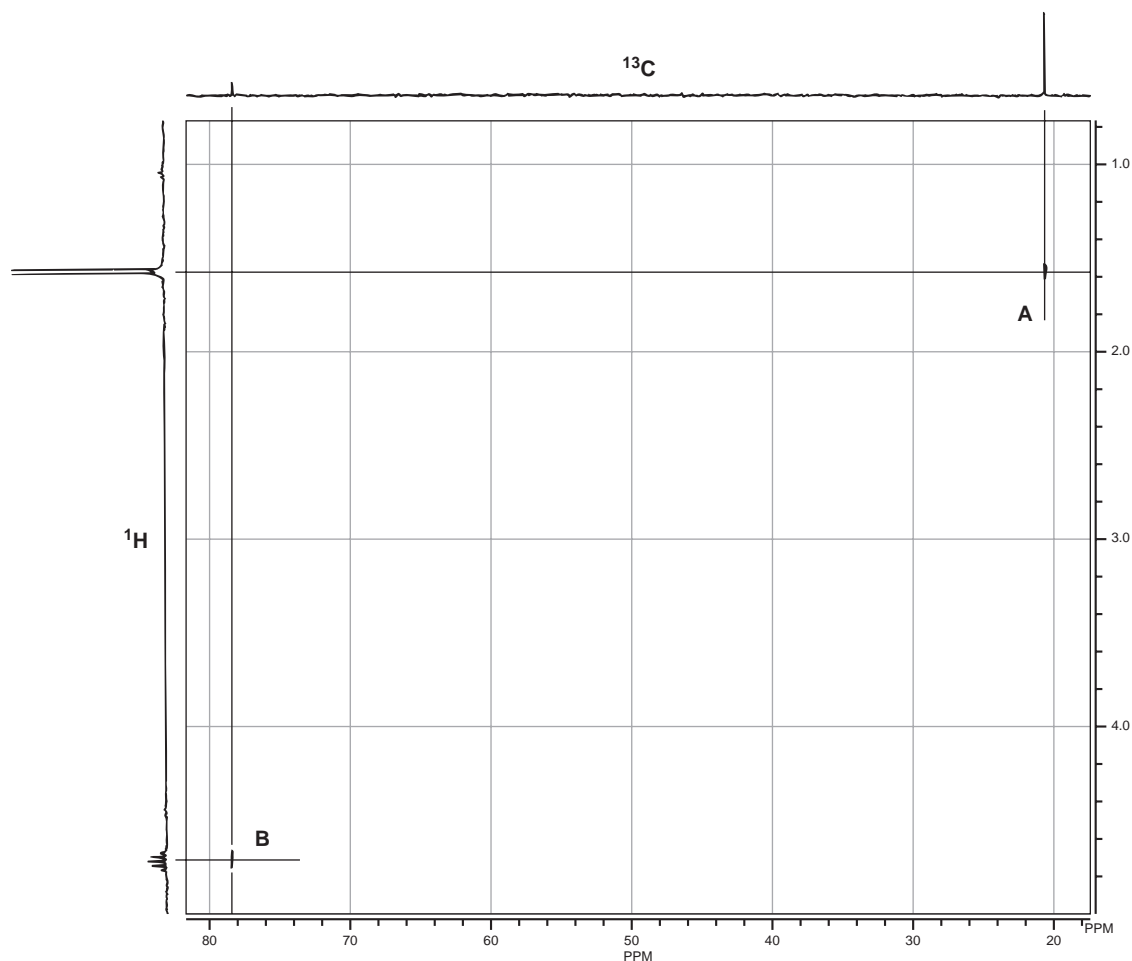
FIGURE 10.16 HETCOR spectrum of 2-nitropropane.

be able to find the doublet for the methyl protons at 1.56 ppm (proton spectrum) and a septet for the methine proton at 4.66 ppm. If you drew a vertical line from the methyl peak of the carbon spectrum (21 ppm) and a horizontal line from the methyl peak of the proton spectrum (1.56 ppm), the two lines would intersect at the exact point **A** on the two-dimensional plot where a spot is marked. This spot indicates that the protons at 1.56 ppm and the carbons at 21 ppm represent the same position of the molecule. That is, the hydrogens are attached to the indicated carbon. In the same way, the spot **B** in the lower left corner of the HETCOR plot correlates with the carbon peak at 79 ppm and the proton septet at 4.66 ppm, indicating that these two absorptions represent the same position in the molecule.

Isopentyl Acetate. A second, more complex example is isopentyl acetate. Figure 10.17 is the HETCOR plot for this substance.
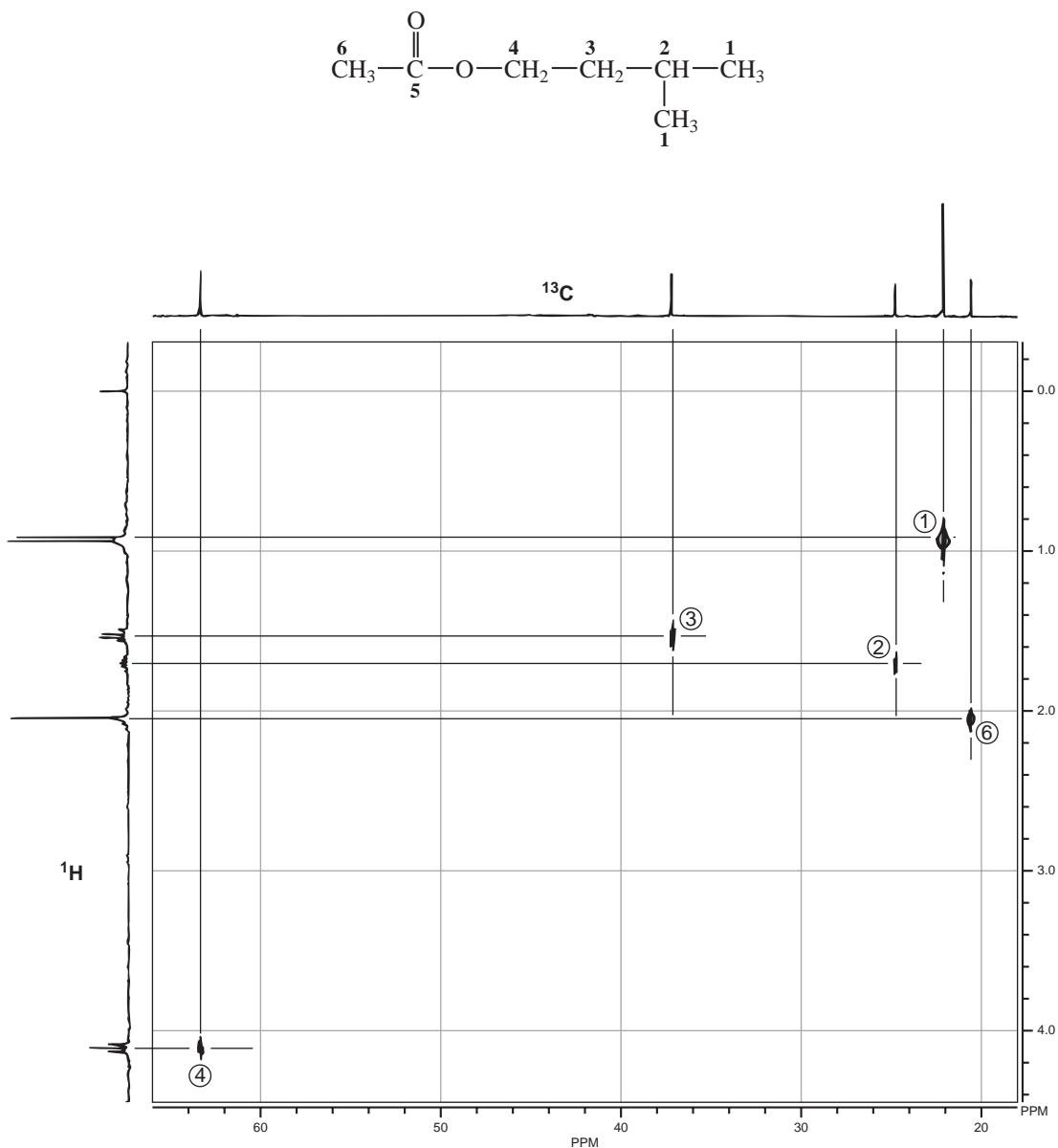
FIGURE 10.17 HETCOR spectrum of isopentyl acetate.

Each spot on the HETCOR plot has been labeled with a number, and lines have been drawn to help you see the correlations between proton peaks and carbon peaks. The carbon peak at 23 ppm and the proton doublet at 0.92 ppm correspond to the methyl groups (**1**); the carbon peak at 25 ppm and the proton multiplet at 1.69 ppm correspond to the methine position (**2**); and the carbon peak at 37 ppm and the proton quartet at 1.52 ppm correspond to the methylene group (**3**). The other methylene group (**4**) is deshielded by the nearby oxygen atom. Therefore, a spot on the HETCOR plot for this group appears at 63 ppm on the carbon axis and 4.10 ppm on the proton axis. It is interesting that the methyl group of the acetyl function (**6**) appears downfield of the methyl groups of the isopentyl group (**1**) in the proton spectrum (2.04 ppm). We expect this chemical shift since the methyl protons should be deshielded by the anisotropic nature of the carbonyl group. In the carbon spectrum, however, the carbon peak appears *upfield* of the methyl carbons of the isopentyl group. A spot on the HETCOR plot that correlates these two peaks confirms that assignment.

4-Methyl-2-Pentanol. Figure 10.18 is a final example that illustrates some of the power of the HETCOR technique for 4-methyl-2-pentanol. Lines have been drawn on the spectrum to help you find the correlations.
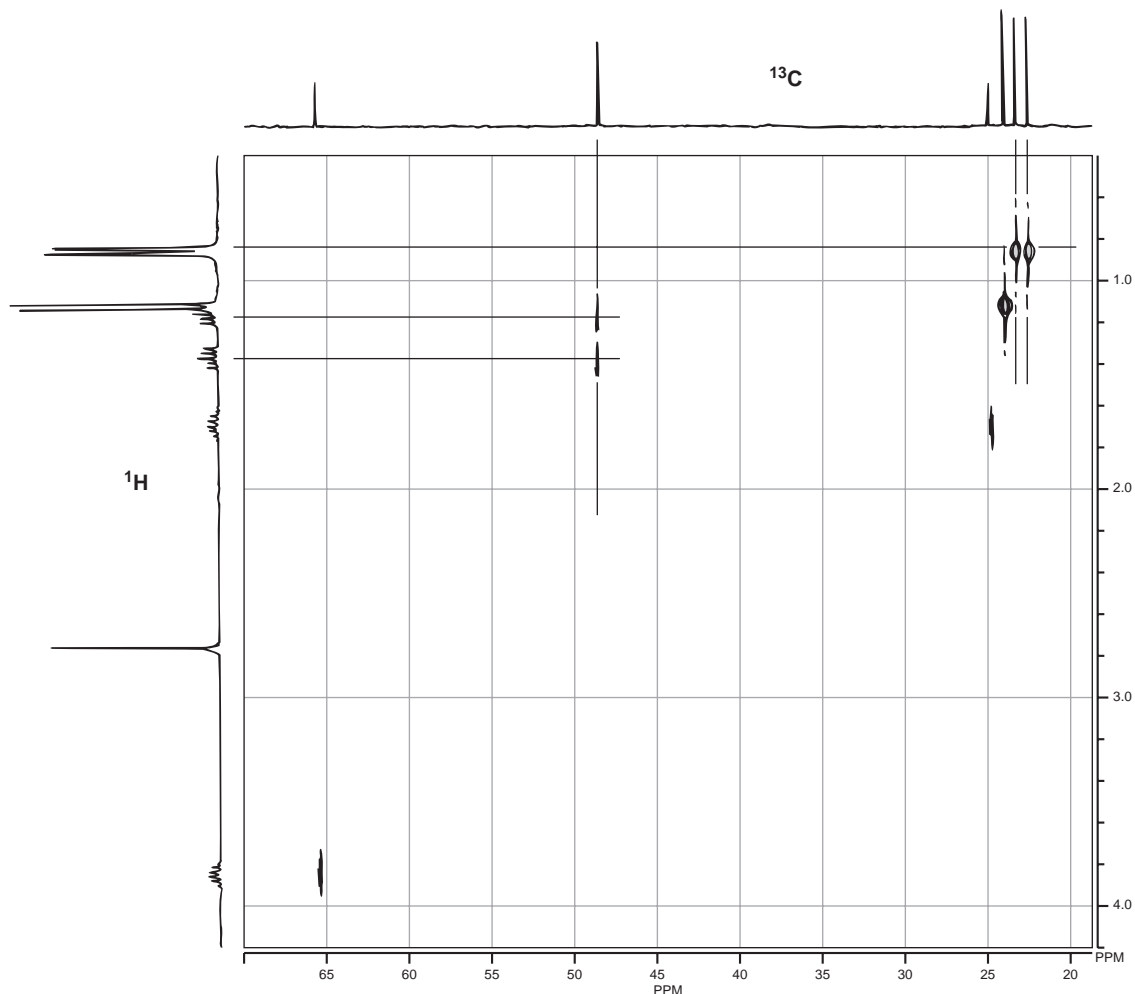
F I G U R E   1 0 . 1 8   HETCOR spectrum of 4-methyl-2-pentanol.

$$
\begin{array}{c}
\overset{5}{CH_3} \\
| \\
\overset{1}{CH_3} - \overset{2}{CH} - \overset{3}{CH_2} - \overset{4}{CH} - \overset{6}{CH_3} \\
| \\
OH
\end{array}
$$
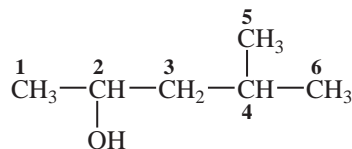
This molecule has a stereocenter at carbon 2. An examination of the HETCOR plot for 4-methyl-2-pentanol reveals *two* spots that correspond to the two methylene protons on carbon 3. At 48 ppm on the carbon axis, two contour spots appear, one at about 1.20 ppm on the proton axis and the other at about 1.40 ppm. The HETCOR plot is telling us that there are two non-equivalent protons attached to carbon 3. If we examine a Newman projection of this molecule, we find that the presence of the stereocenter makes the two methylene protons (**a** and **b**) non-equivalent (they are diastereotopic, see Section 5.4). As a result, they appear at different values of chemical shift.
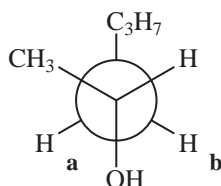
The *carbon* spectrum also reveals the effect of a stereocenter in the molecule. In the proton spectrum, the apparent doublet (actually it is a *pair* of doublets) at 0.91 ppm arises from the six protons on the methyl groups, which are labeled **5** and **6** in the preceding structure. Looking across to the right on the HETCOR plot, you will find two contour spots, one corresponding to 22 ppm and the other corresponding to 23 ppm. These two carbon peaks arise because the two methyl groups are also not quite equivalent; the distance from one methyl group to the oxygen atom is not quite the same as that from the other methyl group when we consider the most likely conformation for the molecule.

A great many advanced techniques can be applied to complex molecules. We have introduced only a few of the most important ones here. As computers become faster and more powerful, as chemists evolve their understanding of what different pulse sequences can achieve, and as scientists write more sophisticated computer programs to control those pulse sequences and treat data, it will become possible to apply NMR spectroscopy to increasingly complex systems.

☐ 10.9 INVERSE DETECTION METHODS

The NMR detection probe that is used for most heteronuclear experiments (such as the HETCOR experiment) is designed so that the receiver coils for the less-sensitive nucleus (the "insensitive" nucleus) are located closer to the sample than the receiver coils for the more sensitive (generally the ^1H) nucleus. This design is aimed at maximizing the signal that is detected from the insensitive nucleus. As was described in Chapter 4, owing to a combination of low natural abundance and a low magnetogyric ratio, a ^{13}C nucleus is about 6000 times more difficult to detect than a ^1H nucleus. A ^{15}N nucleus is also similarly more difficult to detect than a ^1H nucleus.

The difficulty with this probe design is that the initial pulse and the detection occur in the insensitive channel, while the evolution period is detected in the ^1H channel. The *resolution* that is possible, however, is much lower in the channel where the evolution of spins is detected. In the case of a

carbon–hydrogen correlation (a HETCOR), this means that the greatest resolution will be seen in the ^{13}C spectrum (in which every peak is a singlet), and the lowest resolution will be observed in the ^{1}H spectrum (in which maximum resolution is required). In effect, the *lowest* resolution is observed along the axis where the *greatest* resolution is required.

Within the past 10–15 years, the technology of probe design has advanced. Today, an instrument can be fitted with an **inverse detection** probe. In this design, the initial pulse and detection occurs in the ^{1}H channel, where the resolution is very high. The insensitive nucleus is detected during the evolution time of the pulse sequence, for which high resolution is generally not required. The result is a cleaner two-dimensional spectrum with high resolution. Examples of heteronuclear detection experiments that utilize an inverse detection probe are **heteronuclear multiple-quantum correlation** (HMQC) and **heteronuclear single-quantum correlation** (HSQC). Each of these techniques provides the same information that can be obtained from a HETCOR spectrum but is more suitable when the spectrum contains many peaks that are crowded close together. The improved resolution of the HMQC and HSQC experiments allows the spectroscopist to distinguish between two closely spaced peaks, whereas these peaks might overlap into one broadened peak in a HETCOR spectrum.

10.10 THE NOESY EXPERIMENT

The nuclear Overhauser effect was described in Chapter 4, Sections 4.5 and 4.6 (pp. 184–189). A two-dimensional NMR experiment that takes advantage of the nuclear Overhauser effect is nuclear Overhauser effect spectroscopy, or NOESY. Any ^{1}H nuclei that may interact with one another through a dipolar relaxation process will appear as cross peaks in a NOESY spectrum. This type of interaction includes nuclei that are directly coupled to one another, but it also includes nuclei that are not directly coupled but are located near to one another *through space*. The result is a two-dimensional spectrum that looks very much like a COSY spectrum but includes, besides many of the expected COSY cross peaks, additional cross peaks that arise from interactions of nuclei that interact through space. In practice, the nuclei must be within 5 Å of each other for this spatial interaction to be observed.

NOESY spectroscopy has become especially useful in the study of large molecules, such as proteins and polynucleotides. Very large molecules tend to tumble more slowly in solution, which means that nuclear Overhauser effect interactions have more time to develop. Small molecules tumble more quickly in solution; the nuclei move past one another too quickly to allow a significant development of dipolar interactions. The result is that NOESY cross peaks may be too weak to be observed.

Because the cross peaks in NOESY spectra arise from spatial interactions, this type of spectroscopy is particularly well suited to the study of configurations and conformations of molecules. The example of acetanilide demonstrates the capabilities of the NOESY experiment. The structural formula is shown, with the proton NMR chemical shifts of the relevant protons indicated.
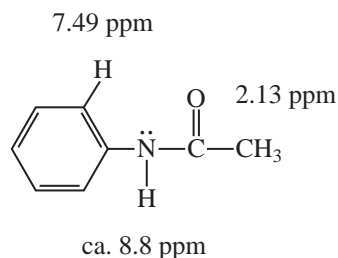
The problem to be solved is to decide which of two possible conformations is the more important for this molecule. The two conformations are shown, with circles drawn around the protons that are close to each other spatially and would be expected to show nuclear Overhauser interactions.

A   B
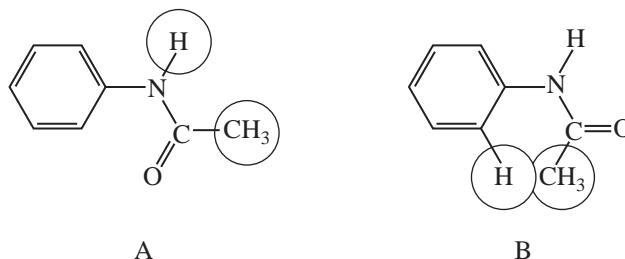
For conformation **A**, the N—H hydrogen is close to the methyl C—H hydrogens. We would expect to see a cross peak in the NOESY spectrum that correlates the N—H peak at 8.8 ppm with the C—H peak at 2.13 ppm. For conformation **B,** the protons that are close to each other are the methyl C—H protons and the *ortho* proton of the aromatic ring. For this conformation, we would expect to see a cross peak that correlates the aromatic proton at 7.49 ppm with the methyl protons at 2.13 ppm. When the actual spectrum is determined, one finds a weak cross peak that links the 8.8-ppm peak with the 2.13-ppm peak. This demonstrates clearly that the preferred conformation for acetanilide is **A.**

Certainly, when one considers solving the three-dimensional structure of a complex molecule such as a polypeptide, the challenge of assigning every peak and every cross peak becomes formidable. Nevertheless, the combination of COSY and NOESY methods finds wide application in the determination of the structures of biomolecules.

10.11 MAGNETIC RESONANCE IMAGING

The principles that govern the NMR experiments described throughout this textbook have begun to find application in the field of medicine. A very important diagnostic tool in medicine is a technique known as **magnetic resonance imaging (MRI).** In the space of only a few years, MRI has found wide use in the diagnosis of injuries and other forms of abnormality. It is quite common for sports fans to hear of a football star who has sustained a knee injury and had it examined via an MRI scan.

Typical magnetic resonance imaging instruments use a superconducting magnet with a field strength on the order of 1 Tesla. The magnet is constructed with a very large inner cavity so that an entire human body can fit inside. A transmitter–receiver coil (known as a **surface coil**) is positioned outside the body, near the area being examined. In most cases, the ^{1}H nucleus is the one studied since it is found in the water molecules that are present in and around living tissue. In a manner somewhat analogous to that used for an X-ray-based CAT (computerized axial tomography) scan, a series of planar images is collected and stored in the computer. The planar images can be obtained from various angles. When the data have been collected, the computer processes the results and generates a three-dimensional picture of the proton density in the region of the body under study.

The ^{1}H nuclei of water molecules that are not bound within living cells have a relaxation time different from the nuclei of water molecules bound within tissue. Water molecules that appear in a highly ordered state have relaxation times shorter than water molecules that appear in a more random state. The degree of ordering of water molecules within tissues is greater than that of water molecules that are part of the fluid flowing within the body. Furthermore, the degree of ordering of water

FIGURE 10.19 MRI scan of a skull showing soft tissues of the brain and eyes.

molecules may be different in different types of tissue, especially in diseased tissue as compared with normal tissue. Specific pulse sequences detect these differences in relaxation time for the protons of water molecules in the tissue being examined. When the results of the scans are processed, the image that is produced shows different densities of signals, depending on the degree to which the water molecules are in an ordered state. As a result, the "picture" that we see shows the various types of tissue clearly. The radiologist can then examine the image to determine whether any abnormality exists.

As a brief illustration of the type of information that can be obtained from MRI, consider the image in Figure 10.19. This is a view of the patient's skull from the spinal column, looking toward the top of the patient's head. The light-colored areas represent the locations of soft tissues of the brain. Because bone does not contain a very high concentration of water molecules, the MRI image provides only a somewhat dim view of the bones of the spinal column. The two bulbous features at the top of the image are the person's eyes.

Figure 10.20 is another MRI scan of the same patient shown in Figure 10.19. On the left side of the image is an area that appears brightly white. This patient has suffered an **infarct,** an area of dying tissue resulting from an obstruction of the blood vessels supplying that part of the brain. In other words, the patient has had a stroke, and the MRI scan has clearly shown exactly where this lesion has occurred. The physician can use very specific information of this type to develop a plan for treatment.

The MRI method is not limited to the study of water molecules. Pulse sequences designed to study the distribution of lipids are also used.

The MRI technique has several advantages over conventional X-ray or CAT scan techniques; it is better suited for studies of abnormalities of soft tissue or of metabolic disorders. Furthermore, unlike other diagnostic techniques, MRI is noninvasive and painless, and it does not require the patient to be exposed to large doses of X-rays or radioisotopes.
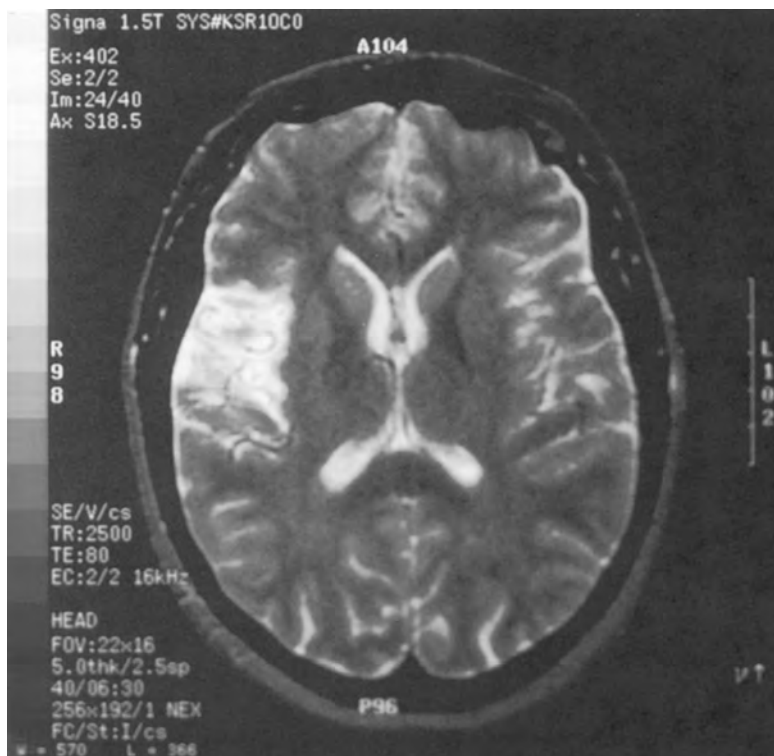
F I G U R E   1 0 . 2 0   MRI scan of a skull showing the presence of an infarct.

10.12 SOLVING A STRUCTURAL PROBLEM USING COMBINED 1-D AND 2-D TECHNIQUES

This section shows you how to solve a structural problem using the various spectroscopic techniques. We will make use of ^{1}H, ^{13}C, HETCOR (gHSQC), COSY, and DEPT NMR techniques. We will also make use of infrared spectroscopy to solve the structure of this example.

A.   Index of Hydrogen Deficiency and Infrared Spectrum

The compound has a formula $C_6H_{10}O_2$. Your first order of business should be to calculate the index of hydrogen deficiency, which is 2. Let's now look at the infrared spectrum shown in Figure 10.21 to determine the types of functional groups present that would be consistent with an index of 2. The spectrum shows a strong C=O peak at 1716 and a strong peak at 1661 cm^{-1} for a C=C. Even though the C=O peak appears near the expected value for a ketone, the presence of the C=C is more likely to indicate that the compound is a conjugated ester with the C=O stretch shifted from the normal 1735-cm^{-1} value found in unconjugated esters to the lower value due to resonance with the double bond. The strong C—O bands in the region of 1350 to 1100 cm^{-1} would support the idea of an ester. The out-of-plane C—H bending patterns shown in Figure 2.22 on p. 42 may be useful to help decide the type of substitution on the C=C bond. For example, the band at 970 cm^{-1} would indicate a *trans* double bond. Notice that a weak peak appears at 3054 cm^{-1}, indicating the presence of a sp^2 C—H bond. The other C—H stretching bonds below 3000 cm^{-1} indicate sp^3 C—H bonds.
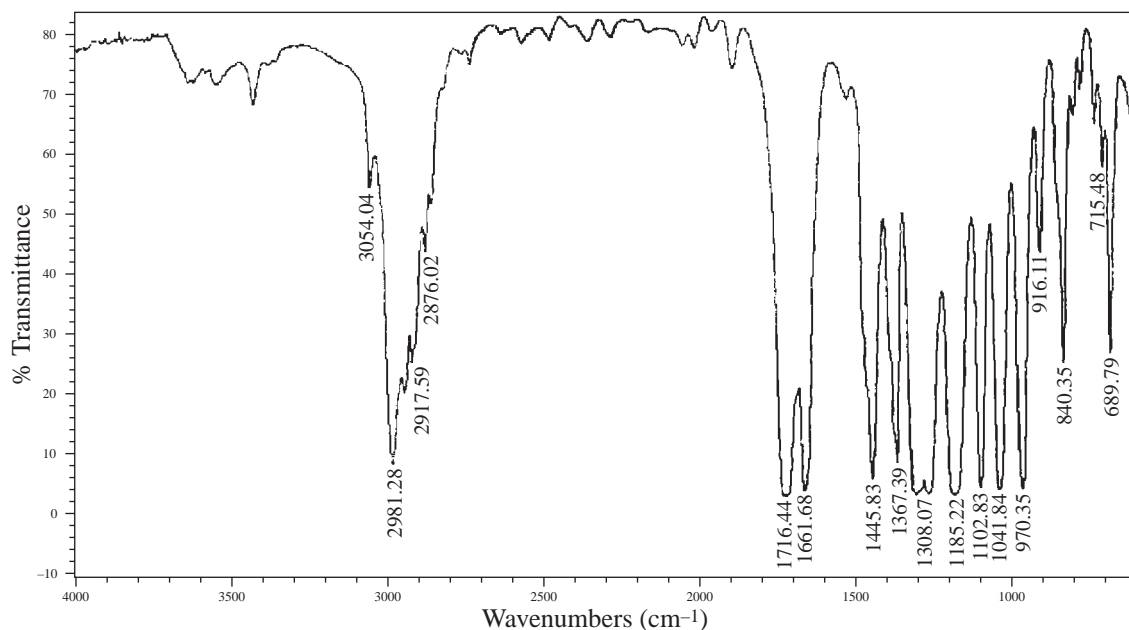
FIGURE 10.21 Infrared spectrum of $C_6H_{10}O_2$.

B. Carbon-13 NMR Spectrum

Next, look at the proton decoupled ^{13}C spectrum shown in Figure 10.22 on p. 618. Notice that there are six peaks in the spectrum matching the six carbons in the formula. Read Section 4.16 starting on p. 206 to determine how to make use of the ^{13}C spectrum. Three of the peaks appear to the right of the solvent peaks ($CDCl_3$) and represent sp^3 carbon atoms. The peak at about 60 ppm suggests a carbon atom attached to an electronegative oxygen atom. Three peaks appear to the left of the solvent peak. Two of them, appearing at about 122 and 144 ppm, are for sp^2 carbon atoms in the C=C bond. The remaining carbon peak at about 166 can be assigned to the C=O carbon atom.

C. DEPT Spectrum

The DEPT spectrum is shown in Figure 10.23 on p. 618. The beauty of this experiment is that it tells you the number of protons attached to each carbon atom. The type of presentation shown here is different from the type of DEPT presentation shown in Figures 10.10 and 10.12 and Figure 4.9 on p. 194. The plot shown in Figure 10.23 shows the methyl, methylene, and methine carbons on the first three lines as positive peaks. The bottom trace shows all protonated carbon atoms. Carbon atoms without attached protons will not appear in a DEPT spectrum. Thus, the plot does not show the C=O carbon atom because there are no attached protons. However, we know from the normal ^{13}C NMR spectrum that a peak appears at 166.4 ppm and this must be the C=O carbon atom. Notice that the $CDCl_3$ solvent does not appear in the DEPT spectrum but does appear in the normal ^{13}C NMR spectrum as a three-line pattern centering on about 77 ppm. From the DEPT experiment, you can conclude that there are two methyl carbons, appearing at 14.1 and 17.7 ppm. There is one methylene carbon appearing at 59.9 ppm (—O—CH_2—) and two methine carbons for the C=C bond that appear downfield at 122.6 and 144.2 ppm. We now know that the compound is a disubstituted
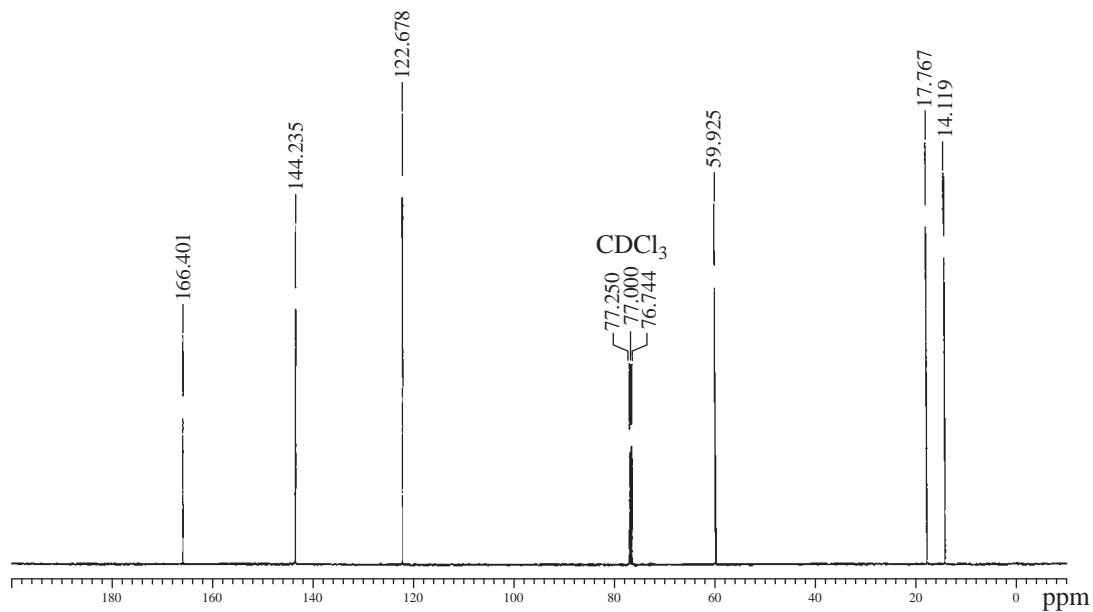
FIGURE 10.22 ^{13}C NMR spectrum for $C_6H_{10}O_2$.
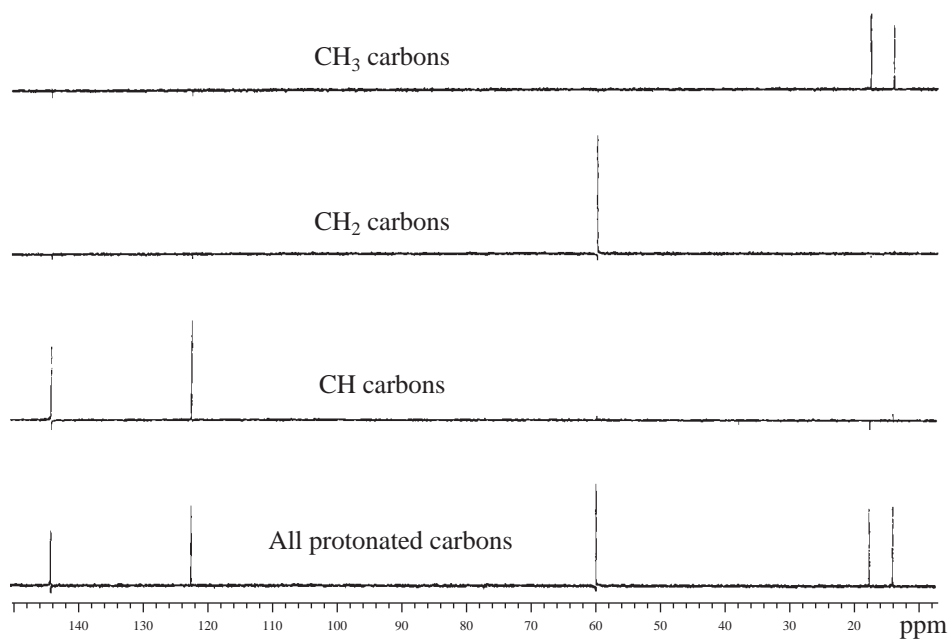
FIGURE 10.23 DEPT spectrum for $C_6H_{10}O_2$.

alkene, which confirms the IR results. Making use of the IR, ^{13}C NMR, and DEPT experiments yields the following structure:
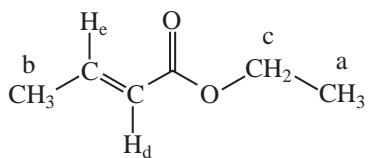
D. Proton NMR Spectrum

The proton spectrum is shown in Figure 10.24. The integral values need to be determined by using the numbers below the peaks. The 10 protons in the spectrum integrate as follows: 1:1:2:3:3. The protons of special interest are shown as expansions in Figure 10.25. The signal centered on 6.97 ppm is a doublet of quartets. What is most apparent is that there is a pair of overlapping quartets (the right-hand quartet is shaded so that you can more easily see the patterns). The doublet part of the pattern results from a vinyl proton H_e being split by the *trans*-proton H_d into a doublet, $^3J_{trans}$. The peaks are numbered on the expansion in Figure 10.25, counting from left to right. In effect the coupling constant for the doublet can be derived by subtracting the Hertz value for the center of the right quartet from the Hertz value for the center of the left quartet. It turns out that it is easier to simply subtract the Hertz value for line 6 from the Hertz value on line 2 or subtracting the value for line 7 from line 3. The averaged value is $^3J = 15.3$ Hz. Also, one can calculate the coupling constant for the quartet part of the pattern that results from the coupling between the vinyl proton H_e and the methyl protons H_b. This is calculated by subtracting the value on line 2 from line 1, line 3 from 2, and so on, yielding an average value of $^3J = 7.1$ Hz. The overall pattern is described as a doublet of quartets, with a $^3J = 15.3$ and 7.1 Hz.

The other vinyl proton (H_d) centered on 5.84 ppm can also be described as a doublet of quartets. In this case, it is much more obvious that it is a doublet of quartets than for the pattern at 6.97 ppm. The Hertz values for peaks in the quartets yield an average value for $^4J = 1.65$ Hz resulting from the long-range coupling between H_d and H_b. The remaining coupling constant for H_d to H_e can be derived by subtracting 2908.55 Hz from 2924.14 Hz, yielding a value for $^3J_{trans} = 15.5$ Hz. This value agrees within experimental error with the $^3J_{trans}$ obtained from the proton at 6.97 ppm, discussed above.

The methyl group (H_b) appearing at 1.87 ppm is a doublet of doublets. The coupling between proton H_b and H_e is calculated by subtracting 931.99 from 939.08 Hz, $^3J = 7.1$ Hz. Notice that this is the same value that was obtained above for H_e. The average value for the distances in Hertz between the smaller peaks yields $^4J = 1.65$ Hz. This value is identical to the one obtained above for H_d.

Finally, the triplet at about 1.3 ppm is assigned to the methyl group (H_a) split by the neighboring methylene group (H_c). In turn, the quartet at about 4.2 results from the coupling to the neighboring methyl group (H_a).
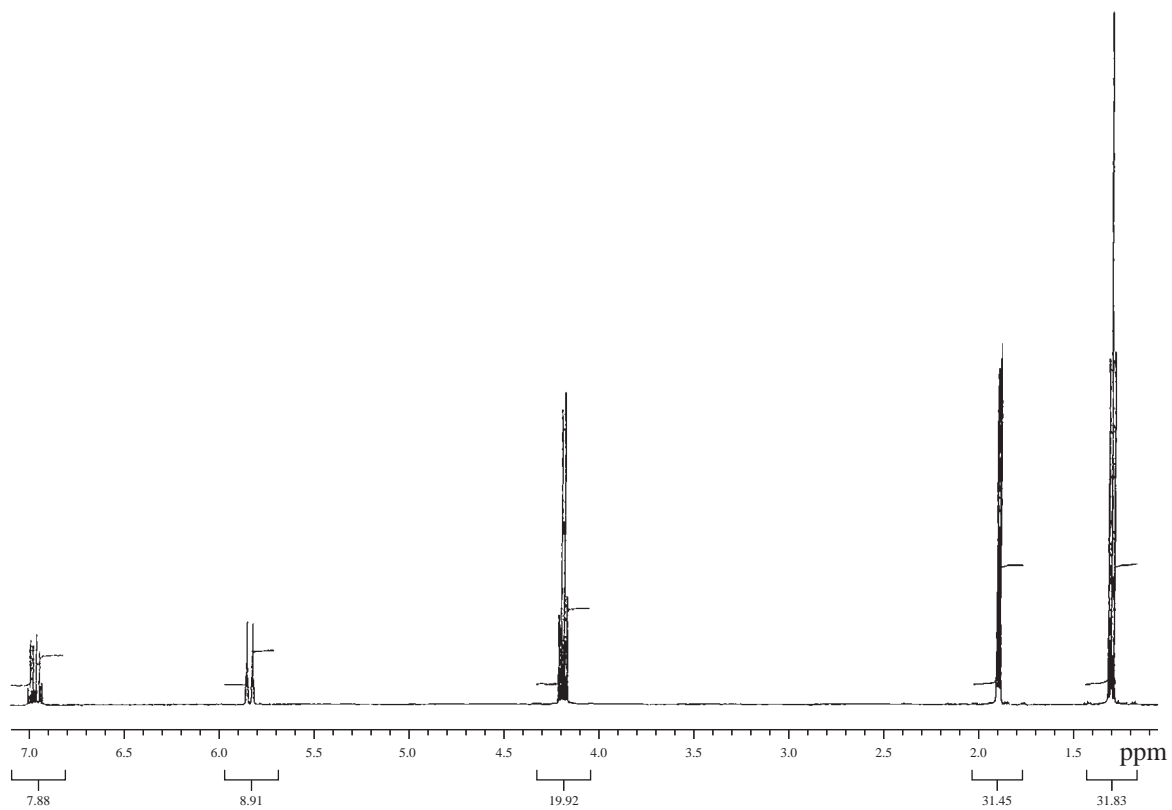
FIGURE 10.24 ^1H (proton) NMR spectrum for $C_6H_{10}O_2$.
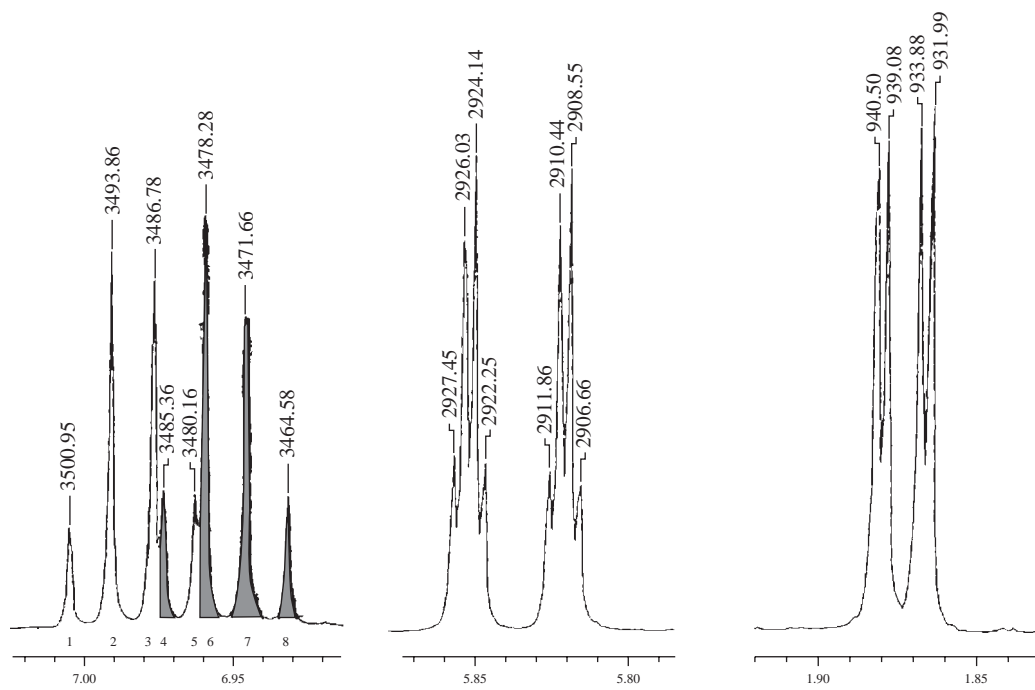
FIGURE 10.25 Proton NMR expansions for $C_6H_{10}O_2$.

E.   COSY NMR Spectrum

The COSY spectrum is shown in Figure 10.26. A COSY spectrum is an **$^1H-^1H$ correlation** with the proton NMR spectrum plotted on both axes. It helps to confirm that we have made the right assignments for the coupling of neighboring protons in this example: ^3J and ^4J. Following the lines drawn on the spectrum, we see that proton H_a correlates to proton H_c in the ethyl group. We also see that proton H_b correlates to both H_d and H_e. Proton H_d correlates to both H_e and H_b. Finally, proton H_e correlates to both H_d and H_b. Life is very good!
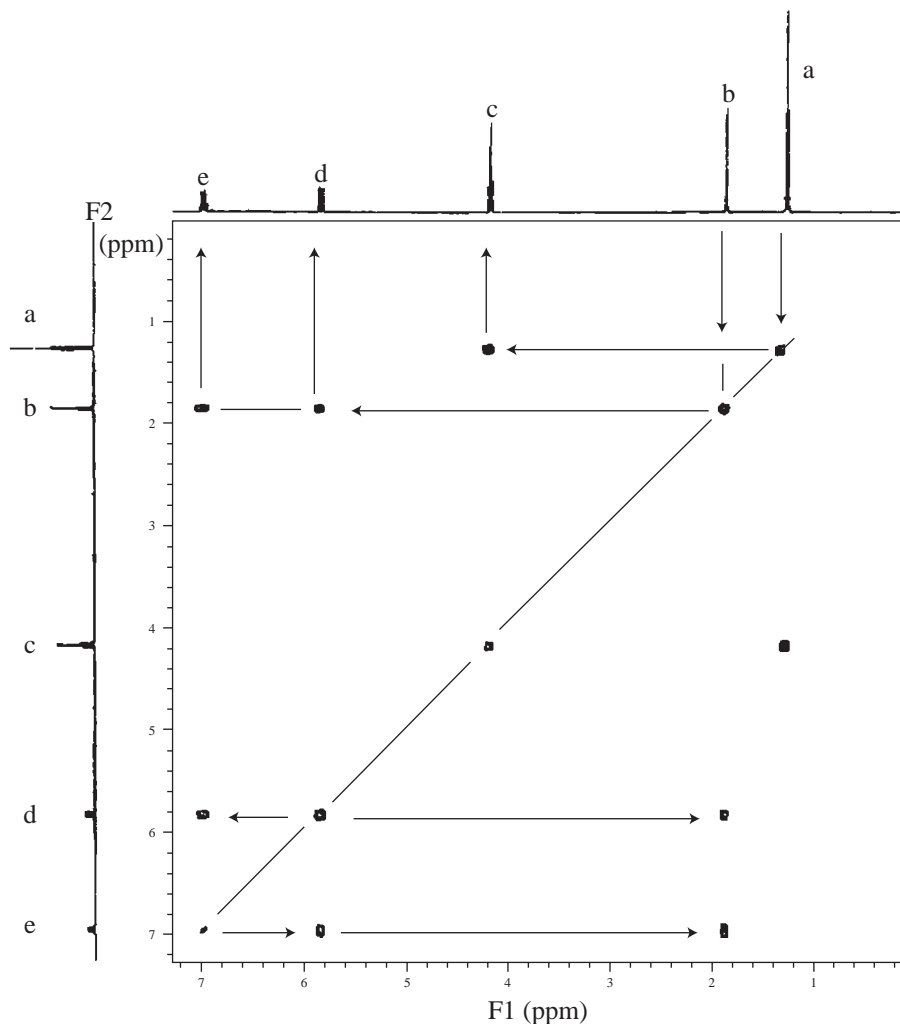
FIGURE 10.26 H—H correlation (COSY) spectrum for $C_6H_{10}O_2$.

F.   HETCOR (HSQC) NMR Spectrum

The HETCOR (HSQC) spectrum is shown in Figure 10.27. This type of spectrum is a **^{13}C–H correlation** with the ^{13}C NMR spectrum and the ^{1}H NMR spectrum plotted on the two axes. The purpose of this experiment is to assign each of the ^{13}C peaks to the corresponding proton patterns. The results support the conclusions already made about the assignments. No surprises here!
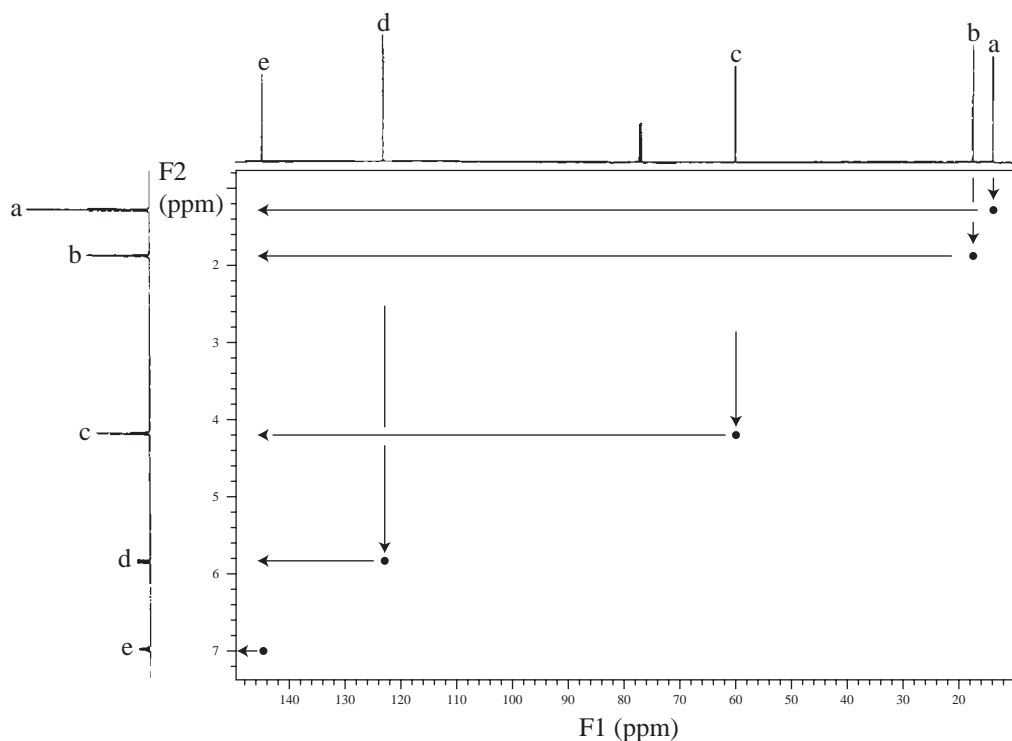
F I G U R E   1 0 . 2 7   C–H correlation (HETCOR/HSQC) spectrum for $C_6H_{10}O_2$.

P R O B L E M S

*1. Using the following set of DEPT-135, COSY, and HETCOR spectra, provide a complete assignment of all protons and carbons for C_4H_9Cl.

PPM
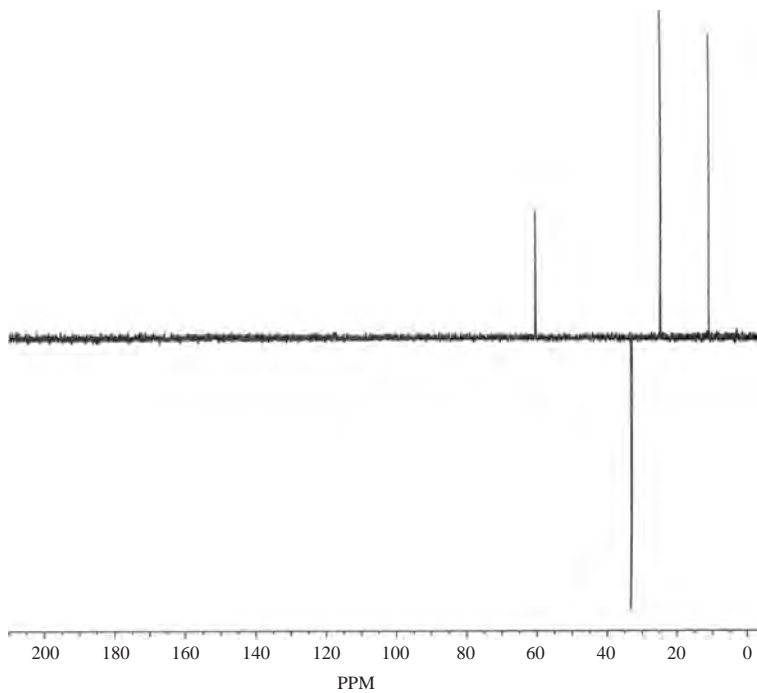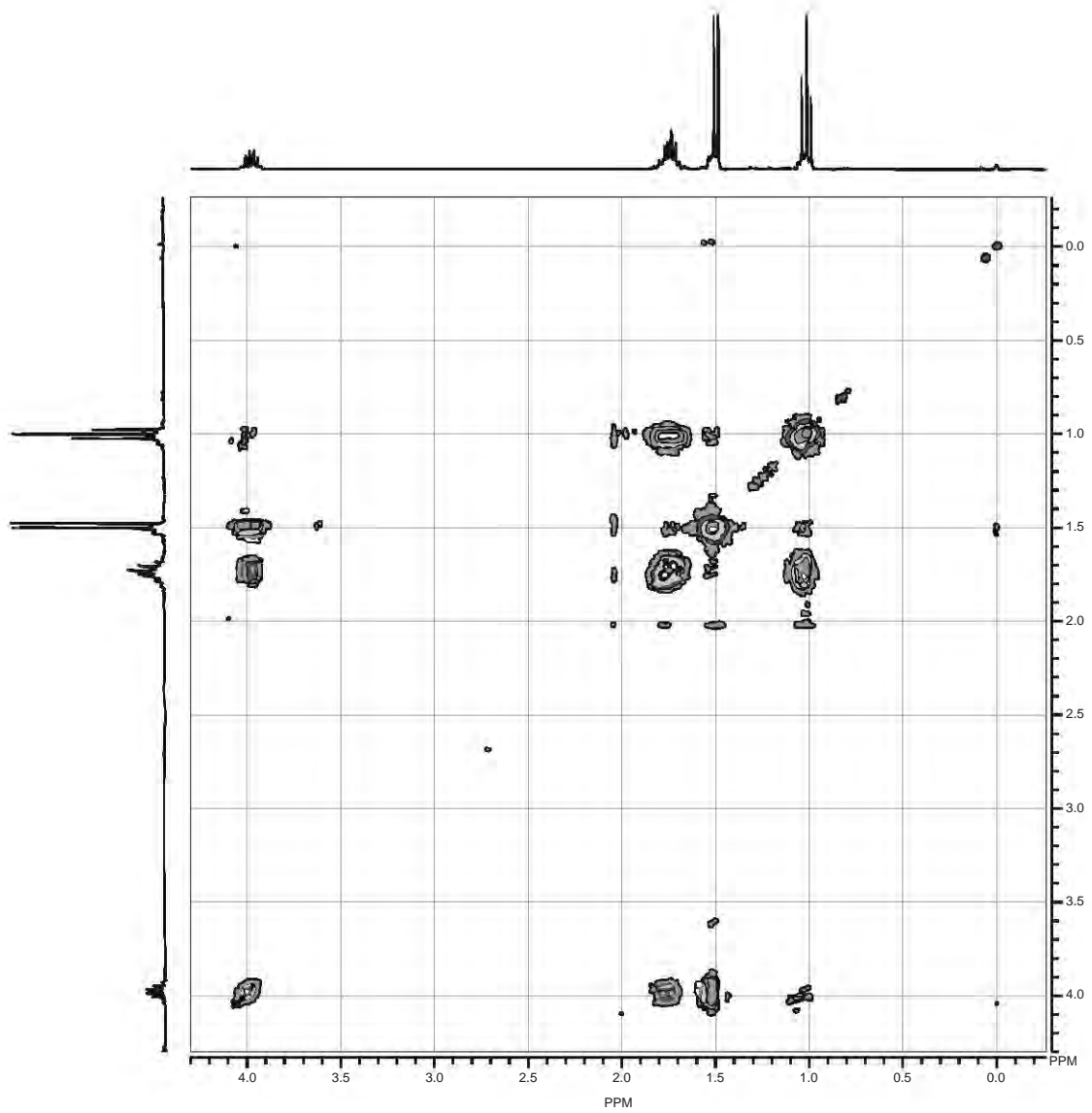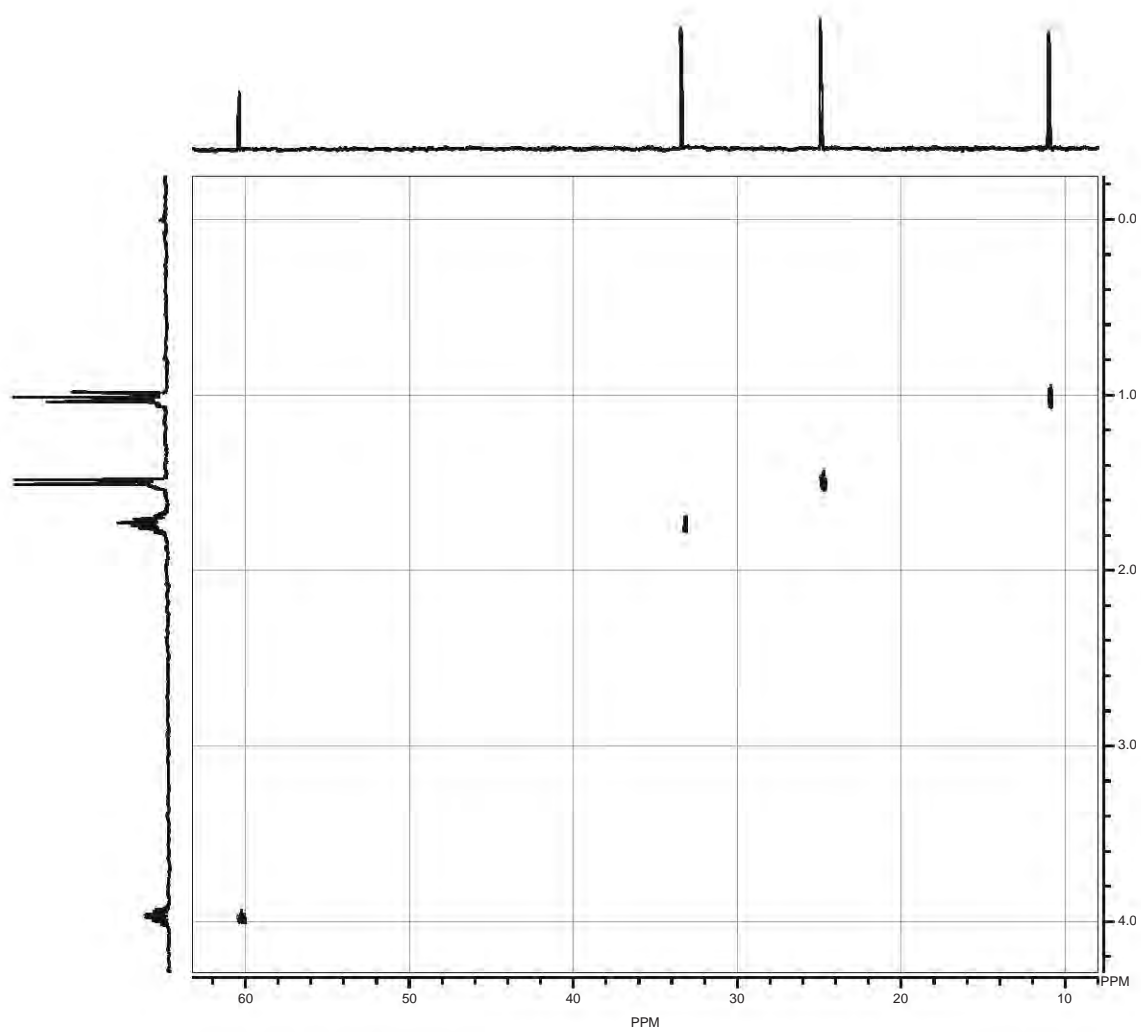
2. Determine the structure for a compound with formula $C_{13}H_{12}O_2$. The IR spectrum shows a strong band at 1680 cm^{-1}. The normal ^{13}C NMR spectrum is shown in a stacked plot along with the DEPT-135 and DEPT-90 spectra. The ^1H NMR spectrum and expansions are provided in the problem along with the COSY spectrum. Assign all of the protons and carbons for this compound.

(ppm)

2521.87 2520.04

(ppm)
8.42 8.40 8.38

2409.48 2407.65 2400.71 2398.88

(ppm)
8.04 8.02 8.00 7.98

2362.70
2353.93
2337.12
2328.35

7.88 7.86 7.84 7.82 7.80 7.78 7.76 7.74
(ppm)

2169.18
2166.80
2160.41
2157.85
2150.17
2147.62

7.24 7.22 7.20 7.18 7.16 7.14
(ppm)
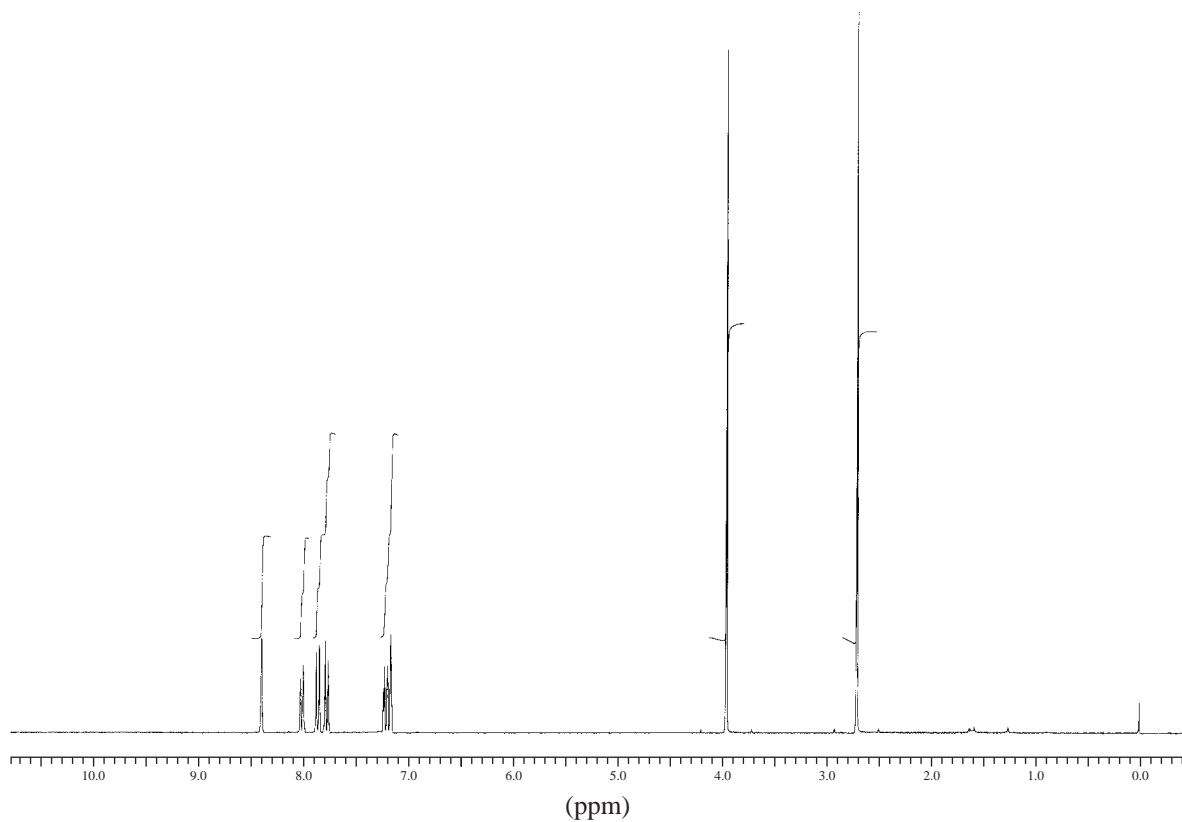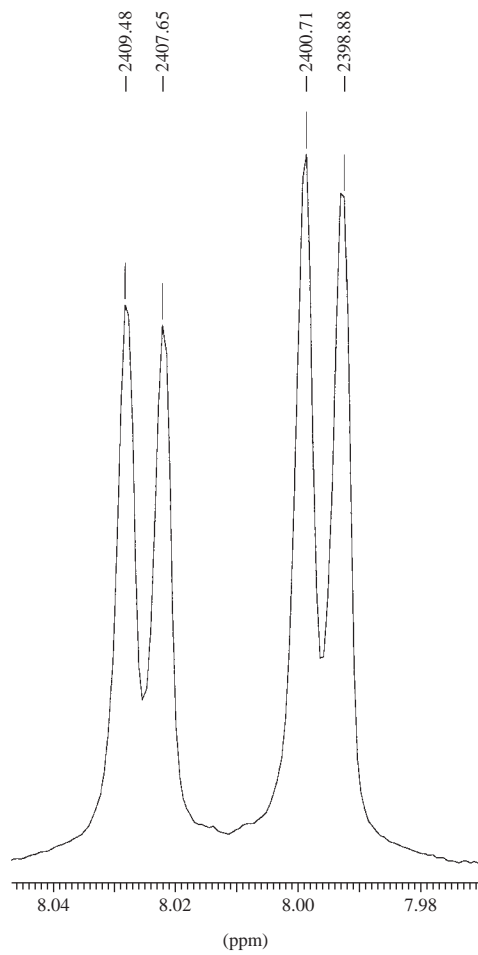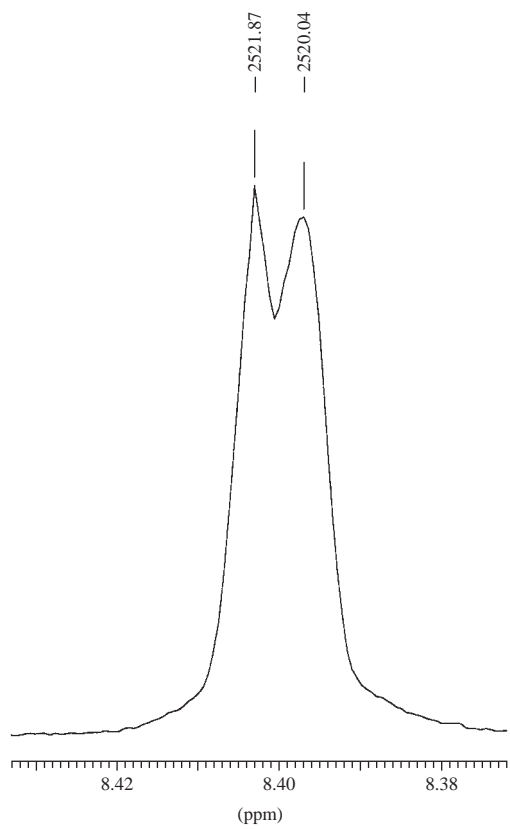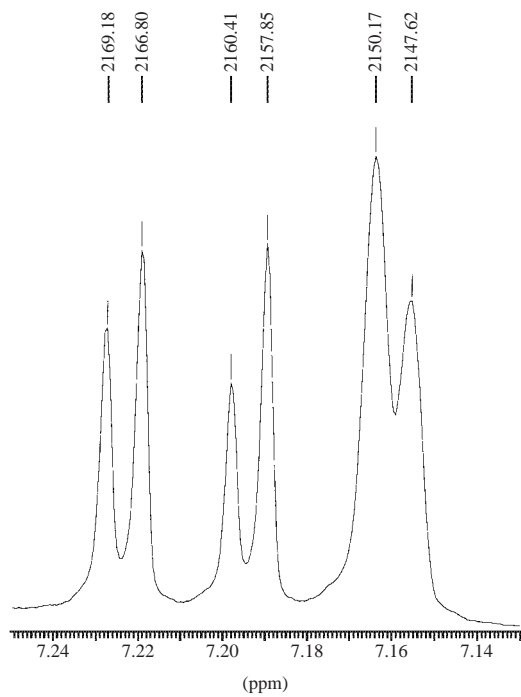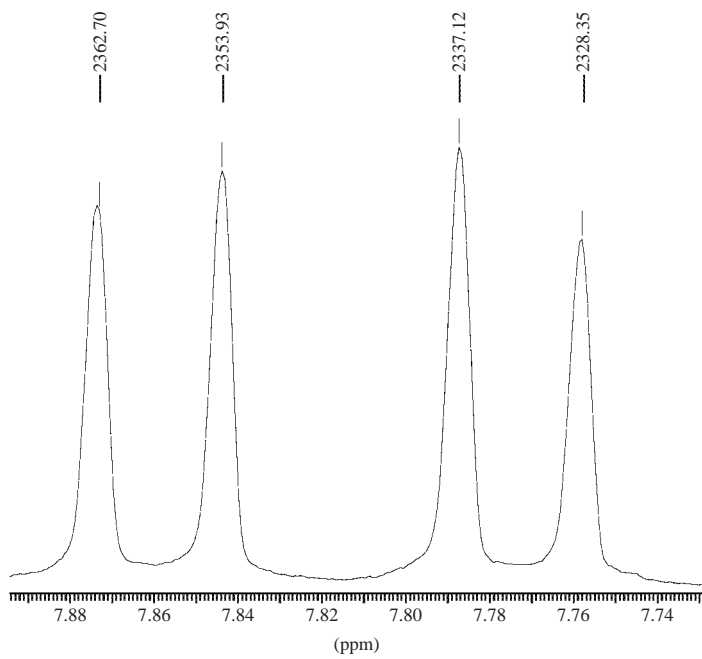
DEPT-90

DEPT-135

Normal
carbon

197.8181

159.6834

137.2069
132.3229
131.0402
129.9955
127.7265
127.0189
124.5814
119.6503

105.6657

77.4156
77.0000
76.5732

55.3435

26.4869

CDCl₃

200   180   160   140   120   100   80   60   40

(ppm)

CHCl₃

CHCl₃

7.2

7.6

(ppm)

8.0

8.4

8.4   8.0   7.6   7.2
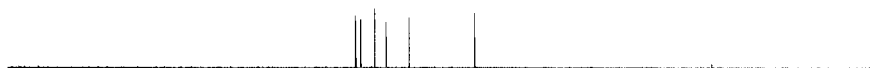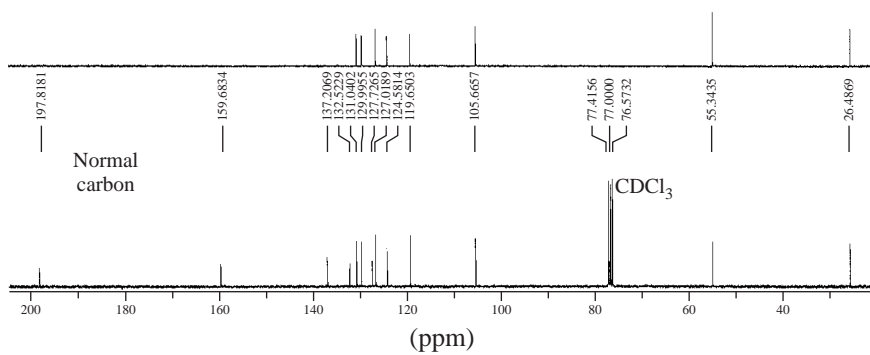
(ppm)
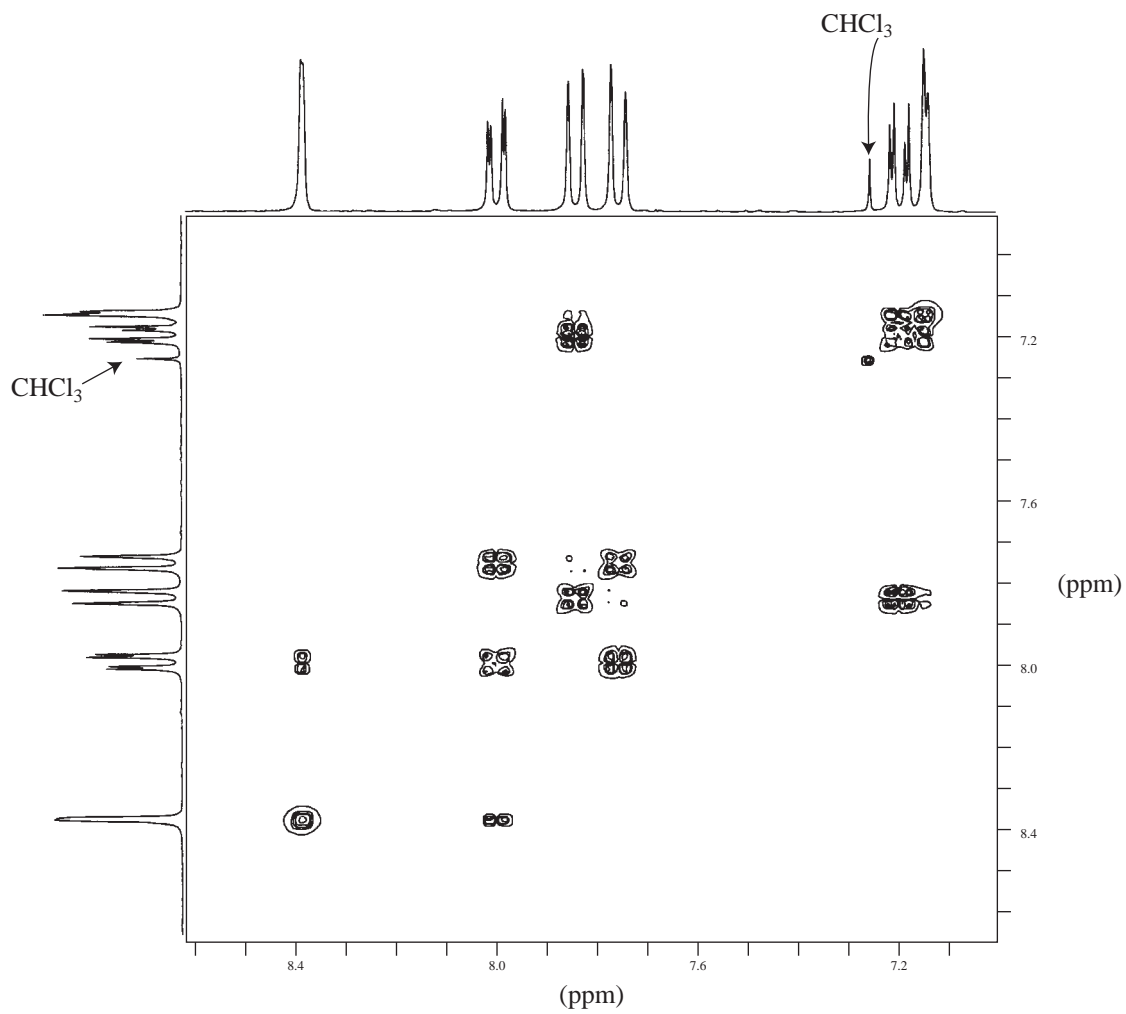
*3. Assign each of the peaks in the following DEPT spectrum of $C_6H_{14}O$. *Note*: There is more than one possible answer.

(ppm)
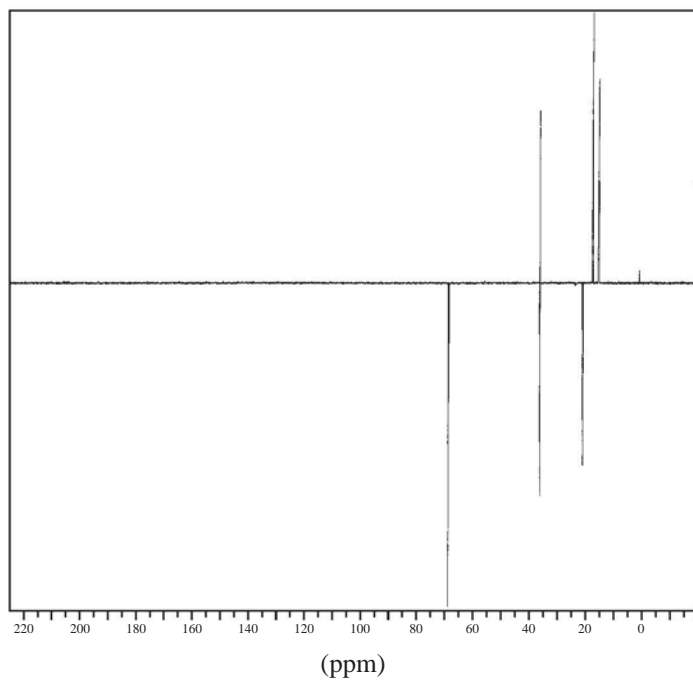
*4. The following HETCOR spectrum is for citronellol. Use the structural formula on p. 607, as well as the DEPT-135 spectrum (Fig. 10.12) and the COSY spectrum (Fig. 10.15), to provide a complete assignment of all carbons and hydrogens in the molecule, especially the assignment of the carbon resonances at C2 and C4.
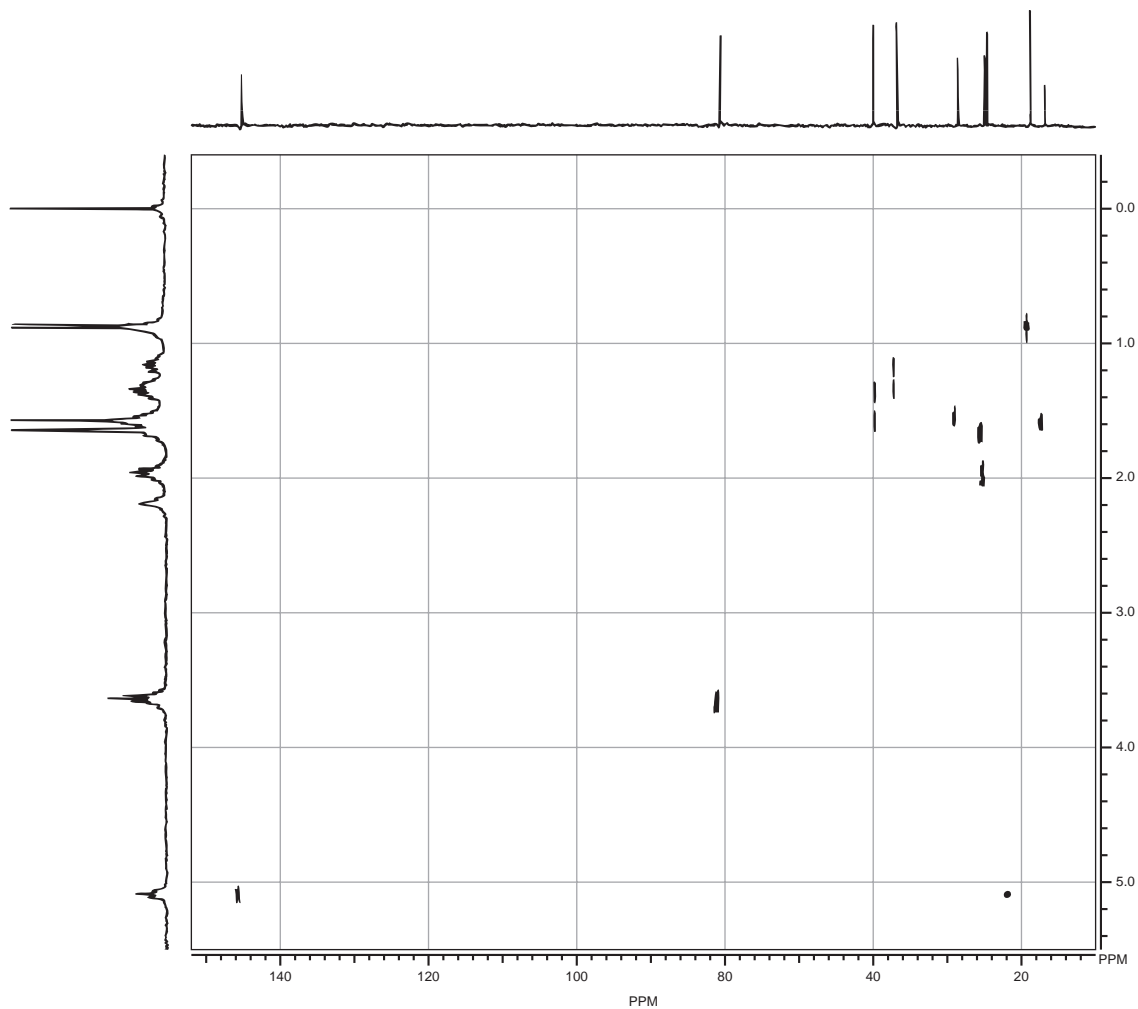
*5. Geraniol has the structure
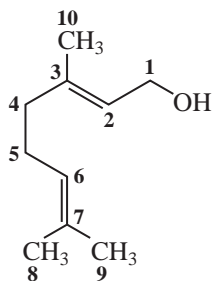
Use the DEPT-135, COSY, and HETCOR spectra to provide a complete assignment of all protons and carbons in geraniol. (*Hint*: The assignments you determined in Problem 4 may help you here.)
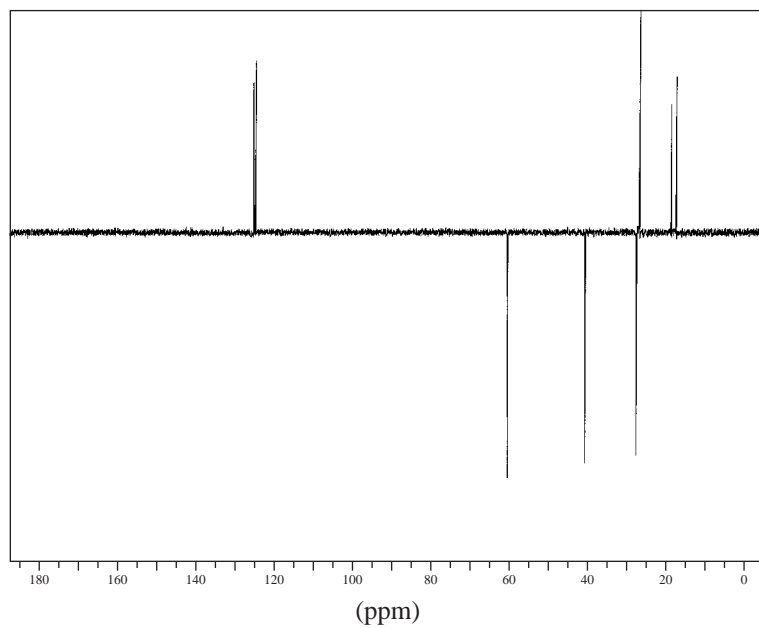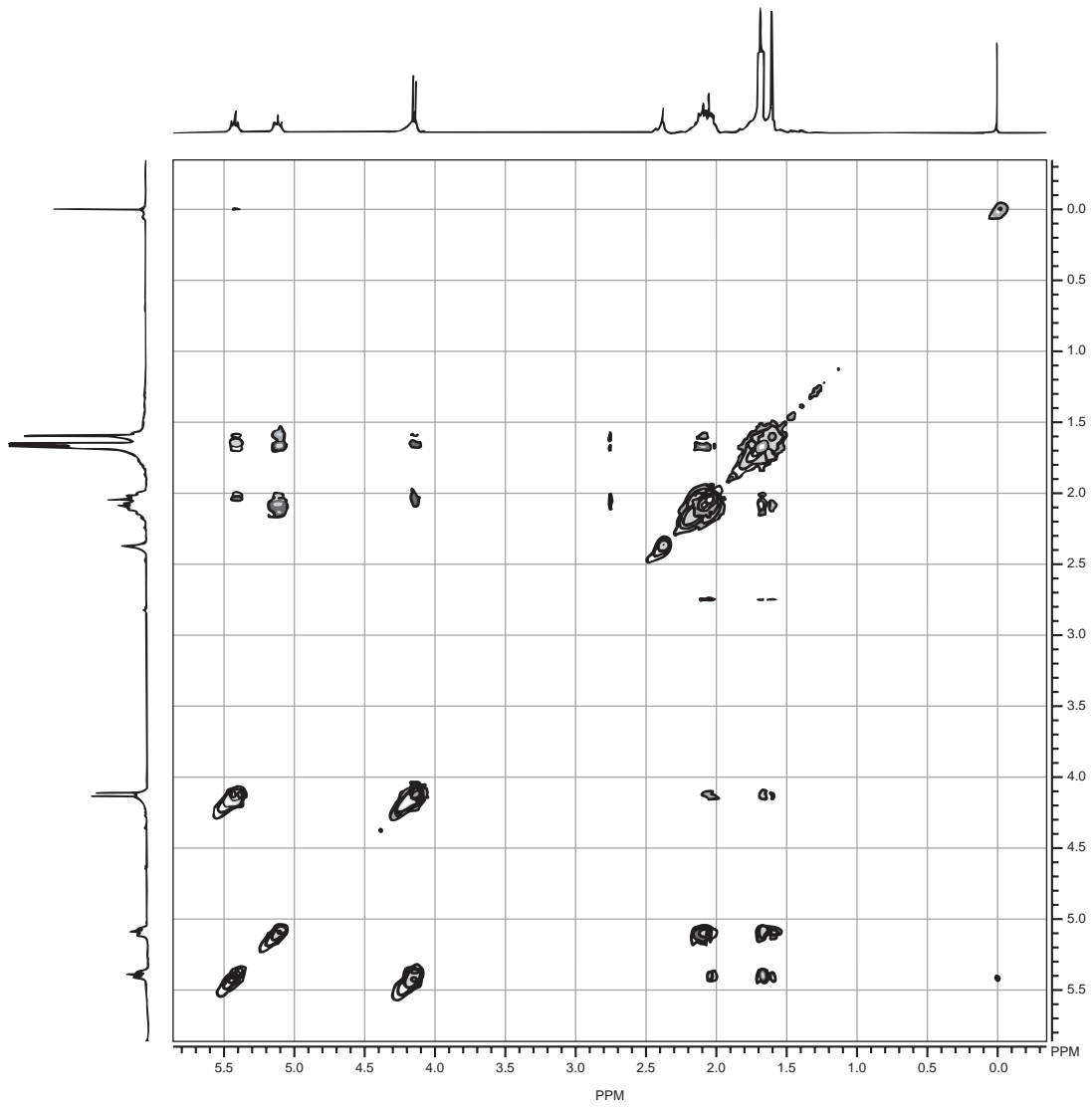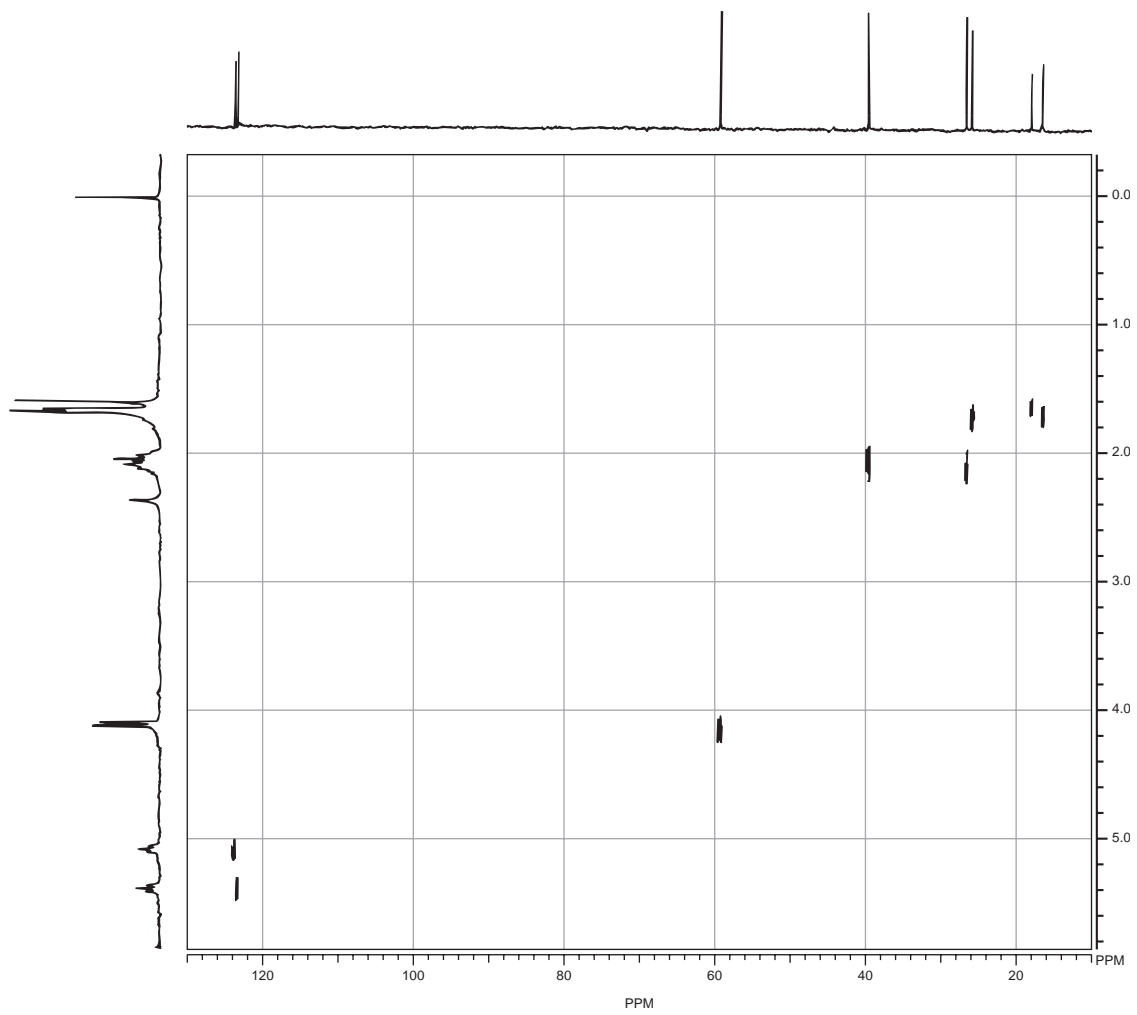
*6. The following set of spectra includes an expansion of the aromatic region of the ^{1}H NMR spectrum of **methyl salicylate** as well as a HETCOR spectrum. Provide a complete assignment of all aromatic protons and unsubstituted ring carbons in methyl salicylate. (*Hint*: Consider the resonance effects of the substituents to determine relative chemical shifts of the aromatic hydrogens. Also try calculating the expected chemical shifts using the data provided in Appendix 6.)

METHYL SALICYLATE EXPANSION

HERTZ

2336.21
2334.89
2334.52
2328.28
2326.99
2326.48
2320.64
2919.50

2256.49

2226.37
2225.78
2224.63
2224.06
2219.12
2217.99
2217.41
2216.37
2210.77
2210.16
2209.00
2208.46

2176.65

2167.22

2122.58

2086.93
2086.61
2078.50
2078.17

2053.30
2052.24
2051.55
2046.08
2045.33
2045.04
2044.31
2038.15
2037.03
2036.44

7.8   7.7   7.6   7.5   7.4   7.3   7.2   7.1   7.0   6.9   6.8

PPM
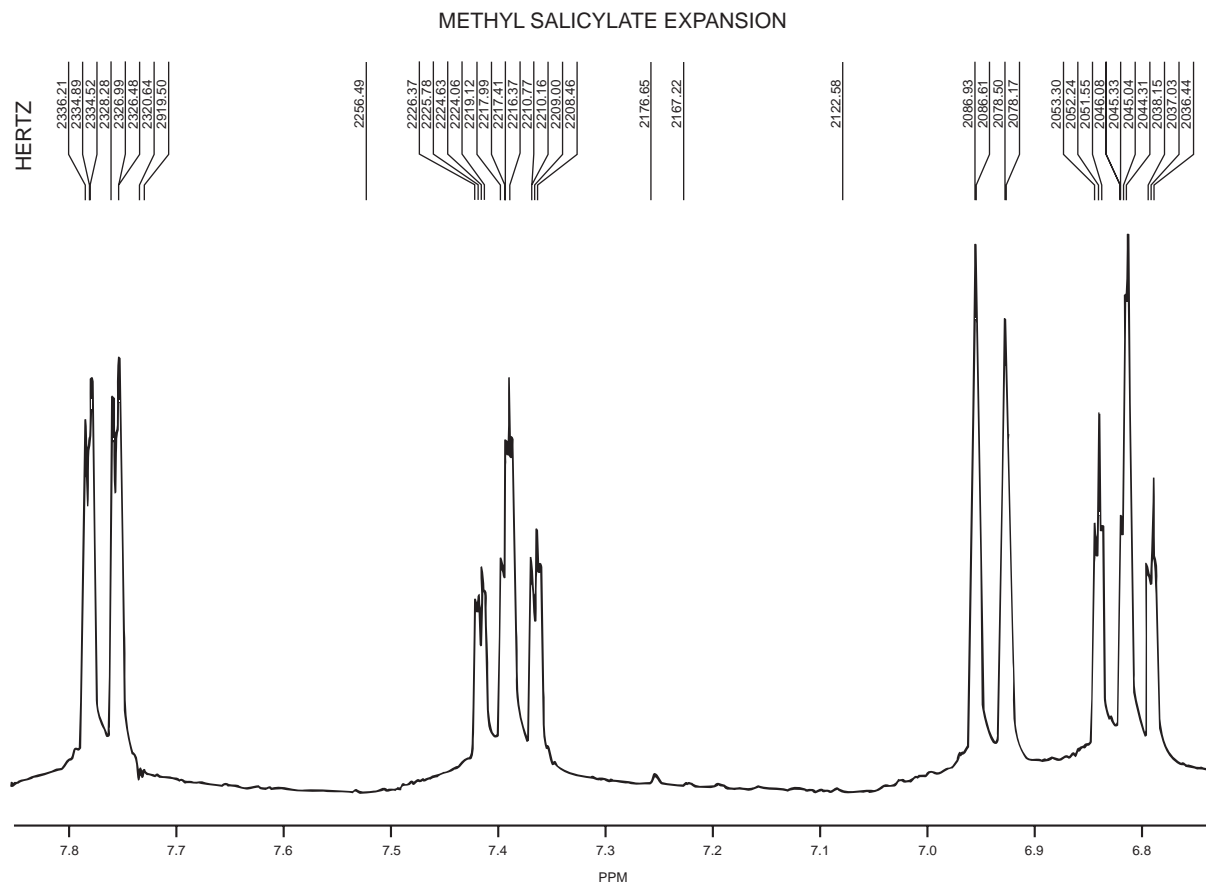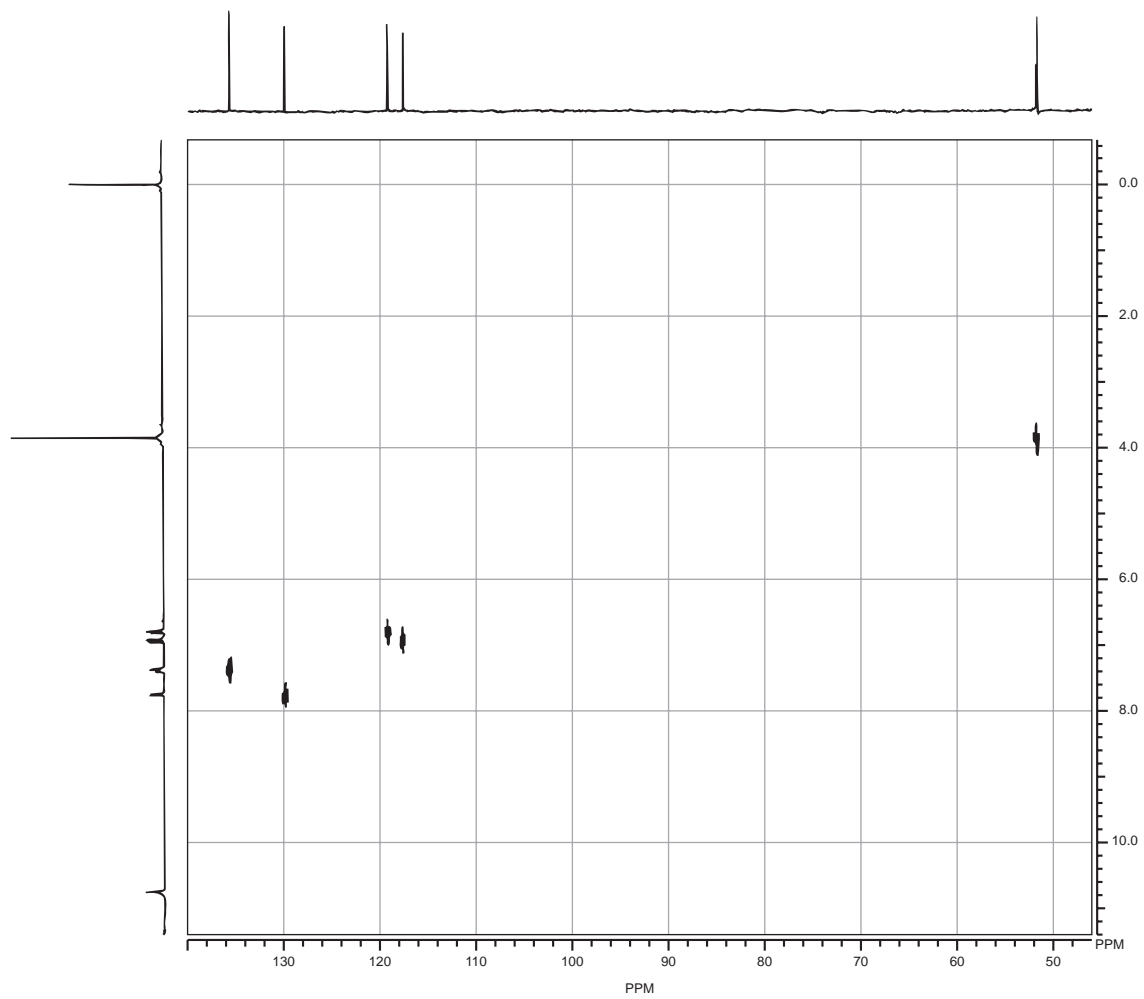
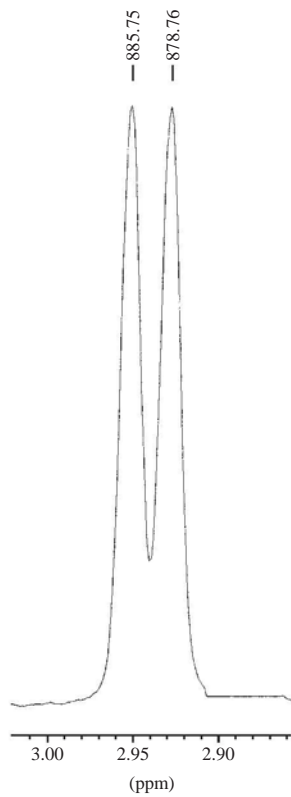**7.** Determine the structure for a compound with formula $C_6H_{12}O_2$. The IR spectrum shows a strong and broad band from 3400 to 2400 cm^{-1} and also at 1710 cm^{-1}. The ^{1}H NMR spectrum and expansions are shown, but a peak appearing at 12.0 ppm is not shown in the full spectrum. Fully interpret the ^{1}H NMR spectrum, especially the patterns between 2.1 and 2.4 ppm. A HETCOR spectrum is provided in this problem. Comment on the carbon peaks appearing at 29 and 41 ppm in the HETCOR spectrum. Assign all of the protons and carbons for this compound.

(ppm)

Top spectrum peaks: 719.92, 713.67, 704.85, 698.59, 655.58, 647.49, 40.50, 32.41
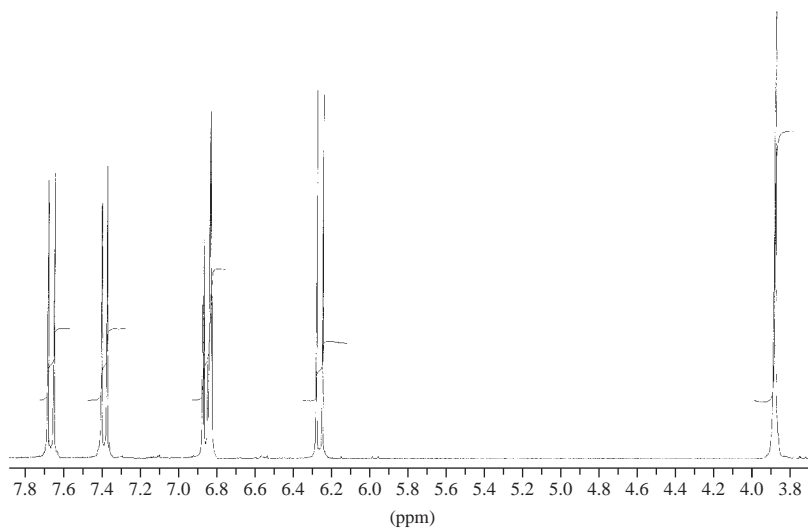
Bottom spectrum peaks: 593.07, 586.45, 579.83, 572.85, 566.23, 559.61, 552.26, 545.64

442.32
436.44
434.60
428.72
427.25
421.36
415.48
413.64
407.76
406.29
400.41
397.83
390.48
382.76
375.77
369.15
362.17
356.28
354.81
349.67

1.48   1.44   1.40   1.36   1.32   1.28   1.24   1.20   1.16
(ppm)

294.15
287.53
279.81
272.45
264.73

1.00   0.96   0.92   0.88
(ppm)

HETCOR

(ppm)

(ppm)
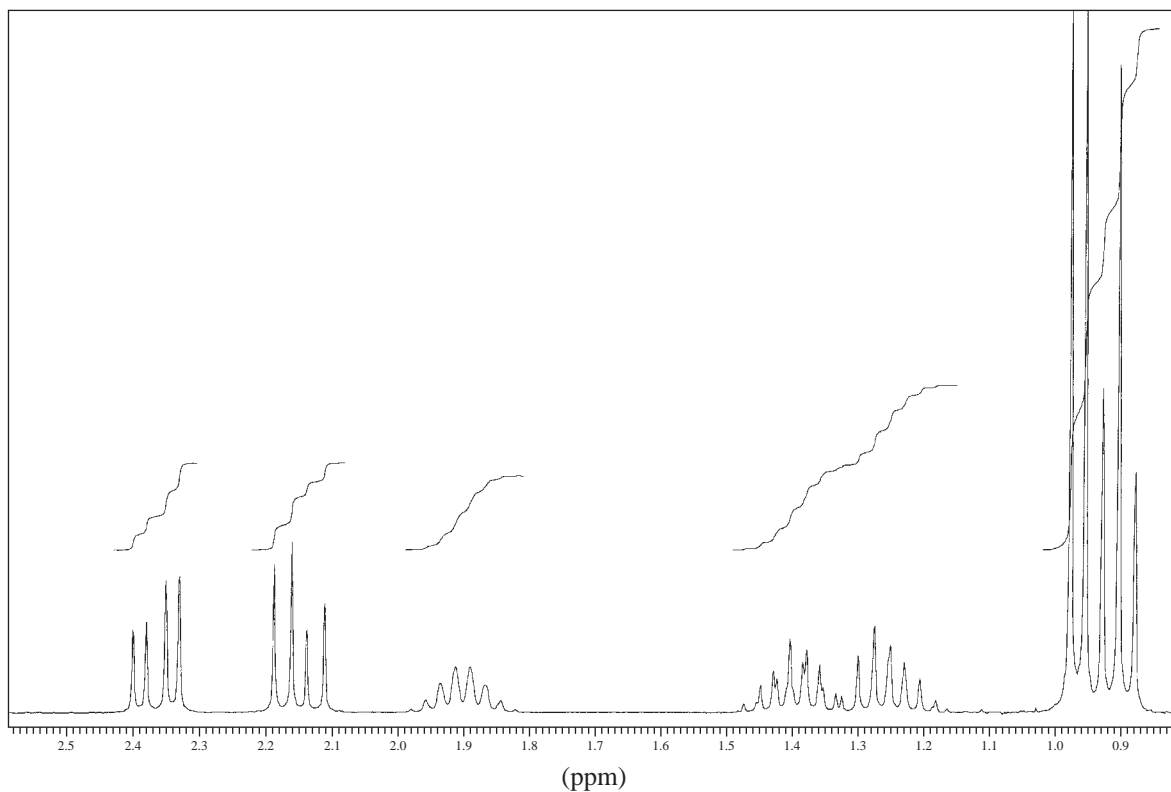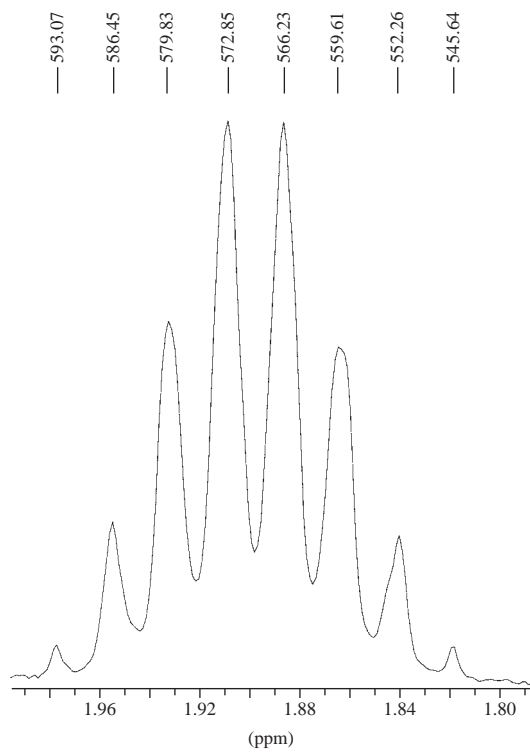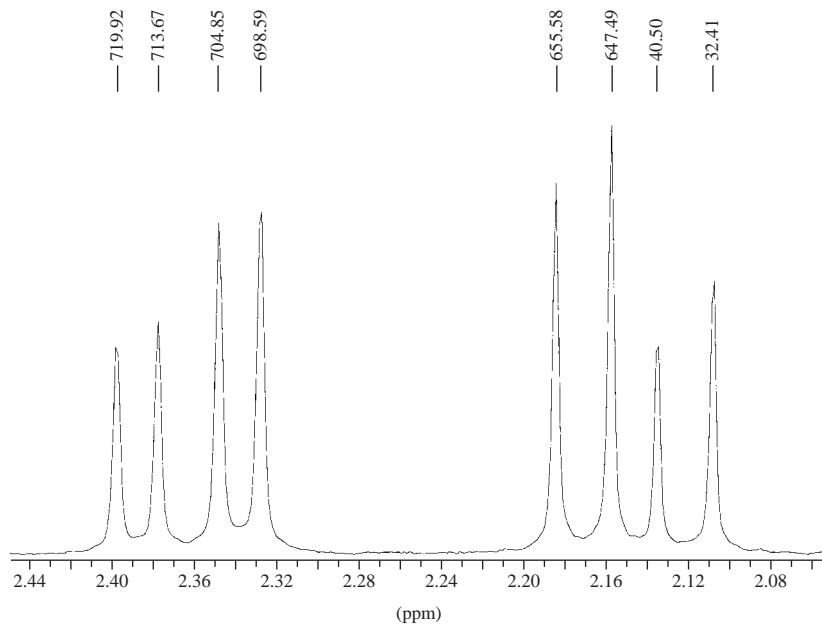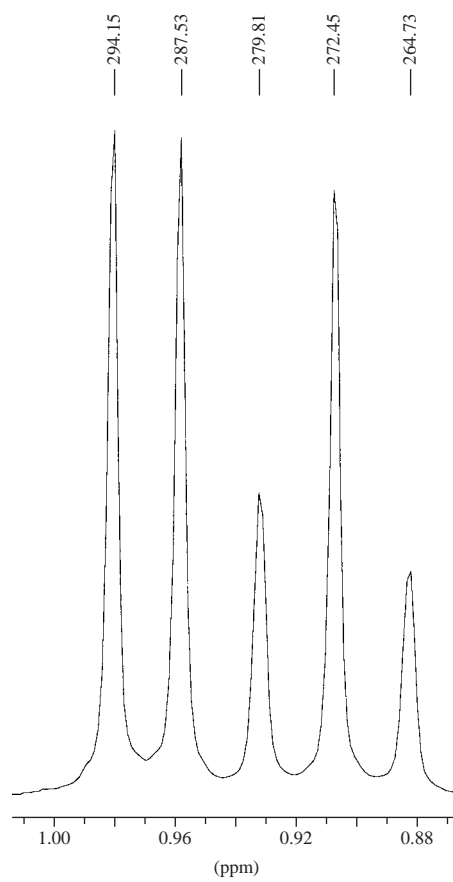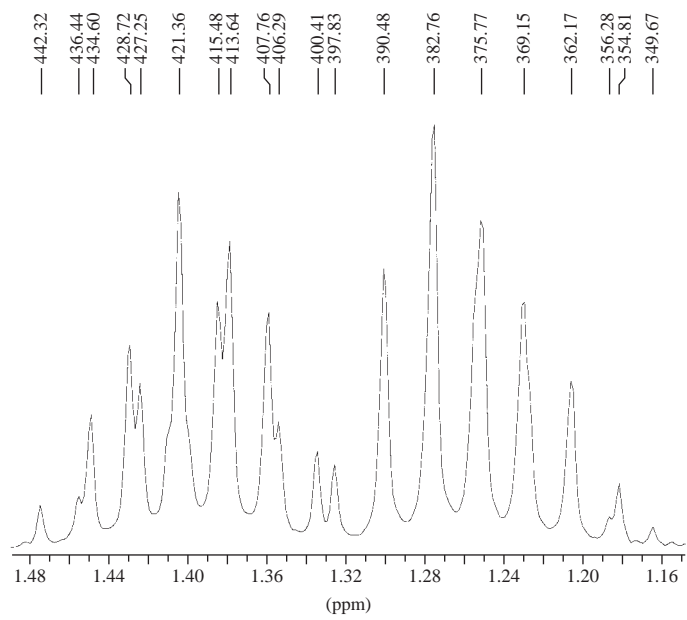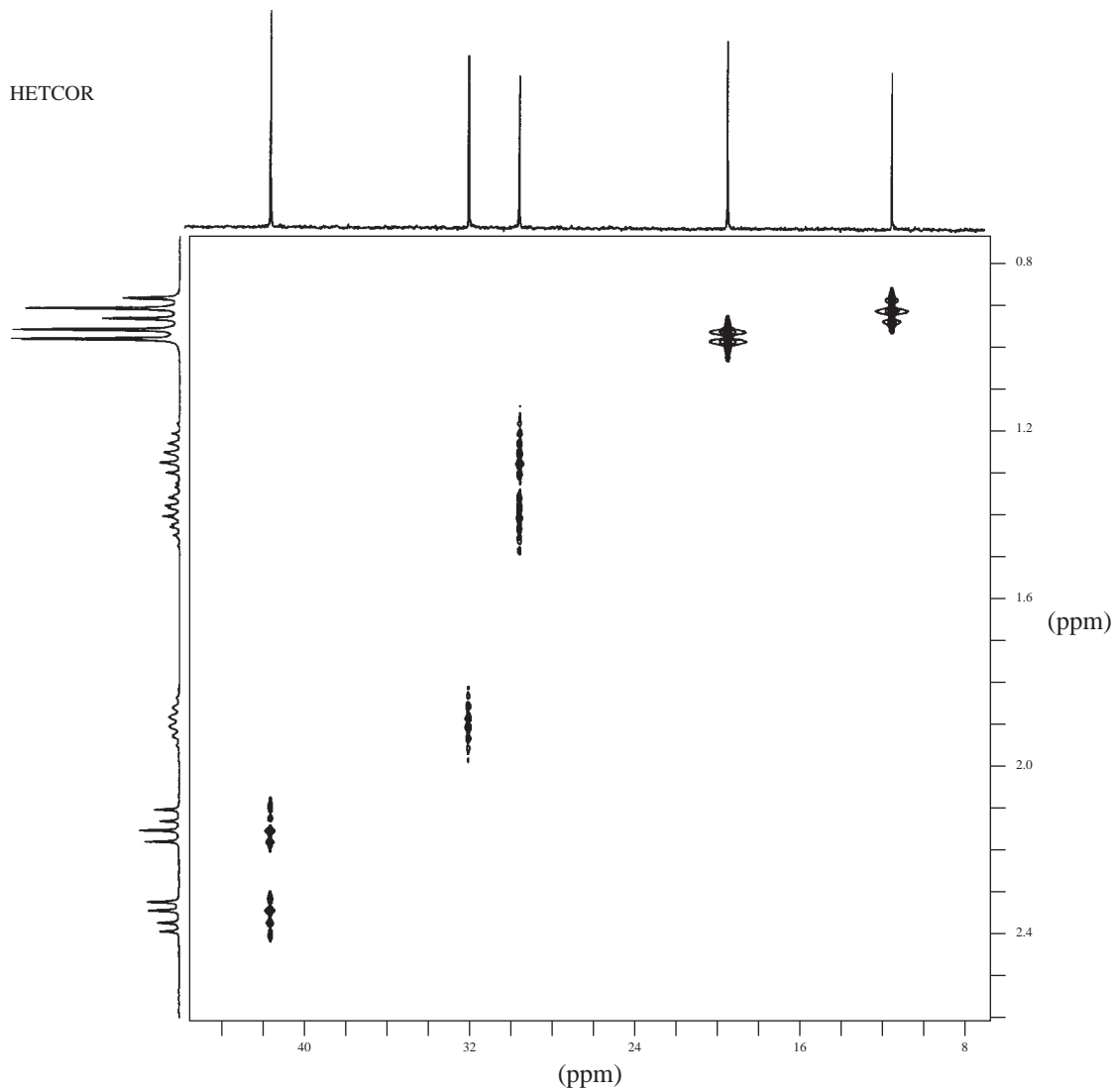
8. Determine the structure for a compound with formula $C_{11}H_{16}O$. This compound is isolated from jasmine flowers. The IR spectrum shows strong bands at 1700 and 1648 cm^{-1}. The ^{1}H NMR spectrum, with expansions, along with the HETCOR, COSY, and DEPT spectra are provided in this problem. The DEPT-90 spectrum is not shown, but it has peaks at 125 and 132 ppm. This compound is synthesized from 2,5-hexanedione by monoalkylation with (Z)-1-chloro-2-pentene, followed by aldol condensation. Assign all of the protons and carbons for this compound.
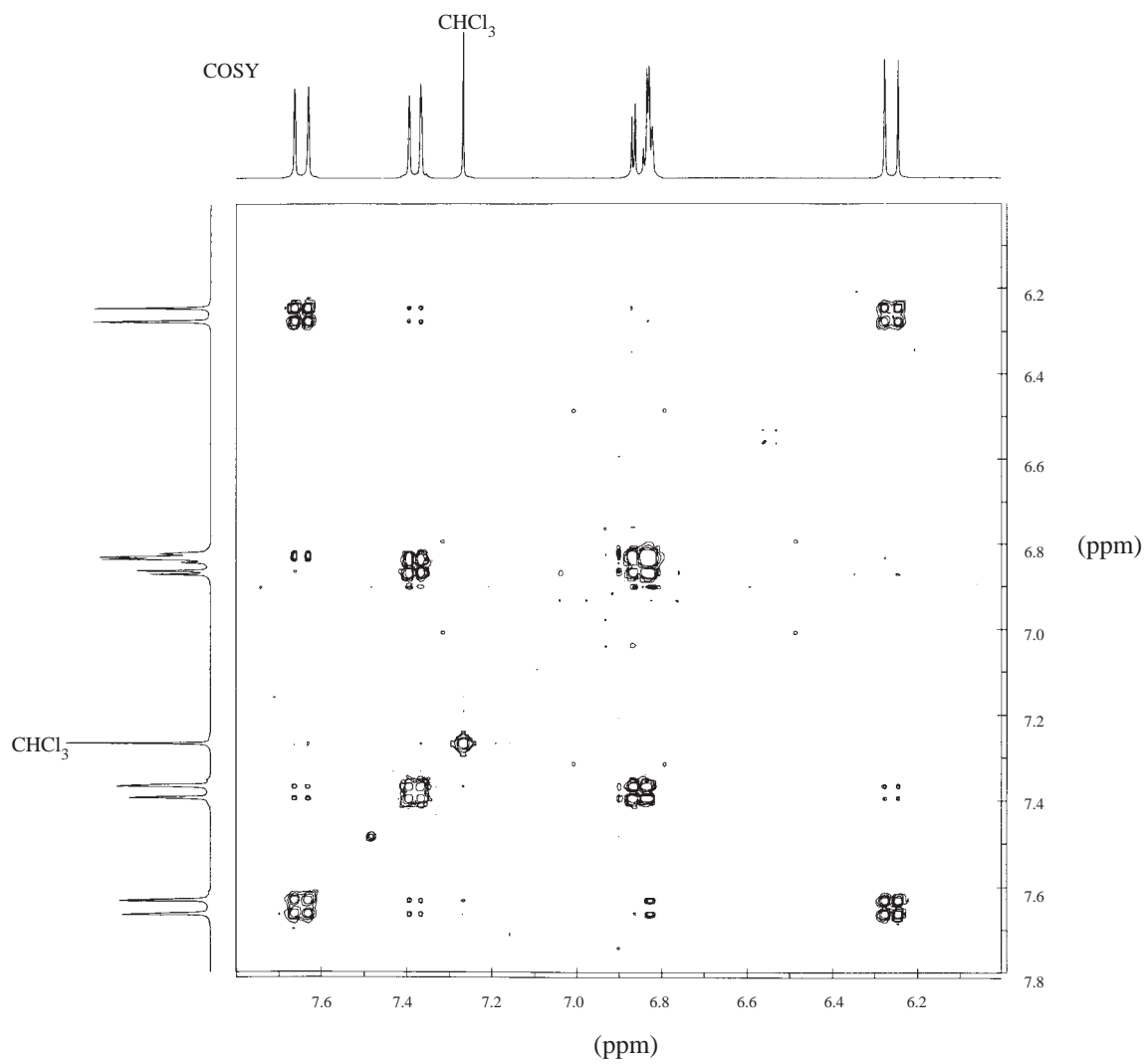

(ppm)

(ppm)

— 885.75
— 878.76

3.00   2.95   2.90
(ppm)

2.55   2.50   2.45   2.40   2.35
(ppm)

HETCOR

(ppm)

(ppm)

COSY

(ppm)

(ppm)

Normal Carbon

209.0915

170.4213

139.3743
132.3202
125.0565

77.4751
77.0557
76.6364

34.2669
31.6459

21.1472
20.5631
17.2832
14.1680

CDCl$_3$

200 180 160 140 120 100 80 60 40 20 0

(ppm)

DEPT-135

132.3202
125.0565

34.2669
31.6459

21.1472
20.5631
17.2981
14.1680

130 120 110 100 90 80 70 60 50 40 30 20 10

(ppm)
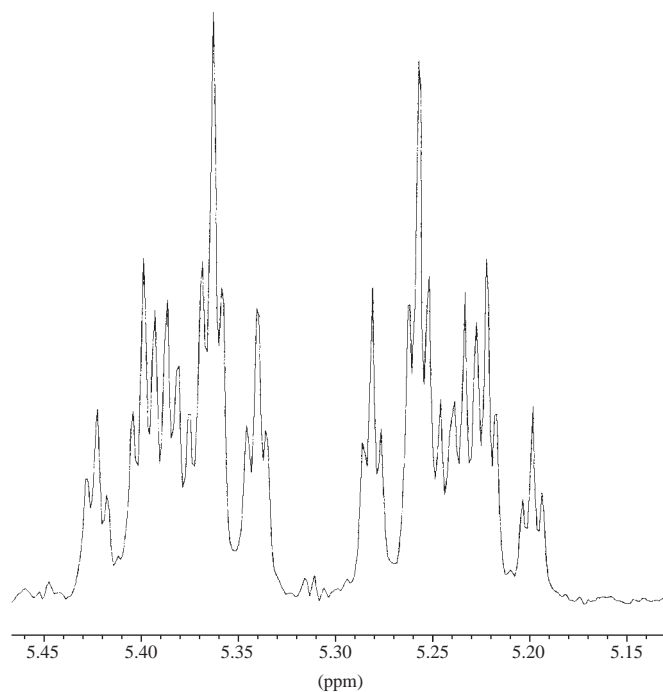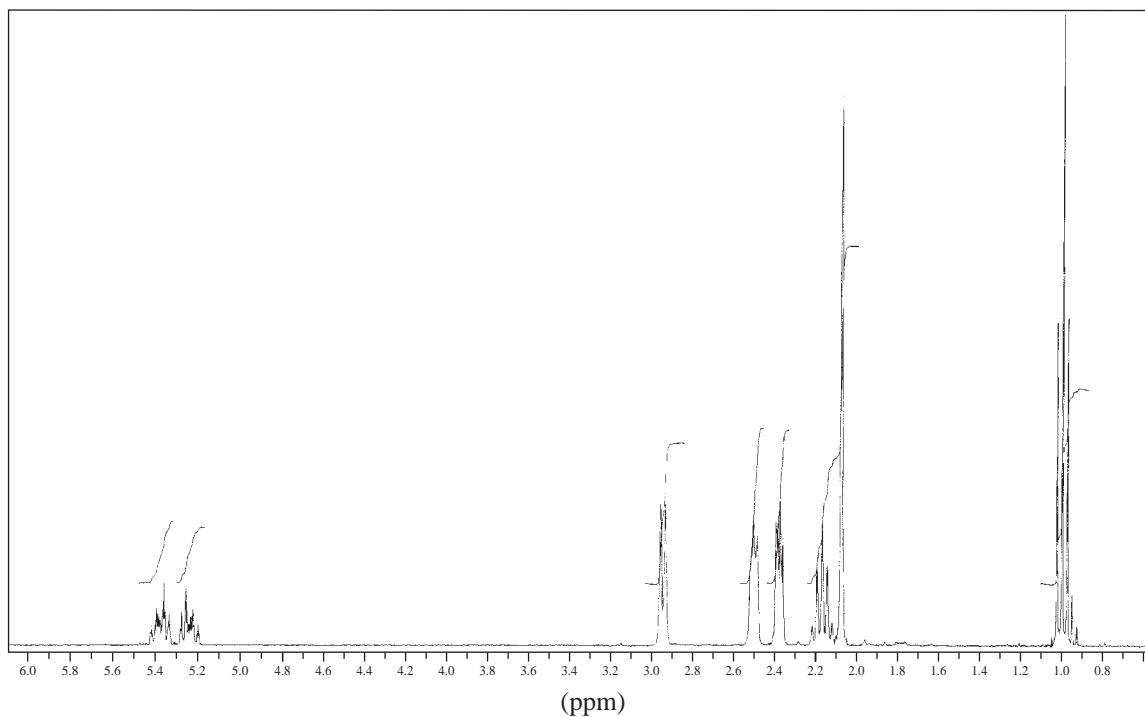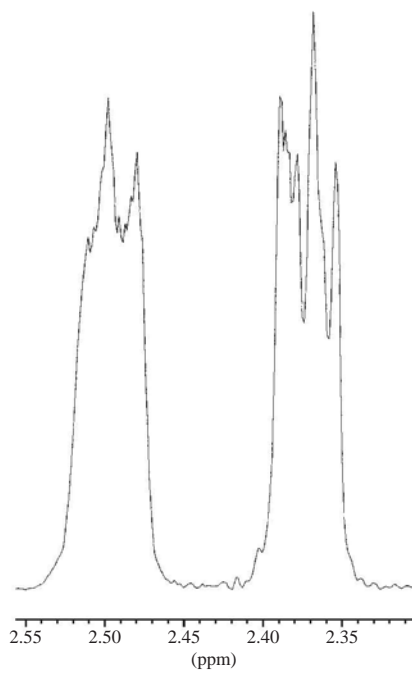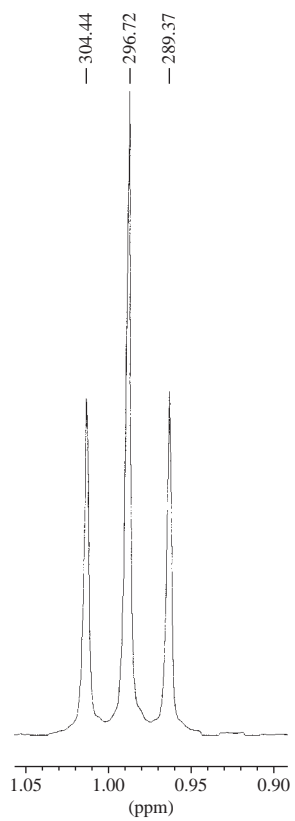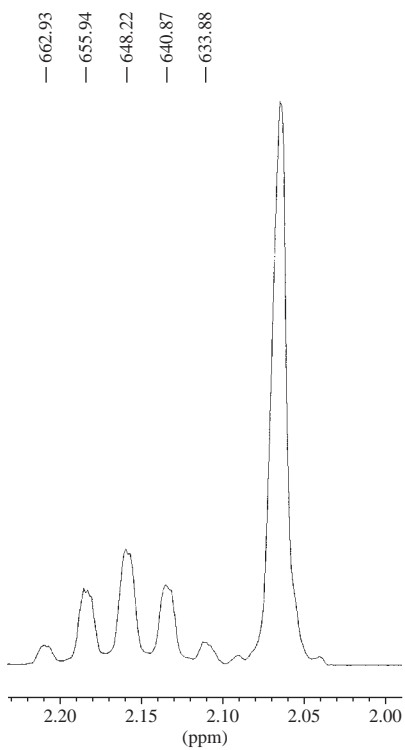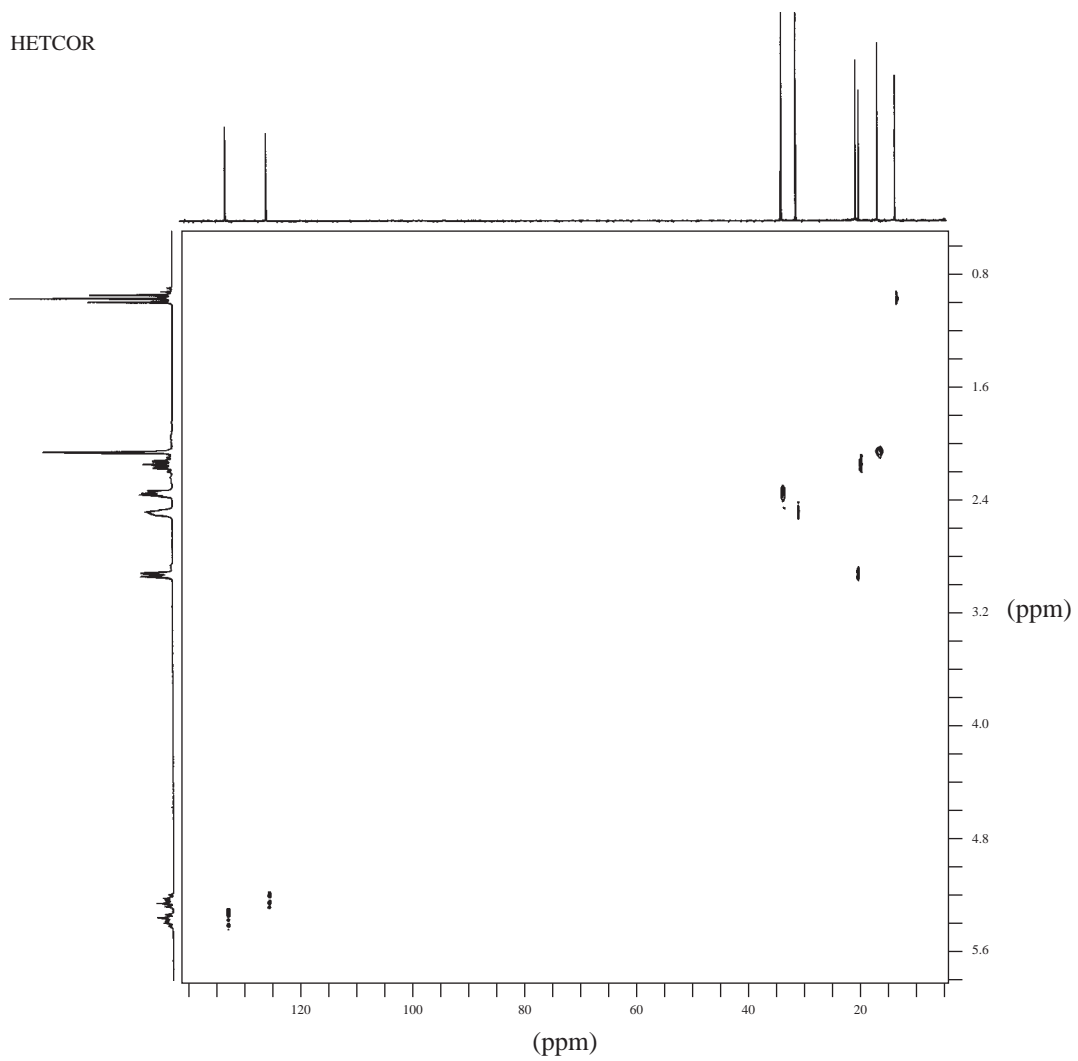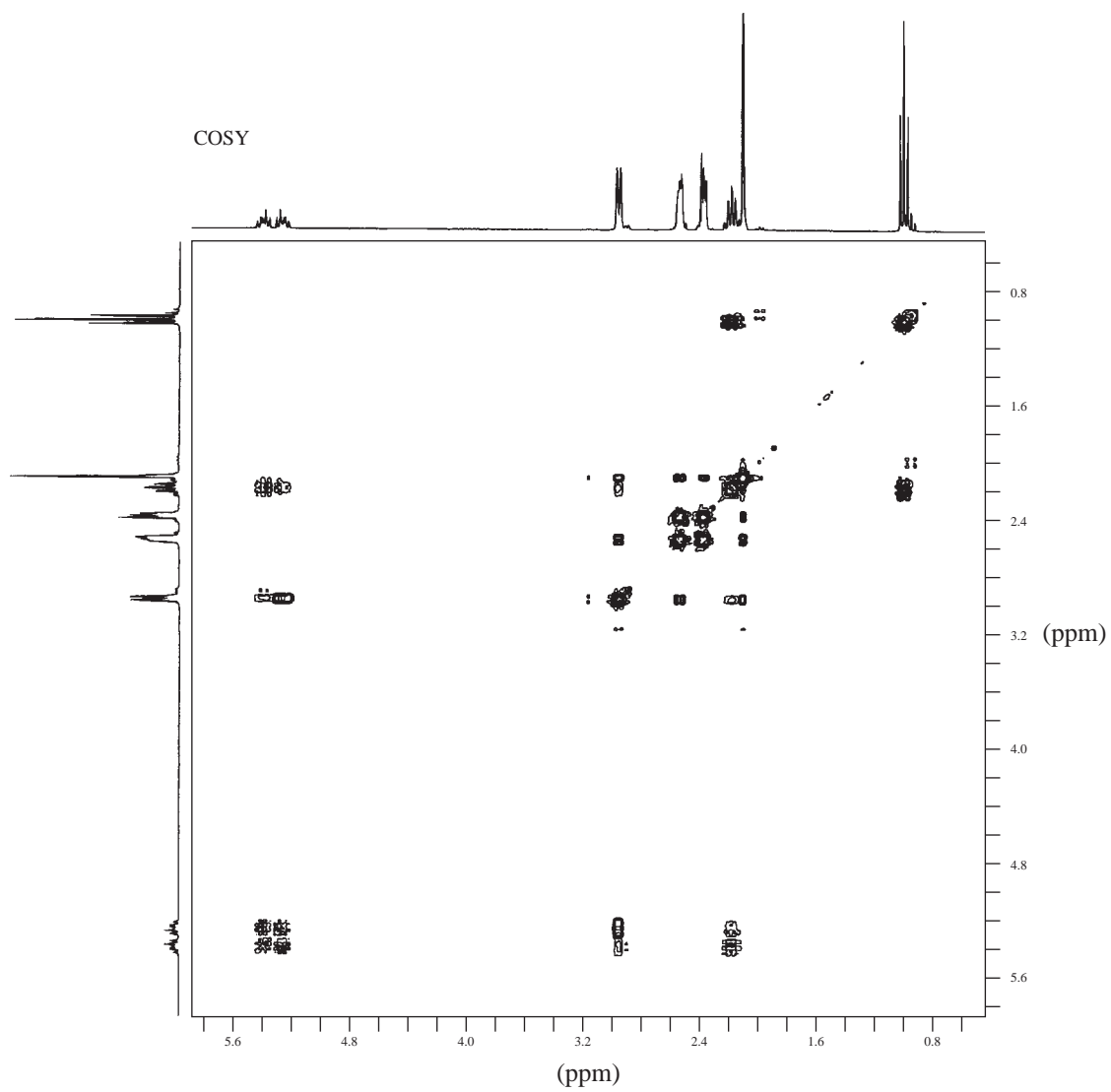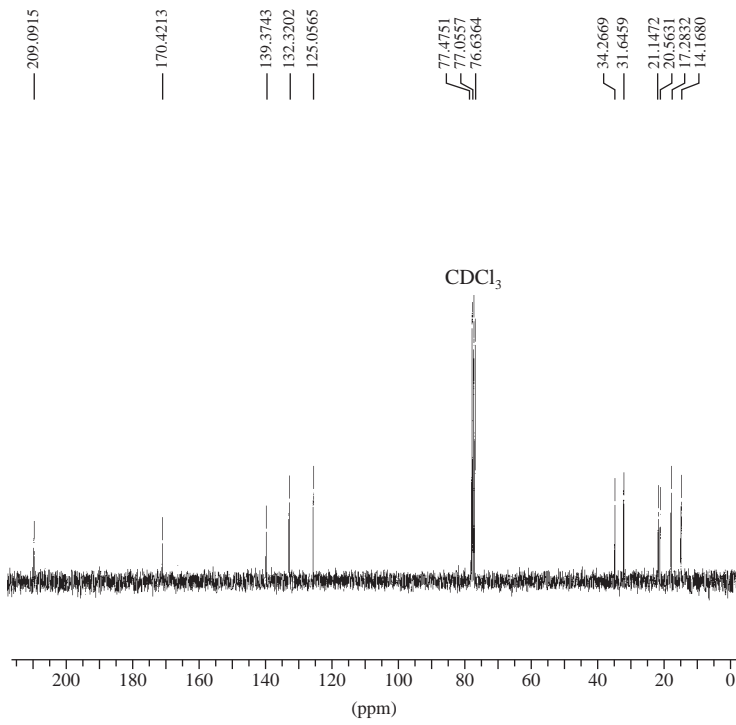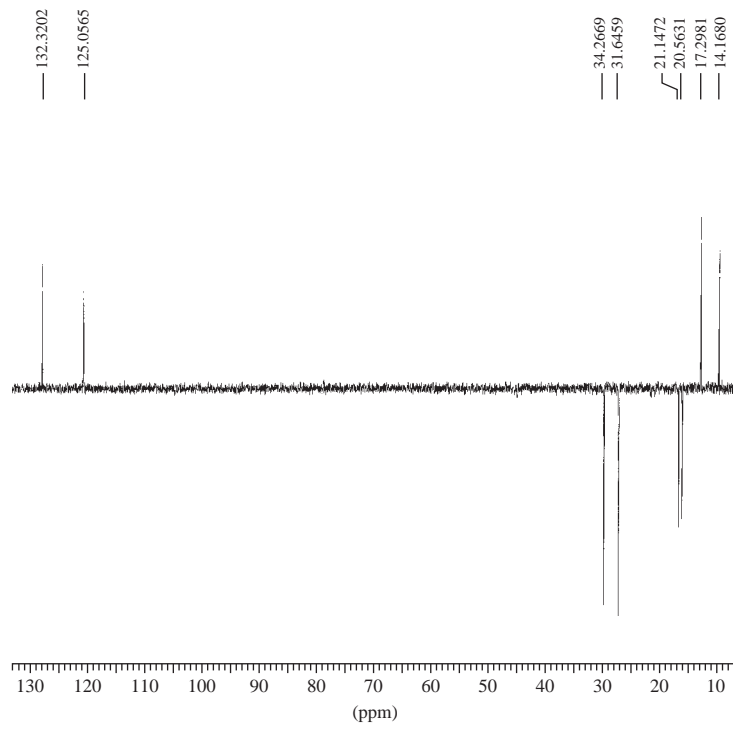
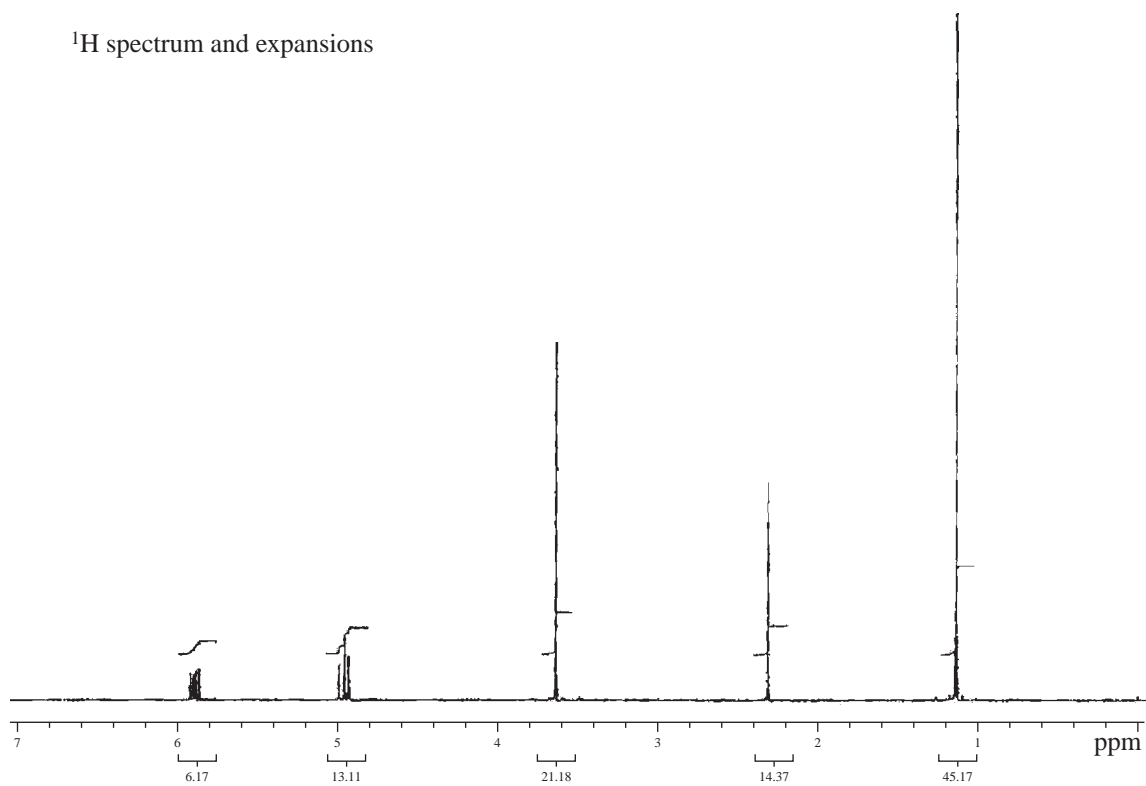**9.** Determine the structure for a compound with formula $C_{10}H_8O_3$. The IR spectrum shows strong bands at 1720 and 1620 cm^{-1}. In addition, the IR spectrum has bands at 1580, 1560, 1508, 1464, and 1125 cm^{-1}. The ^{1}H NMR spectrum, with expansions, along with the COSY and DEPT spectra are provided in this problem. Assign all of the protons and carbons for this compound.

Peaks (ppm) top spectrum: 2061.96, 2059.39, 2053.50, 2051.30, 2049.83, 2047.25; 1883.63, 1874.07

DEPT-90: 143.3635, 128.6748, 112.8865, 112.4111, 100.6843

DEPT-135: 143.3635, 128.6748, 112.8865, 112.4111, 100.6843, 55.6497

NORMAL CARBON: 162.6848, 161.0780, 155.7324, 143.3635, 128.6748, 112.8865, 112.4111, 112.3828, 100.6843, CDCl₃ 77.4221, 77.0000, 76.5743, 55.6497

COSY

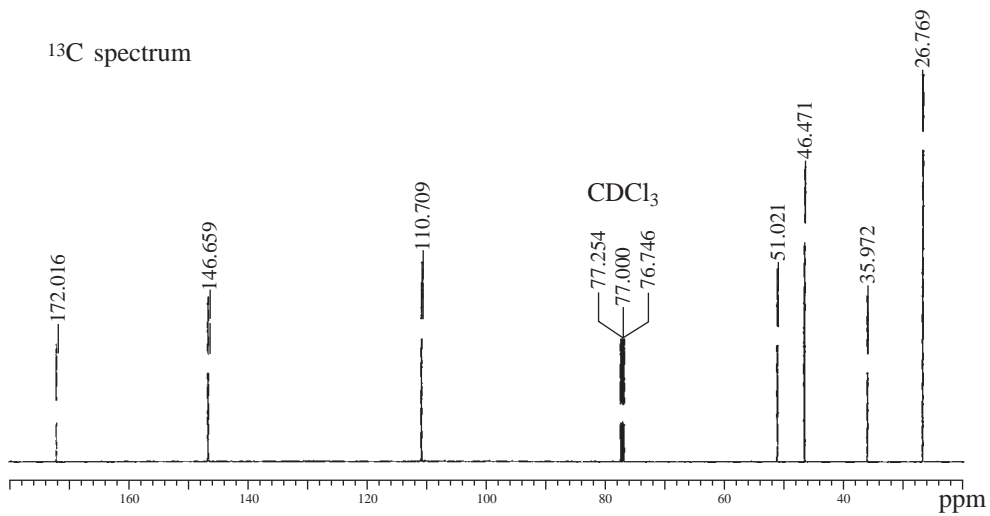CHCl$_3$

CHCl$_3$

(ppm)

(ppm)
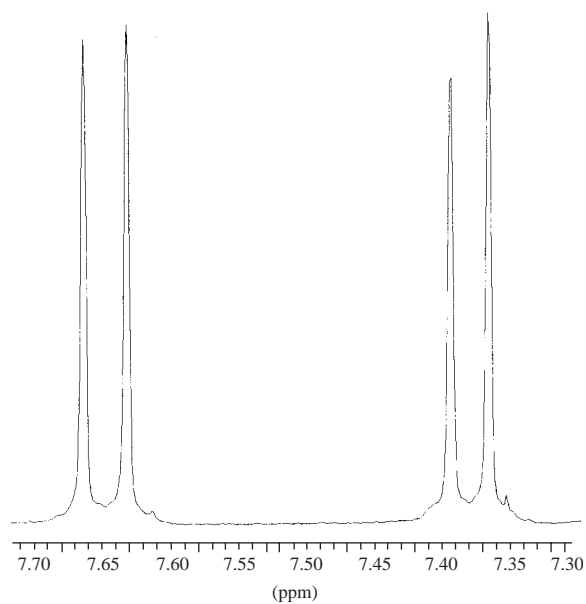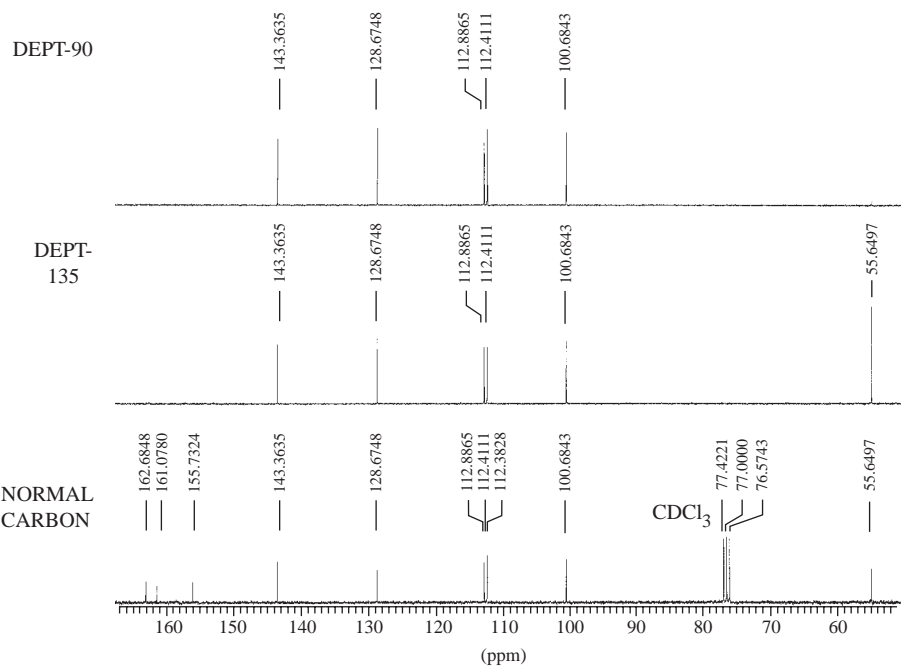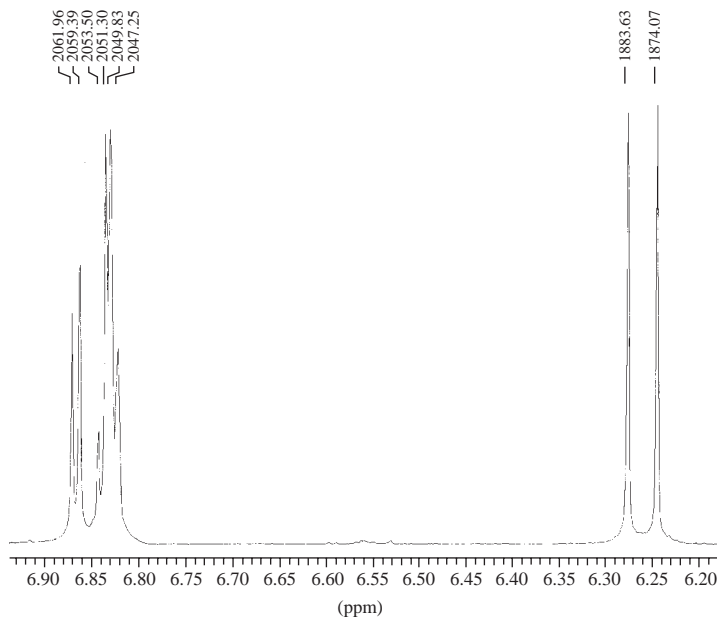
10. Determine the structure for a compound with formula $C_8H_{14}O$. The IR spectrum, ^1H NMR spectrum and expansions, ^{13}C NMR spectrum, DEPT spectrum, COSY spectrum, and HETCOR (HSQC) spectrum are included in this problem.
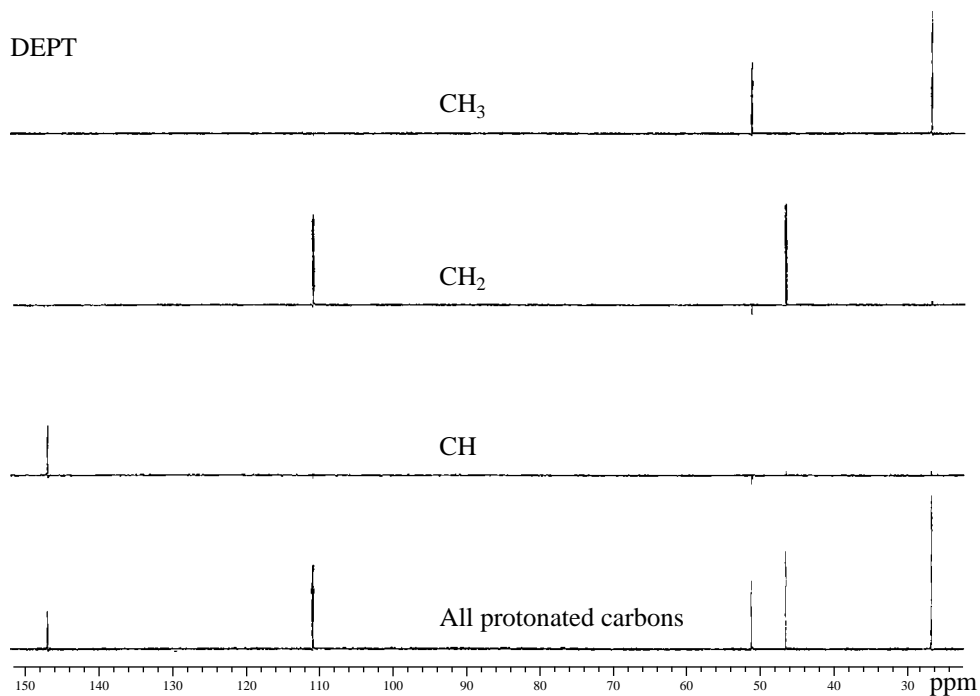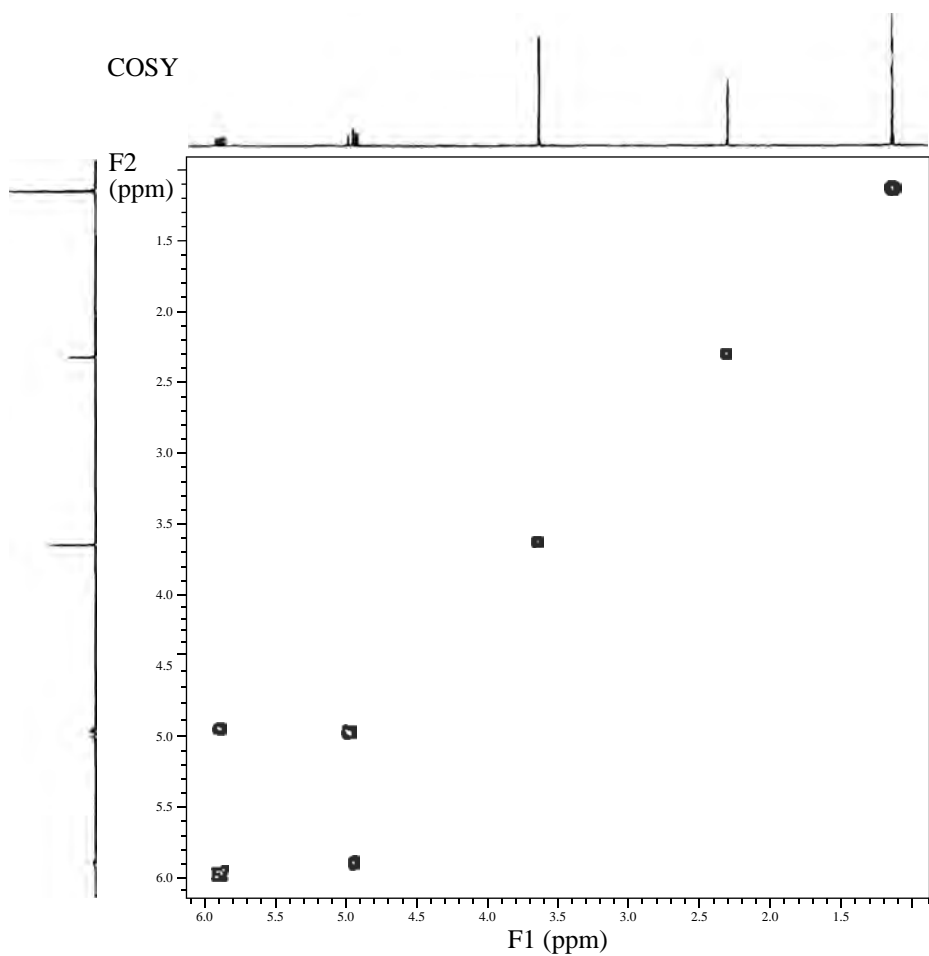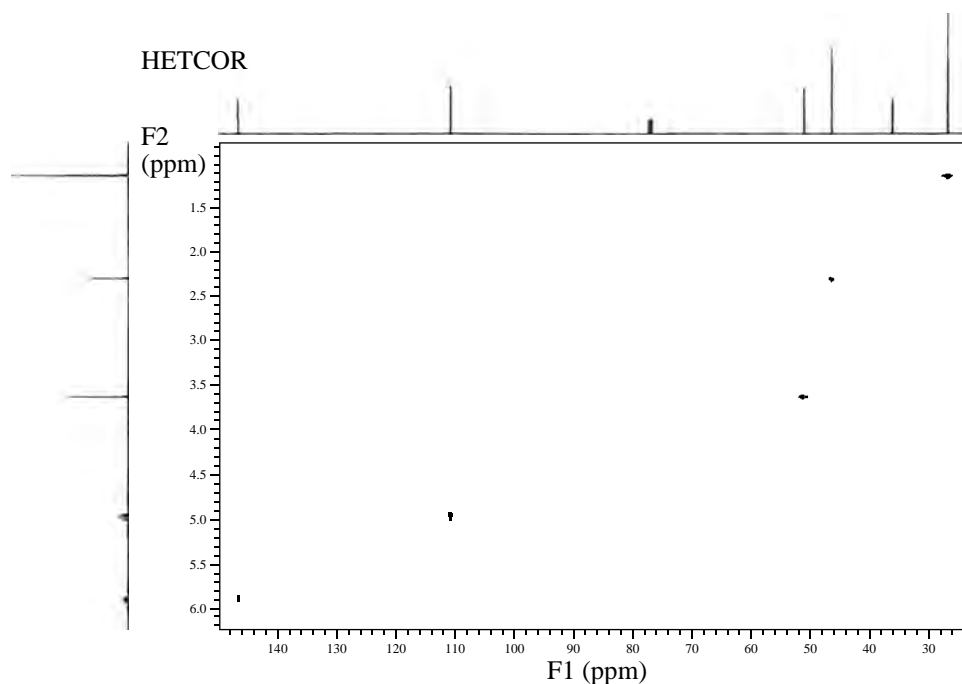
Infrared spectrum

^1H spectrum and expansions

2959.68
2948.93
2942.58
2931.84

5.90
5.85

2495.14
2494.16
2477.55
2476.09
2475.11
2465.34
2464.36

5.00
4.95

¹³C spectrum

172.016
146.659
110.709

CDCl₃
77.254
77.000
76.746

51.021
46.471
35.972
26.769

160   140   120   100   80   60   40   ppm

DEPT

CH$_3$

CH$_2$

CH

All protonated carbons

150   140   130   120   110   100   90   80   70   60   50   40   30 ppm
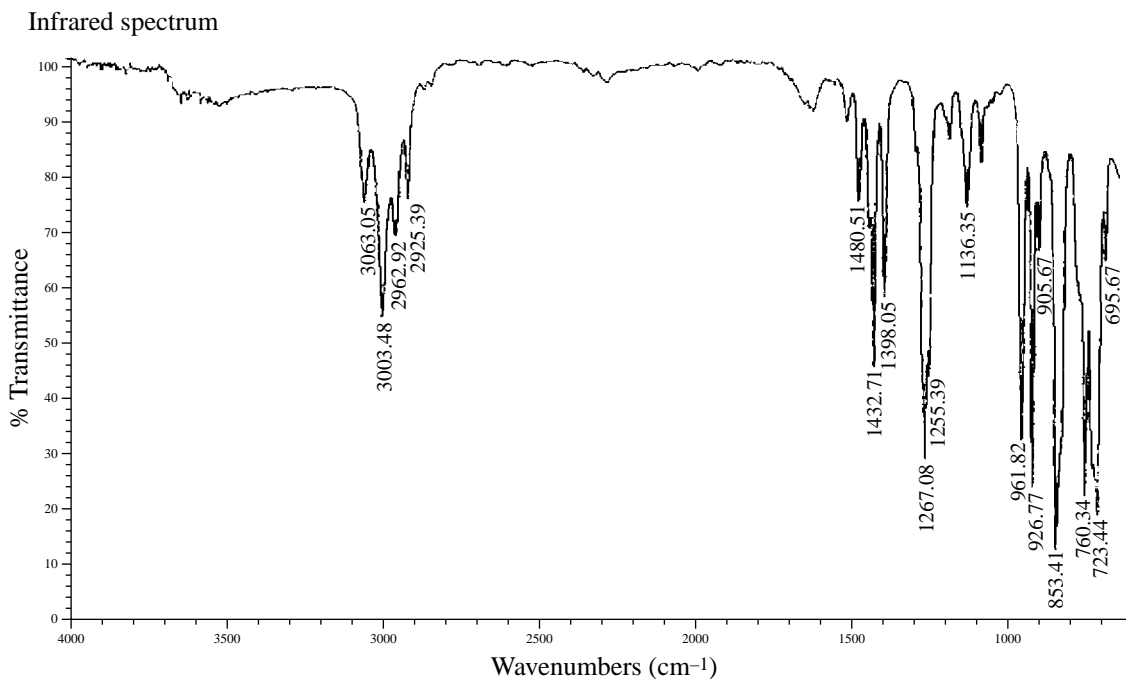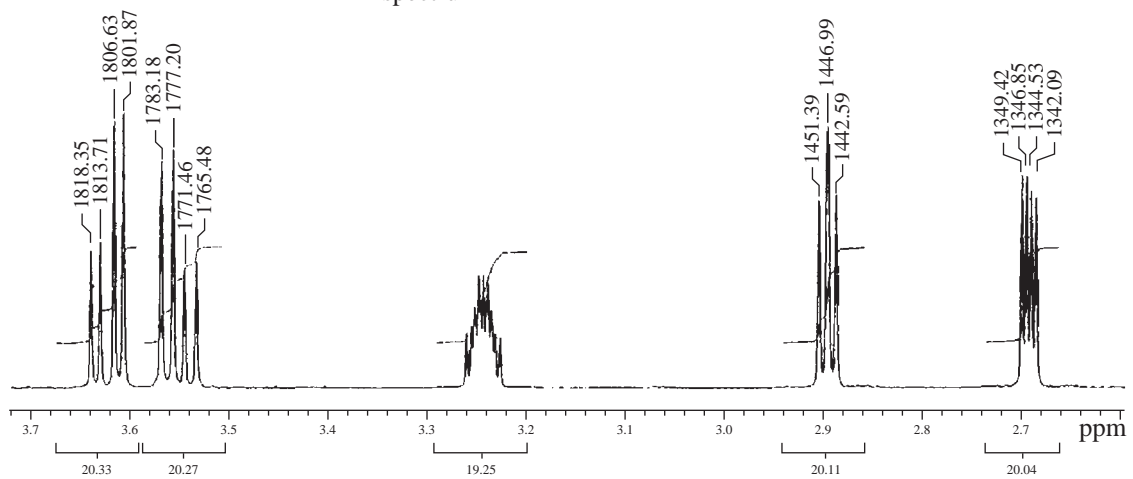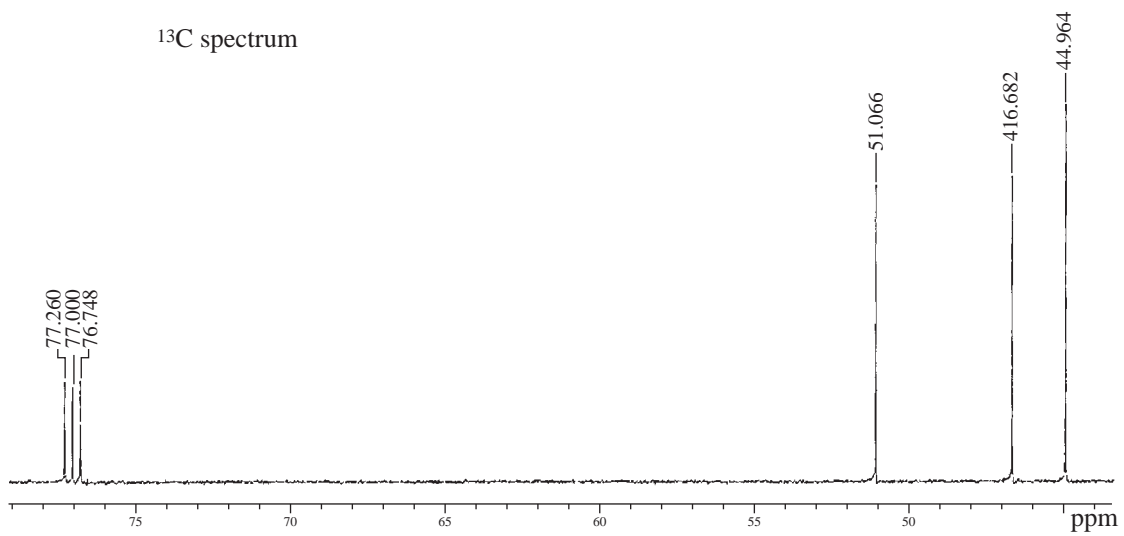
COSY

F2
(ppm)

F1 (ppm)
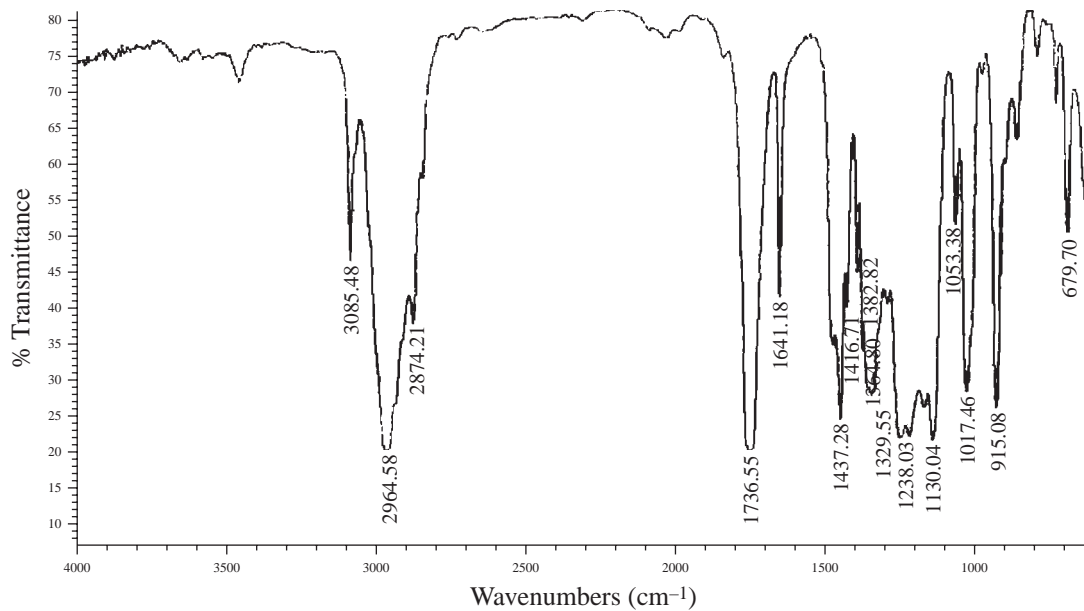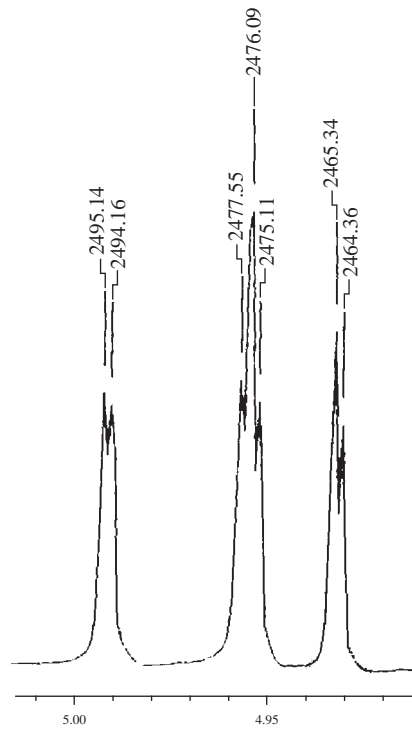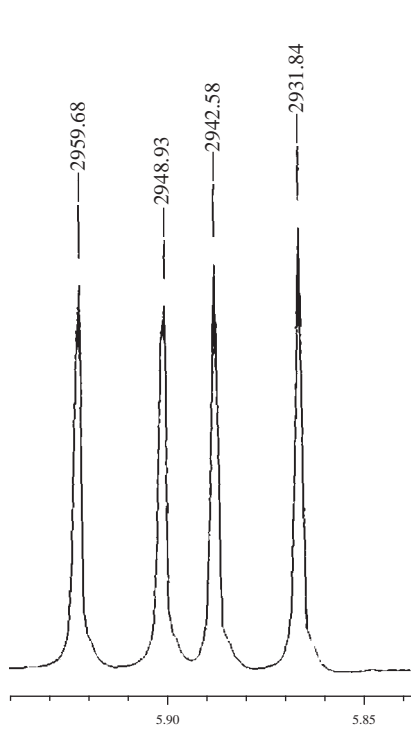
HETCOR

11. Determine the structure for a compound with formula C_3H_5ClO. The IR spectrum, ^1H NMR spectrum and expansions, ^{13}C NMR spectrum, DEPT spectrum, COSY spectrum, and HETCOR (HSQC) spectrum are included in this problem. The infrared spectrum has a trace of water that should be ignored (region from 3700 to 3400 cm^{-1}). You will find it to be helpful to consult Appendix 5 for values of coupling constants. Using these values make complete assignments for each of the protons in the NMR spectrum.
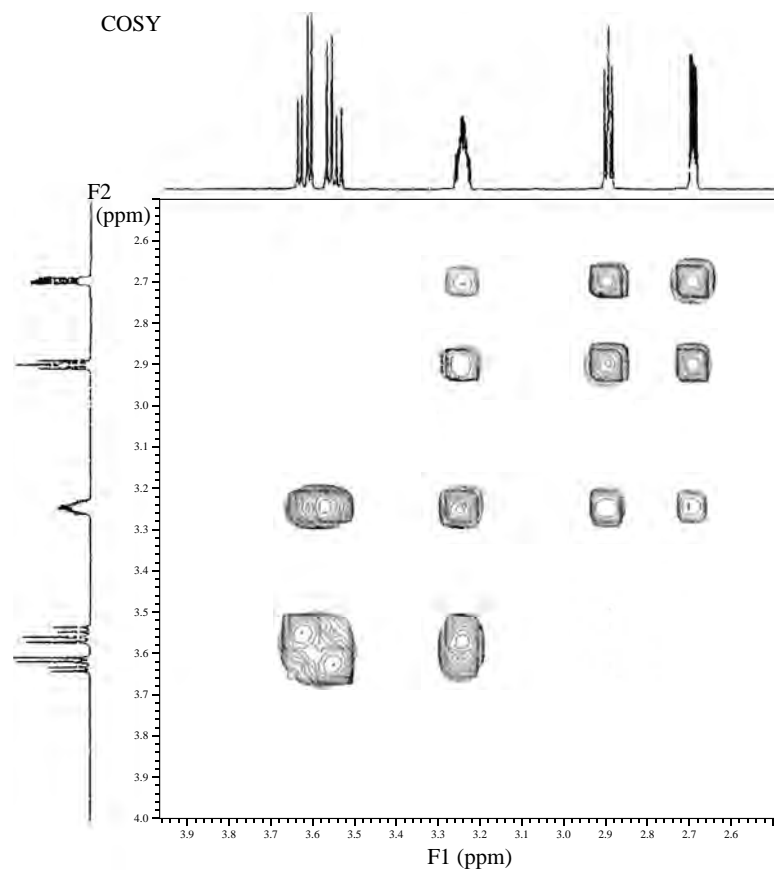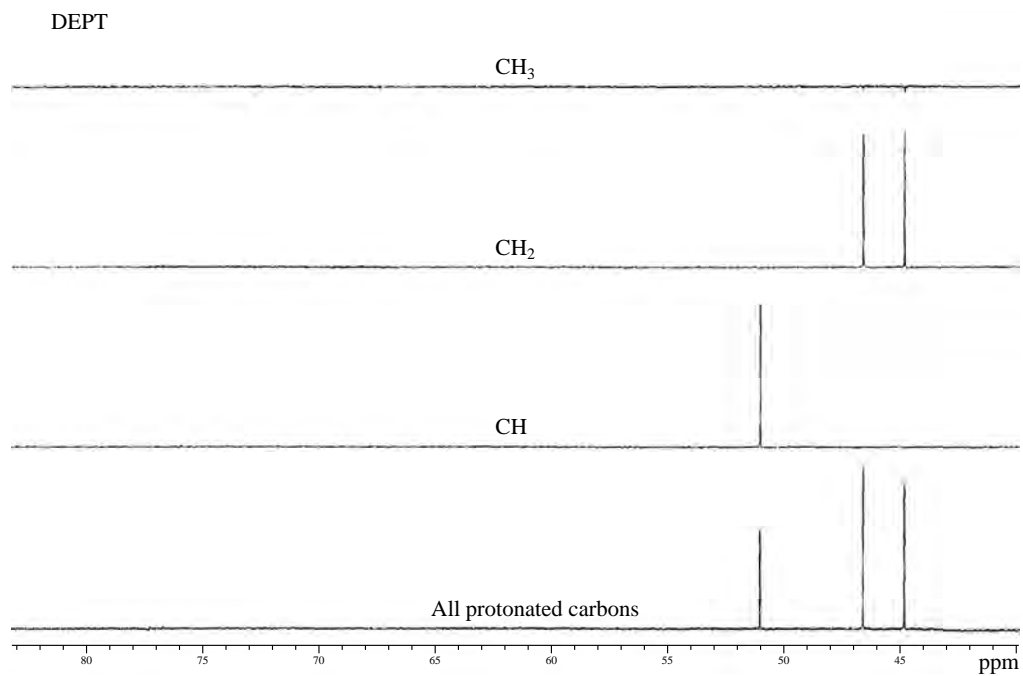
Infrared spectrum

¹H spectrum

1818.35
1813.71
1806.63
1801.87
1783.18
1777.20
1771.46
1765.48
1451.39
1446.99
1442.59
1349.42
1346.85
1344.53
1342.09

3.7 3.6 3.5 3.4 3.3 3.2 3.1 3.0 2.9 2.8 2.7 ppm

20.33   20.27   19.25   20.11   20.04

¹³C spectrum

77.260
77.000
76.748
51.066
416.682
44.964

75 70 65 60 55 50 ppm

DEPT

CH₃

CH₂

CH

All protonated carbons

COSY

F2
(ppm)
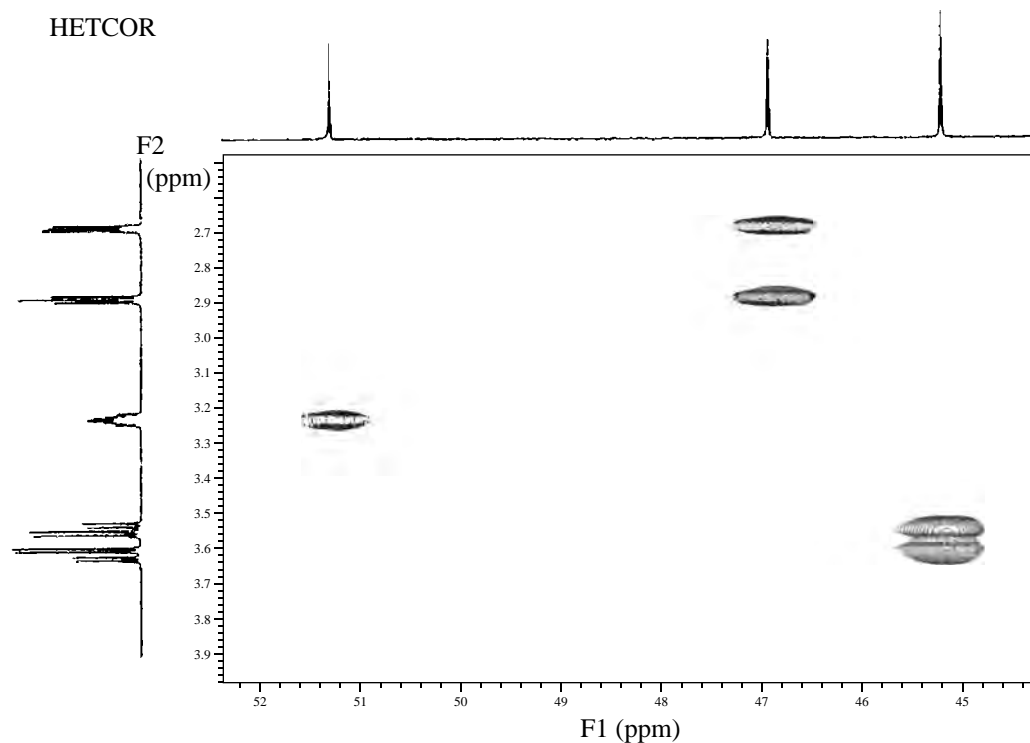
HETCOR

REFERENCES

Becker, E. D., *High Resolution NMR: Theory and Chemical Applications*, 3rd ed., Academic Press, San Diego, CA, 2000.

Croasmun, W. R., and R. M. K. Carlson, eds., *Two-Dimensional NMR Spectroscopy*, VCH Publishers, New York, 1994.

Derome, A. E., *Modern NMR Techniques for Chemistry Research*, Pergamon Press, Oxford, England, 1987.

Friebolin, H., *Basic One- and Two-Dimensional NMR Spectroscopy*, 3rd rev. ed., Wiley-VCH, Weinheim, Germany, 1998.

Sanders, J. K. M., and B. K. Hunter, *Modern NMR Spectroscopy: A Guide for Chemists*, 2nd ed., Oxford University Press, Oxford, England, 1993.

Schraml, J., and J. M. Bellama, *Two-Dimensional NMR Spectroscopy*, John Wiley and Sons, New York, 1988.

Silverstein, R. M., F. X. Webster, and D. J. Kiemle, *Spectrometric Identification of Organic Compounds*, 7th ed., John Wiley and Sons, New York, 2005 (Chapter 6).

Another valuable source of information about advanced NMR methods is a series of articles that appeared in the *Journal of Chemical Education* under the general title "The Fourier Transform in Chemistry." The specific volume and page citations are as follows.

Volume 66 (1989), p. A213
Volume 66 (1989), p. A243
Volume 67 (1990), p. A93
Volume 67 (1990), p. A100
Volume 67 (1990), p. A125

Selected Websites

http://www.chem.ucla.edu/~webnmr
Webspectra: Problems in NMR and IR Spectroscopy (C. A. Merlic, Project Director).

http://www.cis.rit.edu/htbooks/nmr
The Basics of NMR (Joseph P. Hornek, Ph. D.).